Cold fiber solid phase microextraction in solid sample analysis

by
Jun Guo

A thesis
presented to the University of Waterloo
in fulfillment of the
thesis requirement for the degree of
Master of Science
in
Chemistry

Waterloo, Ontario, Canada, 2013

Declaration

I hereby declare that I am the sole author of this thesis. This is a true copy of the thesis, including any required final revisions, as accepted by my examiners.

I understand that my thesis may be made electronically available to the public.

Abstract

The cold fiber solid phase microextraction (SPME) system was improved by minimizing the coating temperature fluctuation range, and the performance of the system was evaluated by investigating the extraction of PAHs from spiked sand samples. The coating temperature can be made relatively constant and the relative standard division (RSD) for most compounds was smaller than 2%.

A simplified cold fiber system without the solenoid valve was modified to connect CO_2 delivery tubing directly to the liquid CO_2 tank. The robustness of this system was evaluated with different sizes of CO_2 delivery tubings. The system is stable, low cost and can be easily controlled, which provides a supplementary extraction strategy to the traditional cold fiber system.

The extraction amount of the analyte in a specific system was calculated theoretically in advance. The extraction amount for the experiment agreed with that of the calculated result. By using theoretical calculations as a guide, desorption efficiency for aged spiked samples was investigated.

In order to achieve better extraction efficiency for PAHs, a programmed coating temperature method was developed and optimized, which led to higher extraction efficiency for most studied analytes compared to the traditional methods. In real sample analysis, certified reference soils were analyzed using cold fiber SPME and the addition of diethylamine successfully realized the exhaustive extraction for volatile compounds and enhanced the recoveries for semi-volatile compounds. Satisfactory extraction amounts for all compounds were achieved by the proposed method after method optimization.

Acknowledgements

I would like to take this opportunity to express my gratitude to all who have provided assistance and support during the process of this research.

First, I would like to thank my supervisor, Dr. Pawliszyn, for providing me with the opportunity to work on such an interesting project with such a great group, and for supporting me when I decided to change my program. His instruction, guidance and encouragement have allowed for the completion of this work.

I would also like to give thanks to my committee members, Dr. Tadeusz Górecki, Dr. Mario Gauthier, and Dr. Wojciech Gabryelski, for their advice as well as the time given to evaluate the work completed throughout this research project.

Additionally, I am very grateful to Dr. Gangfeng Ouyang, Reifen Jiang, and Dr. Heather Lord for their encouragement and valuable suggestions in my research.

I would also like to express my thanks to all the group members for their help and friendship, especially Weiqiang Zhan, Yanwei Zhan, Erica Silva, Sanja Risticevic, Nathaly Reyes G., German Augusto Gomez Rios, Afsoon Pajand Birjandi, Barbara Bojko, Dr. Yugao Guo, Dr. Youfu Du, Dr. Qin Shuai, Ziwei Bai, Yang Yang, Lixian Li, and Huiyu Zhao.

I would like to thank my parents, my husband Changjiu for their love, support and encouragement.

Dedication

I dedicate this thesis to my loving husband Changjiu.

Love Changjiu,
Love Forever.

Table of Contents

List of Figures

List of Tables

List of Abbreviations

AED.....Atomic-emission detector

CW.....Carbowax

DVB..... Divinylb

ECD.....Electron capture detector

EPA.....Environmental Protection Agency

FID.....Flame ionization detection

GC.....Gas chromatography

HPLC.....High performance liquid chromatography

HOCs.....Hydrophobic organic contaminants

LLE.....Liquid-liquid extraction

IMS.....Ion mobility spectrometer

ILs .....Ionic liquids

MAE.....Microwave-assisted extraction

MS.....Mass spectrometry

NAPL.....Non-aqueous phase liquid

NPD.....Nitrogen-phosphorus detector

PDMS.....Poly dimethylsiloxane

PA.....Polyacrylate

PAHs.....Polycyclic aromatic hydrocarbons

PCDD.....Polychlorinated dibenzodioxins

PFE.....Pressurized fluid extraction

PHWE.....Pressurized hot-water extraction

Refs.....References

RSD.....Relative standard division

SPME.....Solid phase microextration

SOM.....Sorbent organic matter

TPR.....Templated resin

Chapter 1

Introduction

1.1 Kinetics of extraction of analytes from solid matrices

The extraction of analytes from a solid matrix is the most challenging of all extraction modes because it involves several fundamental processes in the extraction procedure. Figure 1-1 shows the extraction kinetics of analytes from a solid matrix in a general model [1]. It is assumed that a matrix particle consists of an organic layer on a porous core. The analyte is adsorbed on the surface of the porous core which is impermeable. First the analyte must be desorbed from the surface (A(M, S)), and then diffuses through the organic layer of the matrix (A(M,L)) to reach the matrix/fluid interface (A(M,I)). Then, the analyte must be solvated by the extraction phase (A(EP,P)) and diffuses through the static phase inside the pore to reach the extraction phase portion which is affected by convection. Finally, the analyte transports through the interstitial pores of the matrix and arrives at the bulk of the extraction phase (A(EP,B)) [1].

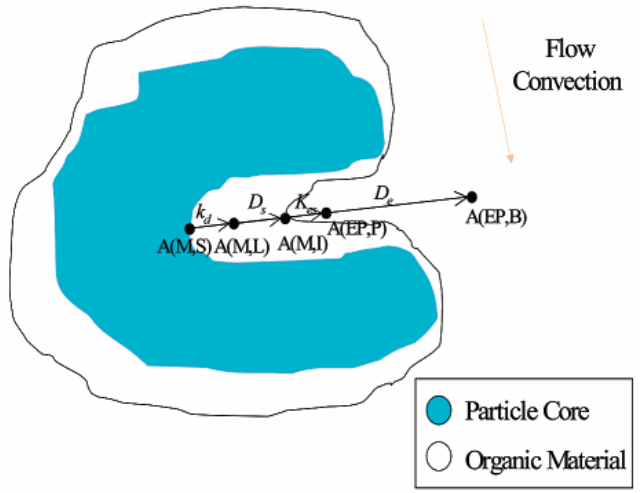

Figure 1-1 Extraction processes of heterogeneous samples containing porous solid particles. k_d is the dissociation rate constant of the analyte in matrix complex; D_s and D_e are the diffusion constants of the analyte in the matrix and the extraction phase, respectively; K_{es} is the distribution constant between the extraction phase and the sample matrix [1].

Extraction of analytes from a solid can be performed directly in a vessel, such as Soxhlet, sonication, and microwave-assistant extraction, or can be combined with elution from the packed tube, such as pressurized fluid extraction and supercritical fluid extraction [2]. The extraction combined with elution from the packed tube is the most efficient approach for the extraction of volatile and semi-volatile compounds. The extraction process is similar to chromatographic elution with packed columns since the extraction phase removes analytes from the matrix continuously [2]. Therefore, mathematical equations in chromatography can be applied to describe the relationship between the matrix parameters and flow conditions. The elution profile for calculating mass of analytes eluted from the vessel in solid matrix extraction is as follows [1]:

$$\frac{m(t)}{m_0} = \frac{\int_{-\infty}^{-\frac{1}{2}L} C(x,t)}{C_0 L} \qquad \text{Equation1-1}$$

Where $m\ (t)$ and m_0 are the mass of the analyte extracted and the total amount in the vessel initially, $C(x,t)$ is the concentration of the analyte at the position x and time t, C_0 is the concentration of the analyte in the matrix at beginning, and L is the length of the vessel [3]. This

equation can only be applied when the analyte is weakly adsorbed on an organic-poor matrix, meaning that the elution and partitioning between the matrix and extraction fluid is reached rapidly. However, under dynamic extraction, the system cannot reach the equilibrium conditions at the beginning of extraction in most practical circumstances due to the slow mass transport rate between the fluid and the matrix. Therefore, the amount of analyte removed from the vessel at elution time *t* can be obtained by convoluting the function of the mass transfer rate between two phases with the elution time profile [3].

In this extraction time profile, the mass transfer and the elution process between the phases occur at same time. Convolution during extraction is the release rate of analyte from the matrix, which describes the overall extraction process as well as the kinetics of these complex processes. It is difficult to obtain the exact mathematical solution of the convolution, but the solution can be represented graphically by using Fourier transform.

In heterogeneous samples, the rate of extraction is frequently controlled by the release of solid-bound analytes from the sample matrix. Desorption of the solid-bound analytes can be achieved by a high sample temperature or by the addition of organic modifiers. Extraction strategies, such as supercritical fluid extraction, pressurized fluid extraction, and microwave-assisted extraction, operate with more energy to accelerate the analytes release from the interface between phases [4]. Furthermore, the addition of an organic modifier, which accelerates interactions between analytes and matrices, can be beneficial in many cases for the extraction in solid matrices.

1.2 Sample preparation techniques from solid matrices

There are several steps in the analytical procedure: sampling, laboratory sample preparation, separation and quantification, statistical evaluation, decision, and action. In the analytical process,

each of these steps is important in obtaining precise and accurate results. Among those, however, sample preparation is always the key to a successful analysis. Sample preparation in different solid materials is an especially complicated task due to the separation of the analytes fraction from solid matrices with very different physical-chemical compositions and characteristics. As a result, sample preparation in complex solid matrices, such as soil, sediments, or other matrices, is difficult to process.

The traditional methods of sample preparation such as liquid-liquid extraction (LLE) are typically time consuming, labor intensive, use extensive amounts of organic solvents, and have a high risk for loss of analytes. Some sample preparation techniques for solids, which use a small quantity or no organic solvent, have been available in recent years. These include: accelerated solvent extraction (ASE), microwave-assisted extraction, supercritical fluid extraction, pressurized hot-water extraction, ionic liquid extraction, and headspace SPME.

1.2.1 Solvent extraction

Solvent extraction is the most traditional extraction strategy for isolating the various analytes from complex solid matrices. In a solvent extraction process, organic solvents like dichloromethane, acetonitrile, cyclohexane, benzene, and their mixtures are usually used as extraction solvents [5], followed by concentration, such as rotary evaporator concentration [6].

Soxhlet extraction is a traditional solvent extraction technique with high extraction efficiency. Although Soxhlet extraction has high extraction efficiency, it is time-consuming, and further concentration steps are required [7].

Compared to Soxhlet extraction, sonication extraction is more time-saving, solvent-saving and is more efficient. Sonication could be carried out at room temperature. The regular procedure

involves extracting analytes with the assistance of sonication in a solvent, such as toluene, methanol, or cyclohexane, for some time; after which, the samples are evaporated under nitrogen, and then dissolved in a small volume of the solvent before the chromatographic analysis.

Pressurized fluid extraction (PFE) is a liquid extraction method using elevated temperature and pressure to enhance extraction efficiency; it applies pressure so that the solvent will not boil during extraction at the elevated temperature [8]. The PFE method is similar to Soxhlet extraction with the exception that the solvents are used near their supercritical region so they have high extraction efficiency [9, 10].

1.2.2 Microwave-assisted extraction

Microwave-assisted extraction (MAE) is an instrumental extraction technique in which both samples and solvents are subjected to heat radiation from electromagnetic wavelengths of various frequencies. Compared to conventional heating, microwave-heating radiation is rapid, reproducible, and has less energy loss. Modern designs of microwave ovens can simultaneously hold at least twelve extraction samples.

The major advantage of MAE is that it can reduce solvent consumption and time; moreover, the heating mechanism of MAE provides selective interaction with chemicals, which greatly enhances the extraction efficiency [11, 12]. The cost of this technique is moderately lower than other extraction methods [13]. In addition, a wider range of solvents can be used in MAE, as the technique should be less dependent on a high solvent affinity. Because microwaves interact selectively with the free water present in the matrix systems, MAE can improve the migration of the compounds out of the matrix, which is another advantage of extraction analytes in complex solids [14, 15]. With localized heating, the temperature increases rapidly near or above the

boiling point of water. Such systems undergo a dramatic expansion, after which the chemicals flow towards the organic solvent. This process is quite different from classical solvent extraction in that the solvent partitions into the extraction solvent by solubilization [16].

The main disadvantage of this method is that the solvent needs to be removed physically from the sample matrix after the extraction and prior to the analysis. An additional purification step may reduce this drawback but could result the loss of analytes. MAE can be directly analyzed without the need for further purification step if coupled with HPLC for analysis [17].

1.2.3 Pressurized hot-water extraction

Pressurized hot-water extraction (PHWE), also known as subcritical water extraction, is a result of the development of SFE. The extraction fluid in PHWE is water. Pressurized hot water is used in the condensed phase with the temperature ranging from 100 ℃ (boiling point of water) to 374 ℃ (the critical point of water). As the temperature of water rises under pressure, the hydrogen-bonding network of water molecules weakens, resulting in a decrease in its polarity. Therefore, subcritical water becomes more hydrophobic and organic than ambient water, promoting the miscibility of light hydrocarbons with water [18]. In PHWE, the density of water remains almost the same over this temperature range so that the effect of pressure on the properties of water is very small [19]. PHWE is a green solvent extraction method used to extract organic compounds from a solid matrix like soil. Hawthorne [20] proved that water could be transformed into a solvent for organic compounds under high temperatures and controlled pressurized conditions. The extraction efficiency for PHWE was found to be comparable with the other reference methods such as Soxhlet extraction [21, 22].

1.2.4 Alternative extraction methods

One alternative solid matrix extraction technique consists of replacing conventional organic solvents with other extractive agents such as micellar media [23]. Micellar media have been successfully proved to be an alternative for the extraction of volatile and non-volatile organic compounds from solids [24]. Ionic liquids (ILs) are low melting point ionic compounds that have high thermal stabilities and negligible vapor pressures and are therefore green solvents. Research shows that many compounds tend to have high partition coefficients with IL-aggregates. The method based on IL-aggregates as the extractive agent showed good recovery with short extraction times and small amounts of IL solution. Furthermore, the clean-up step prior to analysis is not required because the IL-extract can be directly injected in a HPLC or GC [25].

Thermal desorption is another alternative solid matrix extraction technique which does not require solvents or high pressure extraction equipment. This technique is commonly coupled with GC by direct injection of a solid sample to the cold injector. The carrier gas is temporarily not available while the injector is rapidly heated to the desired temperature, approximately between 200-500 ℃, to volatilize targeted compounds. The carrier gas is then restored and the isothermally extracted compounds are swept onto the GC column, providing a direct and rapid analysis of a contaminated solid such as soil [26]. This technique, however, requires prior calibration to allow a non-linear response to sample size and concentration of contaminants [27].

Although some sample preparation techniques could achieve high recovery and good sensitivity, there is still an increasing demand for solvent-free extraction methods with speed, sensitivity, convenience, and automation. Headspace SPME is a new preparation technique for solid samples.

Headspace SPME is a solvent-less sample preparation strategy designed to extract volatile compounds from solid samples. After extraction, the fiber coating is transferred directly to the

injection port of an analytical instrument such as GC for quantitative analysis without any pretreatment. All processes could be carried out automatically with the headspace SPME using the autosampler and minimize the loss the compounds during the process of desorption. This method is fast, simple, and convenient, and the extraction is highly efficient. It is preferable for lower molecular weight compounds. Table 1-1 summarizes features of the solvent and comments on different sample preparation techniques for solid samples.

Table1-1 Comparison of the different extraction methods for solid samples.

Extraction method	Solvent	Comments	Reference
LLE	Organic solvents	The most traditional method Time consuming Large solvent consumption	[28,29]
MAE	Organic solvents	Small solvent consumption Low cost Short extraction time	[30,31]
ASE	Organic solvents	Good recovery Low selectivity Short extraction time	[32]
Supercritical fluid extraction	CO_2	Environmentally friendly Use of high pressure equipment Low recovery of heavy compounds	[33]
PHWE	Water	High extraction efficiency Short extraction time Green solvent	[34]
Ionic liquid extraction	Ionic liquids	Short extraction time Small amount of IL	[25]
Headspace SPME	Solvent-less	No solvent needed Easy to operate Short extraction time Fully automated system	[35]

1.3 Headspace SPME

1.3.1 SPME

SPME was invented in 1990 by Pawliszyn and is used as a rapid sampling and sample preparation method both in the laboratory and on-site [36]. It does not require solvents or complicated apparatus with the advantage of combining sampling, isolation, and enrichment into one step [37]. This technique uses a small diameter fused silica or metal fiber coated with a small volume of stationary phase attached to a plunger with outer needle protects the fiber (Figure 1-2).

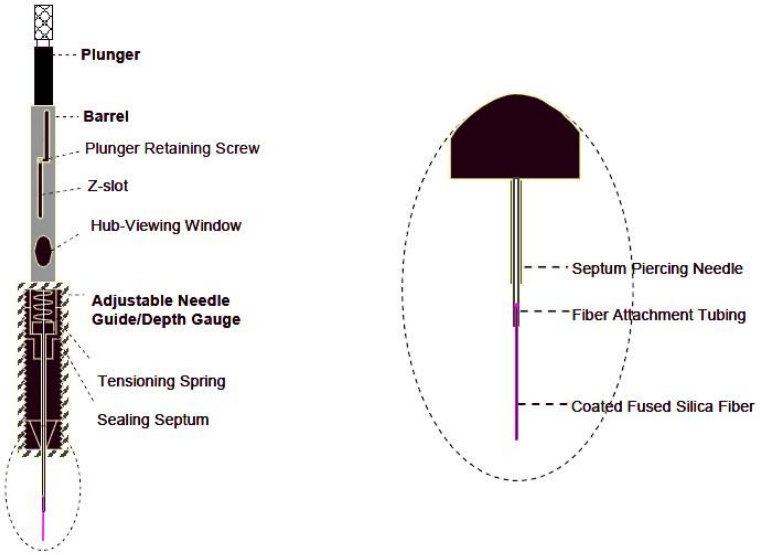

Figure 1-2 Design of the first commercial SPME device [44].

During the extraction the fiber is exposed to either a gaseous or a liquid sample or the headspace of a solid sample and analytes are partitioned between the sample matrix and the fiber coating. After a period of time, the fiber is withdrawn into the outer needle and transferred to the injector of an analytical instrument for thermal desorption, separation, and quantification. The desorption step is normally carried out by placing the fiber coating into a hot injector in a gas

chromatography (GC) [38], or in a SPME-high performance liquid chromatography (HPLC) interface [39, 40].

The coating selection is the first step in the SPME method development because the sensitivity of SPME is mostly affected by the partition coefficient of the analyte between the sample matrix and the fiber coating [41]. Several coatings are currently commercially available: polydimethylsiloxane (PDMS) with different thicknesses, polyacrylate (PA), the mixed phases of PDMS-divinylbenzene (DVB), Carbowax (CW)-DVB, Carboxen-PDMS, and CW-templated resin (TR). The most widely used coating is PDMS, which is a very rugged liquid coating and able to withstand high injector temperatures. PDMS is considered a non-polar phase and particularly suitable for the non-polar analytes; it can also extract more polar compounds [41]. In mixed phase coatings, DVB porous microspheres are immobilized on the fiber, and carbowax or PDMS hold them together with the fiber (Figure1-3). In addition to commercial coatings, custom made coatings have been developed to extract some specific analytes [42, 43].

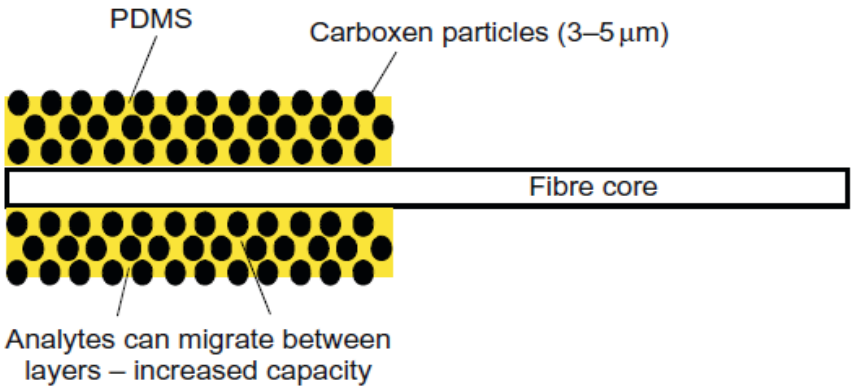

Figure 1-3 Close-up view of Carboxen-PDMS fiber [44].

Extraction efficiency is related to the distribution constant which is a characteristic parameter that describes the properties of a coating and its selectivity toward the analyte in contrast with

other matrix components. Sensitivity is always limited by the volume of the coating. If the partition coefficient of the analyte is relatively high, for example, in case of high boiling point compounds, thin coatings can achieve the extraction equilibrium and desorption begins in a relatively short time [41]. On the other hand, thicker coatings allow the extraction of larger amounts of the analytes enabling their transport to the chromatographic injector without significant loss, but resulting in longer extraction time [41, 44].

There are two extraction mechanisms based on the coating structure: adsorption and absorption. For absorption, the analytes partition into the extraction phase, in which the molecules are solvated by the coating molecules. The diffusion coefficient in the coating enables the molecules to penetrate the whole volume of the coating within a reasonable extraction time if the coating is thin. PDMS and PA coatings are polymeric phases that extract analytes via absorption. The coating for adsorption has a glassy structure, so that sorption occurs only on the porous surface of the coating. Only a limited surface area is available for adsorption; if this area is substantially occupied, compounds with poor affinity towards the phase are frequently displaced by analytes with stronger binding, or with higher concentrations. The CW/DVB and CW/TPR are mixed coatings in which the primary extraction phase is a porous solid that extracts analytes through adsorption. [45]

Equilibrium can be established between the sample matrix and the extraction phase if the extraction time is long enough. When equilibrium conditions are reached, exposing the fiber for a longer time does not result in the accumulation of more analytes. Equilibrium extraction is the most frequently used quantification method for SPME and extraction is considered complete when the analyte concentration has reached equilibrium between the sample matrix and the extraction phase. Equilibrium conditions in a two-phase system can be described by Equation 1-2:

$$n = \frac{K_{fs} V_f V_s C_0}{K_{fs} V_f + V_s}$$ Equation 1-2

where n is the amount of the analyte extracted by the coating, K_{fs} is the distribution constant between the fiber coating and the sample matrix, V_f and V_s are the volume of the fiber coating and the sample respectively, and C_0 is the initial concentration of the analyte in the sample [34]. This equation shows that a linear relationship exists between the amount of analyte extracted by the fiber coating (n), and the initial concentration of the analyte in the sample matrix (C_0), which is the analytical basis for quantification using SPME.

Typically, SPME is considered an equilibrium technique, but it may also be utilized for the exhaustive extraction of analytes under some conditions. When the sample volume is very small, and the distribution coefficient of the analyte between the sample matrix and the fiber coating is very large, such as the extraction of semi-volatile organic compounds from a small volume sample matrix ($V_s << K_{fs} V_f$), Equation 1-2 can be simplified to:

$$n = C_0 V_s$$ Equation 1-3

Equation 1-3 implies that all analytes in the sample matrix are extracted onto the fiber coating. Therefore, the amount of analyte extracted by the coating can be calculated with the analyte concentration in the sample and the volume of the sample. Exhaustive extraction calibration is suitable for small sample volumes and very large distribution coefficients. Cold fiber device can offer an opportunity to extract the total amount of analytes in a sample and is suitable for exhaustive extraction calibration [46].

1.3.2 Headspace SPME

There are three basic extraction modes for SPME: direct extraction, membrane protected SPME, and headspace extraction.

In the direct extraction mode, the coated fiber is directly inserted into the sample and the analytes are transported from the sample matrix to the extraction phase. For gaseous samples, natural convection of air is sufficient to facilitate a fast equilibration. For aqueous samples, in order to make aqueous extraction faster, some level of agitation is required to increase the analytes' diffusion from the sample matrix to the fiber coating. To reach an efficient agitation, in the case of aqueous matrices, rapid sample flow, fast fiber or vial movement, stirring, or sonication is required. These approaches are applied to reduce the effects of fluid shielding and small diffusion coefficients of the analytes in aqueous matrices.

The membrane-protected SPME technique is used for the extraction of analytes in polluted samples such as humic acids or proteins. In such cases, the coating is easily damaged by direct extraction and such membrane materials can protect the coating from damage.

In headspace sampling, the fiber is inserted into the headspace above the aqueous or solid matrix. Only relatively volatile and semi-volatile analytes are extracted. During the extraction, the analytes are transported to the fiber through the headspace and there is no direct contact between the fiber coating and the sample. In this case, coating is protected from damage by high molecular mass proteins or humic matter and this mode allows for a change in pH of the matrix (Figure 1-4).

The headspace SPME can be coupled with GC for analyzing volatile organic compounds in areas such as food, beverages, plants, and environmental matrices. The application of the headspace

SPME device can eliminate the problems in the previous headspace techniques, such as the enrichment of trace compounds, large and expensive equipment devices, and the adsorption of some analytes in the internal wall of the syringe. Headspace SPME can also extend headspace sampling to less volatile analytes due to the concentration effect in the fiber coating.

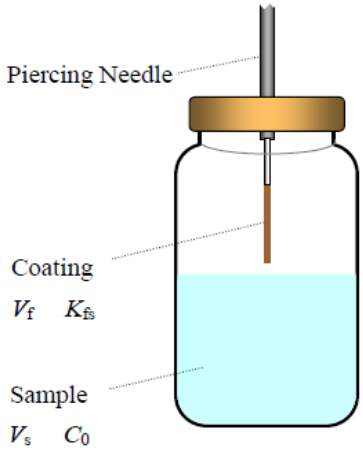

Figure 1-4 Extraction mode of headspace SPME. V_f is the volume of fiber coating; K_{fs} is the fiber/sample distribution coefficient; V_s is the volume of sample; C_0 is the initial concentration of analyte in the sample.

1.3.2.1 Thermodynamics of headspace SPME

Equation 1-2 assumes equilibrium conditions in a two-phase system between the sample matrix and the fiber and no headspace is present in the system [34]. However, Equation 1-2 can be modified for a headspace mode system by considering the volumes of the individual phases and the distribution constants between phases (Equation 1-4) [34].

$$n = \frac{K_{fh}K_{hs}V_fV_s}{K_{hs}V_{hs} + V_s + K_{fh}K_{hs}V_f}C_0 \qquad \text{Equation 1-4}$$

Where n is the mass of the analyte extracted on the fiber between the three phases (the sample, the headspace, and the fiber); K_{fh} and K_{hs} are the partition coefficients of the analyte between the fiber and the headspace, and between the headspace and the sample respectively; V_{hs} is the volume of the headspace; and C_0 is the initial concentration of the analyte in the sample matrix.

The other parameters are the same as in Equation 1-2. Compared with Equation 1-2, it may be noted that, except for the extra term of K_{hs} V_{hs}, which is related to the capacity of the headspace, the two equations are the same. Both equations describe the mass (n) extracted by the fiber coating after equilibrium has been reached. K_{hs} is relatively small for most analytes. The amount absorbed by the coating from the headspace will not be affected if the volume of the headspace is much less than the volume of the sample matrix ($V_{hs} << V_s$). Therefore, the detection limit of the headspace SPME is expected to be very close to those of the direct SPME from some samples.

1.3.2.2 Kinetics of headspace SPME

The speed of headspace SPME extraction is determined by the kinetics of the extraction process, including the analytes transport from the sample matrix to the headspace and finally to the fiber coating. The kinetics process determines the total sampling time of the headspace SPME. The geometry of the headspace SPME extraction is illustrated in Figure l-5a.

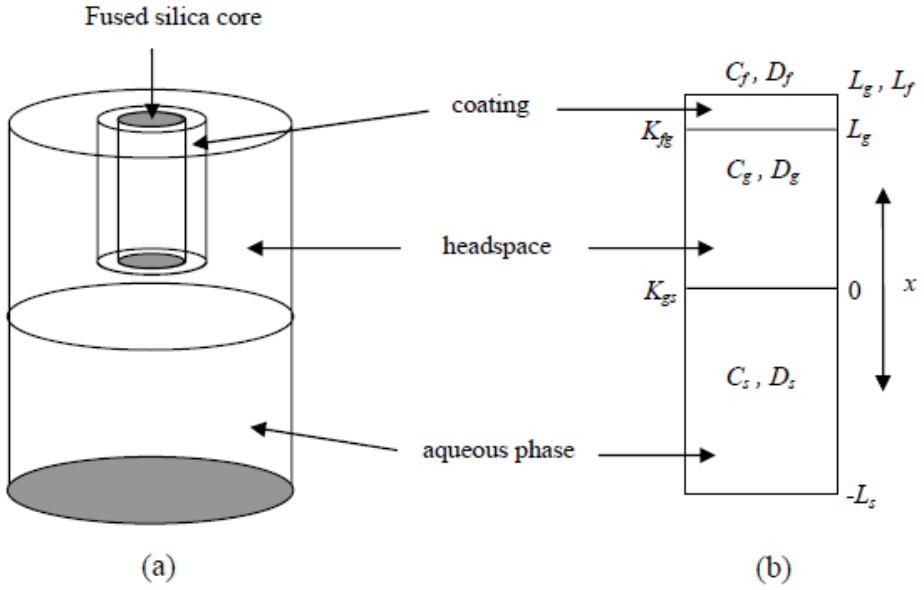

Figure 1-5 (a) Geometry of headspace SPME sampling; (b) one-dimensional model of the system. K_{fg} and K_{gs} are the fiber coating/headspace and headspace/sample matrix partition coefficients, respectively; D_g, D_f, and D_s are the diffusion coefficients of the analyte in the headspace, coating, and sample matrix respectively; L_g, L_f, and L_s are the thicknesses of the headspace, coating, and sample matrix, respectively [44].

In this mode, analytes in the aqueous sample are transferred to the headspace in a closed container. Chemical equilibrium is established between the aqueous solution and the headspace before the extraction. A fiber coated with a thin layer of polymer is inserted into the headspace of the container and the fiber coating starts to extract the analytes from the headspace. Two processes are involved: analytes are transported from the sample matrix to the headspace, and then to the fiber coating, until finally the equilibrium is reached in the system. Figure1-5b illustrates a one-dimensional diffusion model, in which diffusion only occurs in one direction. This process can be described by Fick's second law:

$$\frac{\partial C}{\partial t} = \frac{\partial^2 C}{\partial x^2} \qquad \text{Equation 1-5}$$

Where *t* is the time and *x* is the position; *C(x,t)* is the analyte concentration at time *t* and position *x*. At any given moment (*t*), the mass of the analyte absorbed by the fiber coating can be calculated by:

$$m(t) = \int_{L_s}^{L_s+L_f} C(x,t)dx \qquad \text{Equation 1-6}$$

Assuming that the initial concentration C_0 of the sample solution is loaded into a vessel, and the equilibrium is achieved between the headspace and the sample matrix before the headspace SPME extraction, the concentration of the analyte in the headspace and in the sample can be calculated. After the extraction begins, the concentrations of the analyte in any position (*x*), at any given time (*t*) can be obtained.

During the headspace SPME extraction process, the equilibrium in the three phases is achieved when the concentration of the analyte is kept constant within each of the three phases. Also, the concentration ratios between two adjacent phases are in accordance with the distribution

coefficients between these two phases [44]. The time that is required to reach the equilibrium is related to the thickness of the coating (L_f), the diffusion coefficients of the analyte in the headspace phase and the sample (D_g and D_s), the distribution coefficient of the analyte between the headspace and the sample (K_{gs}), and between the fiber coating and the headspace (K_{fg}), respectively.

For static headspace SPME, the equilibrium time t_e, i.e. the time when 95% of the total mass of an analyte is extracted from the sample, can be estimated [44].

When the amount of the analyte extracted by the fiber coating is small compared to the amount present in the sample matrix, the diffusion coefficient of the analyte in the sample (Ds), and the distance of analytes diffuse through the sample (Ls) controls the mass transfer rate in the sample [44]. The mass transfer rate to the headspace is related to the headspace/sample distribution coefficient (K_{gs}), the length of the headspace phase (L_g), and the diffusion coefficient of the analyte in the headspace (D_g). The equilibrium time also increases with the increase of the fiber thickness and the coating/sample distribution coefficient (K_{fs}).

It should be emphasized that the increase in headspace capacity causes a loss in method sensitivity. In a headspace SPME system, the analyte is distributed between all three phases involved (the headspace, the fiber coating and the sample matrix). Therefore, the amount of analyte extracted by the fiber coating at equilibrium in a headspace SPME system can only be equal to or smaller than the amount extracted without headspace is present (direct SPME). For some semi-volatile analytes, by increasing the headspace capacity, the equilibration time might dramatically shorten while maintaining sufficient sensitivity.

1.3.3 Applications of headspace SPME in solid sample analysis

The headspace SPME technique has been widely used for the analysis of environmental pollutants in solid samples. Hundreds of papers addressing solid sample analysis with headspace SPME have been published in recent years. Table 1-2 summarizes some of the solid matrix applications of headspace SPME in environment, which are reported by Ouyang [47]. Most applications have been assisted by sonication and microwaves due to the strong binding of the analytes with the solid matrices. In most situations, headspace SPME can only extract analytes with high volatilities; however, using cold fiber SPME can realize the extraction of both volatile and semi-volatile analytes without any further assisted procedure.

Table 1-2 Recent applications of headspace SPME in solid environmental samples.

Analytes	Matrix	Fiber	Detection	Refs
BTEX	Sand	PDMS-cold fiber	GC-MS	[46]
BTEX	Sand	CAR-PDMS	GC-MS	[48]
BTEX	Soil	CAR-PDMS	GC-FID	[49]
Organotin compounds	Sediment	PDMS	GC-MS	[50]
Dichlorophenol	Soil	PA	GC-ECD/NPD	[51]
2-Chloroethyl ethyl sulfide	Soil	Acrylate/silicone co-polymer sol-gel	GC	[47]
PCDD	Soil	PDMS	GC-MS-MS	[52]
Butyltin compounds	Sediment	PDMS	GC/MIP AED	[53]
Methylphosphonates	Soil	PDMS PDMS-DVB	IMS	[54]
Fungicides	Soil	PA	GA-MS	[55]
Chlorophenols	Soil	PA	GC-ECD	[56]

1.4 Cold fiber SPME

1.4.1 Introduction

As discussed above, SPME has been successfully applied to the extraction of volatile and semi-volatile organic compounds from gas, liquid, and solid samples. Headspace SPME is appropriate for the analysis of volatile compounds in food, as well as environmental and clinical matrices. In the headspace SPME mode, in order to achieve a good extraction efficiency, analytes must be released effectively from their matrix into the headspace. Accelerating mass transport by vigorous agitation can often shorten the equilibrium time, but in high viscosity matrices such as oil, soil, and sludge, the process is complicated by the presence of particles or macromolecules in the sample. Desorption of analytes from the complex matrix often limits the entire mass transfer process and higher energy is required to isolate the analytes from solid particles.

The simplest and most effective way is to heat the sample at high temperature, which provides enough energy to overcome the energy barriers between the analytes and the matrix. This thermal energy can enhance the mass transfer process within the matrix, and increase the vapor pressure of the analyte in the system. On the other hand, an increase in sample temperature also decreases the distribution coefficients of the analytes between the fiber coating and the sample matrix, which leads to poor extraction amount.

The cold fiber SPME device was developed to overcome this drawback. In this system, the sample matrix is heated to a high temperature (it accelerates desorption of the analytes from matrix components), and simultaneously the fiber coating is kept cool (it increases distribution coefficients of the analytes between the headspace and the extraction phase). In this heating-cooling system, a temperature gap is created between the hot sample/headspace and the cold fiber coating, which significantly increases the extraction efficiency.

1.4.2 Theory

In a cold fiber SPME system, the sample matrix is heated to a high temperature while the extraction phase temperature is kept low. In order for cold fiber SPME to be considered an exhaustive extraction, more than 90% of total mass of the analyte initially existed in the sample should be transferred to the extraction phase. In the headspace SPME system, the ratio of the mass absorbed by the coating at equilibrium to the total mass of the analyte initially in the sample (n/n_0), should be larger than 0.9. Equation 1-4 can be written as:

$$\frac{n}{n_0} = \frac{K_{fh}K_{hs}V_f}{K_{fh}K_{hs}V_f+K_{hs}V_{hs}+V_s} \qquad \text{Equation 1-7}$$

Where n is the amount of the analyte extracted by the coating, and n_0 is the total mass of the analyte initially in the sample. One practical approach to increase the n/n_0 ratio is to increase the partition coefficient of the analyte between the fiber coating and the headspace (K_{fh}), which may be achieved by using different coatings with different polarities [41]. Another approach for a higher n/n_0 ratio is to increase the partition coefficient (K_{hs}) of the analyte between the headspace and the sample matrix. The simplest way is to heat the sample at a high temperature, which has been discussed in the last section.

The distribution coefficient of the analyte between the fiber coating and the headspace affected by temperature may be described by Equation 1-8 [44]:

$$K = K_0 exp\frac{-\Delta H}{R}\left(\frac{1}{T}-\frac{1}{T_0}\right) \qquad \text{Equation 1-8}$$

where K_0 is the distribution coefficient of the analyte between the fiber coating and the headspace when the sample matrix and the fiber coating are both at temperature T_0; K is the distribution coefficient of the analyte between the fiber coating and the headspace when sample

matrix temperature is at T_0 and the fiber coating is at temperature T, ΔH is the molar change in enthalpy during the transfer of the analyte from the sample matrix to the fiber coating, and R is the gas constant. ΔH is considered constant over the temperature ranges of SPME experiments [41]. Since the extraction from the headspace into the fiber coating is an exothermic process, which means $\Delta H < 0$. Therefore, with the increase of the temperature gap between the fiber coating and the headspace, the distribution coefficient of the analyte between the fiber coating and the headspace increases.

1.4.3 Design of cold fiber SPME system

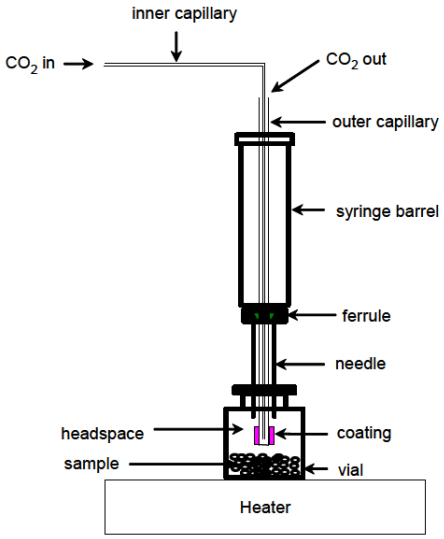

Figure 1-6 Design of cold fiber SPME device.

Cold fiber SPME device (Figure 1-6) utilizes liquid carbon dioxide (CO_2) to cool down SPME coating temperature, which is delivered to the inside surface of a hollow tubing from a liquid CO_2 tank. One end of the hollow tubing is sealed and a piece of PDMS hollow fiber coated outside of the tubing end serves as the extraction phase. In this device, liquid CO_2 comes out of the delivery tubing, evaporates and turns into CO_2 gas quickly. Thermal energy is absorbed from the surrounding environment during evaporation, which results in cooling down the coating

temperature. The coating temperature depends on the flow rate of liquid CO_2 which is controlled by the inner diameter of tubing. The temperature of the fiber coating is monitored by thermocouples, with one end locates inside the hollow tubing along with the liquid carbon dioxide delivery tubing, and the other end connects to a purpose-built temperature controller.

The cold fiber device is designed to be operated automatically with an autosampler. After extraction, the fiber is transferred to a GC injection port for desorption automatically.

1.4.4 Applications of cold fiber SPME system

Cold fiber SPME has been applied in many areas, including extraction of aroma profile from tropical fruits [57], extraction of perfume and flavor compounds from shampoo samples [58], extraction of off-flavor compounds in cork stopper samples [59], and extraction of fragrances from Iranian rice samples [60]. Most target analytes have high volatilities. Haddadi studied the desorption kinetics of PAHs from solid samples [35], which provides simple relationships to predict the desorption behavior of PAHs from solid matrix. More studies are required to extract both volatile and semi-volatile compounds from complex solid matrices.

1.5 Thesis objective

The first objective of this thesis is to develop and evaluate the cold fiber system with the aim of improving a simple, robust system. The application of cold fiber SPME for analyzing volatile and semi-volatile compounds in laboratory spiked and naturally contaminated solid samples is the next purpose of the present study.

Chapter 2 evaluates the traditional cold fiber system and modifies the system with better stability and precision. A new simplified cold fiber system without the solenoid valve is introduced.

In chapter 3, theoretical calculations of the distribution coefficients and the extraction amounts for analytes with cold fiber are shown. Those verification results for BTEX are compared with experimental results, and more applications of the theoretical verification are presented.

Chapter 4 describes the applications of cold fiber system in solid sample analysis. Firstly is the method development and optimization for PAHs from laboratory contaminated sand samples, followed by the extraction of the analytes from real soil samples.

Finally, Chapter 5 summarizes the overall conclusions of the research in this thesis, and makes recommendations for future considerations.

Chapter 2

Improvement and evaluation of cold fiber system

2.1 Introduction

2.1.1 Design of cold fiber device [61]

The primary schematic of the cold fiber SPME device is shown in Figure 2-1. The barrel of a 100 µl gas-tight syringe is used as the barrel of the cold fiber device. The plunger is made from a 22XX-gauge (O.D. 0.71 mm, and I.D. 0.6 mm) stainless steel tubing with a length of 165 mm. One end of the tubing is welded to a half-round open cap, which provides the plunger motion coupling for the autosampler injection arm. The large inner volume of this half-round shape also provides sufficient space to allow the CO_2 tubing to bend with the axial motion of the autosampler arm. The other end of plunger is sealed after mounting the K-type thermocouple wires, which are made from alumel and chromel wires. The plunger tip must have a gas-tight seal to prevent any leakage after the CO_2 is delivered to the end of the syringe tip. The insulation coatings at the end of the thermocouple wires are removed and welded together so that the

movement of the fiber does not change the position of thermocouple probe. The other end of the thermocouple wires is connected to a temperature controller to monitor the temperature of the syringe tip as well as the fiber coating. A 1 cm piece of PDMS hollow tubing is soaked in hexane for sufficient swelling and then is placed on the tip of the plunger. After the hexane evaporates, the coating tightly attaches to the plunger tubing. The thickness of the PDMS coating is 178 μm and the volume of extraction phase is about 2.4 μl.

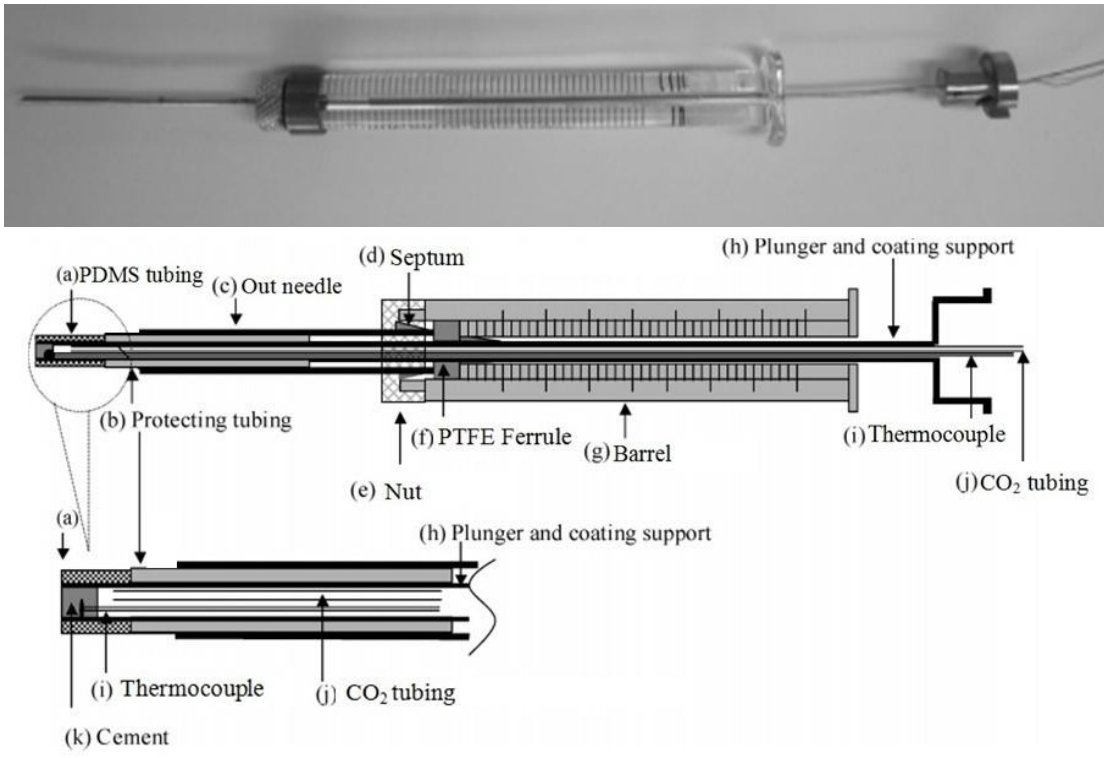

Figure 2-1 Schematic of cold fiber SPME device [62].

CO_2 delivery tubing is made of a 30RW-gauge (O.D. 0.30 mm, and I.D. 0.15 mm) stainless steel tubing and liquid CO_2 is transferred from the cylinder to the internal surface of hollow tubing. In this device, liquid CO_2 comes out from the delivery tubing, evaporates, and turns into CO_2 gas quickly. Thermal energy is absorbed from the surrounding environment during the evaporation,

resulting in cooling of the coating temperature. The coating temperature depends on the flow rate of liquid CO_2, which is controlled by the inner diameter of the delivery tubing. With larger inner diameter tubings, the fiber coating temperature can drop to a lower temperature than that with smaller inner diameter of the tubings. The length of CO_2 tubing will not affect the fiber coating temperature.

The pierce needle of the device is made of a 4.5 cm 18XX-gauge (O.D. 1.27 mm, and I.D. 1.14 mm) stainless steel tubing that the end is beveled to pierce through the sample vial septum and GC injector septum. A manually cut septum is placed between the needle nut and syringe barrel to provide a tight connection.

A 2 cm piece of 19XX-gauge (O.D. 1.08 mm, and I.D. 0.95 mm) stainless steel protection tubing is attached using glue onto the plunger about 2 cm away from syringe tip. The outer diameter of the protection tubing is a little larger than that of the fiber coating, but smaller than the inner diameter of the outer needle so that it will protect the coating when pushing and pulling the syringe from the external needle. The outer needle often strips the coating without using the protection tubing.

After the cold fiber device is installed, a leakage check of the syringe is performed by inserting the syringe into a 10 ml SPME vial containing the mixture solution of methanol-water (20:80, v/v). The vial is heated to higher than 100 ℃ while liquid CO_2 is delivered into the tubing. If no bubbles come out from the syringe tip, the connection is gastight. The connection between the syringe barrel and the needle nut is checked by injecting the outer needle of the device into the GC injector and monitoring the column flow rate.

2.1.2 The automation of cold fiber system

2.1.2.1 Fully automated system with GC

The fiber coating temperature is detected by thermocouples, with one end located inside the fiber coating and the other end connected to a temperature controller. The fiber coating temperature is real-time monitored by the temperature controller with a defined preset value for the coating. A solenoid valve is used to control the delivery of liquid CO_2; its inlet connects to the liquid CO_2 tank and the outlet connects to the CO_2 delivery tubing. When the real temperature of the fiber coating is higher than the preset value, the temperature controller will turn the solenoid valve "open" to deliver the liquid CO_2 to the syringe tip to cool down the fiber coating temperature until it reaches the preset value. The digital line of the solenoid valve is put into the backboard of the temperature controller for the liquid CO_2 delivery control.

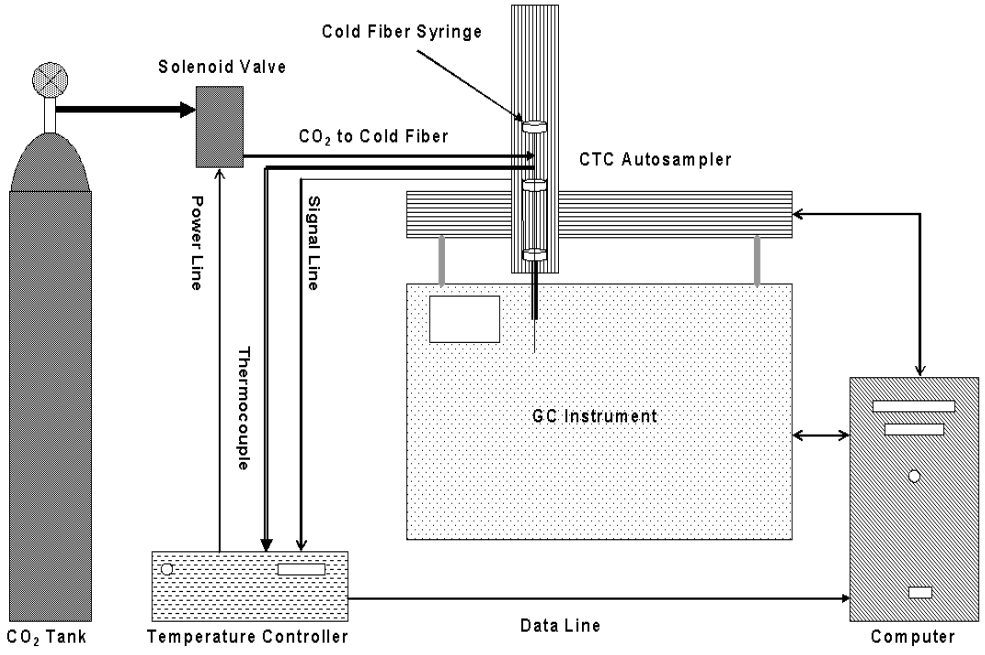

Figure 2-2 Scheme of fully automated cold fiber SPME [61].

The cold fiber SPME system is operated automatically with an autosampler, which is equipped with a 100 µl syringe holder that is suitable for the cold fiber SPME device. A temperature controlled six-vial agitator tray is installed to heat the sample vial at a specific temperature up to 200 ℃. During the extraction, the outer needle of the cold fiber device is not flexible enough for the sample agitation by rotating the agitator tray [62]. However, the high temperature can help the analytes to be released into the headspace, and the temperature gap between the coating and the headspace facilitates the absorption process. The hole of the autosampler needle guide and GC septum nut are enlarged for the outer needle of the device and a liquid injection liner with 2 mm inner diameter is used.

Figure 2-3 Injection liner and modified septum nut of cold fiber device.

At the beginning of an extraction procedure, the autosampler transports the sample vial to the high temperature agitator and exposes the fiber coating to the headspace of the sample for the extraction. After the extraction, the fiber withdraws inside the outer needle and is then automatically transferred to GC injection port for the thermal desorption. After desorption, the

sample vial is transported to the sample tray and the autosampler prepares for the next extraction. The thermal desorption process in a GC injector for the fully automated cold fiber SPME is shown in Figure 2-4.

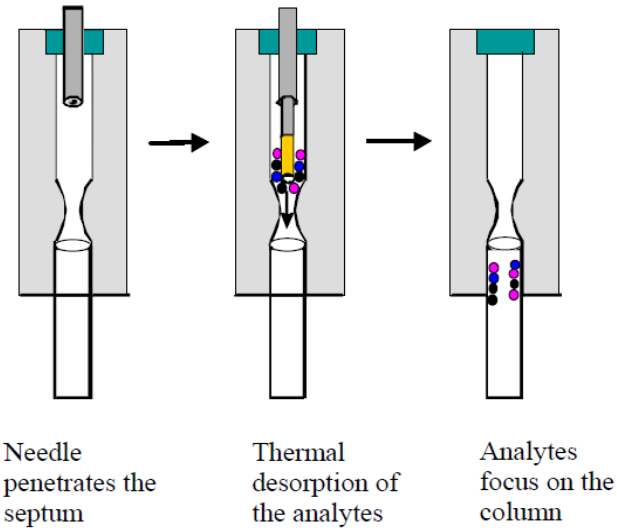

Figure 2-4 Thermal desorption process in a GC injector of the cold fiber SPME fiber [63].

2.1.2.2 The working principle of a solenoid valve

A solenoid valve (shows in Figure 2-5) is an electromechanical valve controlled by an electric current for use with liquid or gas. The flow is switched on or off using a two-way valve. The solenoid and the valve are the two main parts of a solenoid valve. The solenoid converts electrical energy into mechanical energy, which closes or opens the valve mechanically [64]. A direct acting valve has only a small flow circuit, which is in the elastic diaphragm (section E in Figure 2-6). It prevents the fluid from passing through the valve because the fluid pressure is balanced between the input portion and the output portion diaphragm (section A and F in Figure 2-6). This valve multiplies the small flow by using it to direct the flow through a larger orifice. A spring may be used to hold the valve open or closed while the valve is not activated [65].

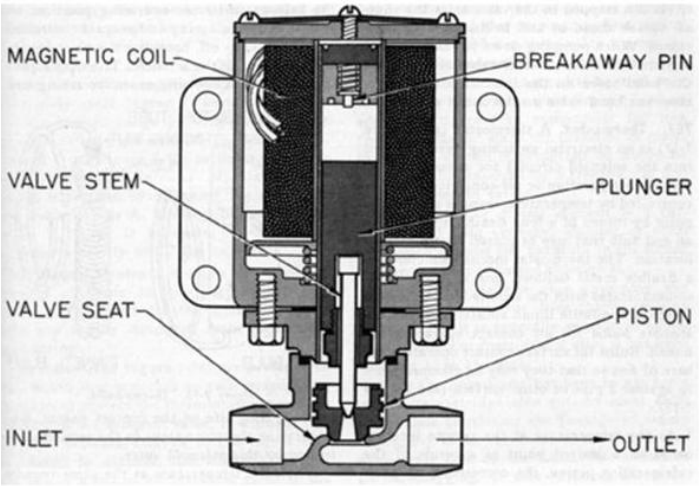

Figure 2-5 Typical diagram of a two-way solenoid valve [64].

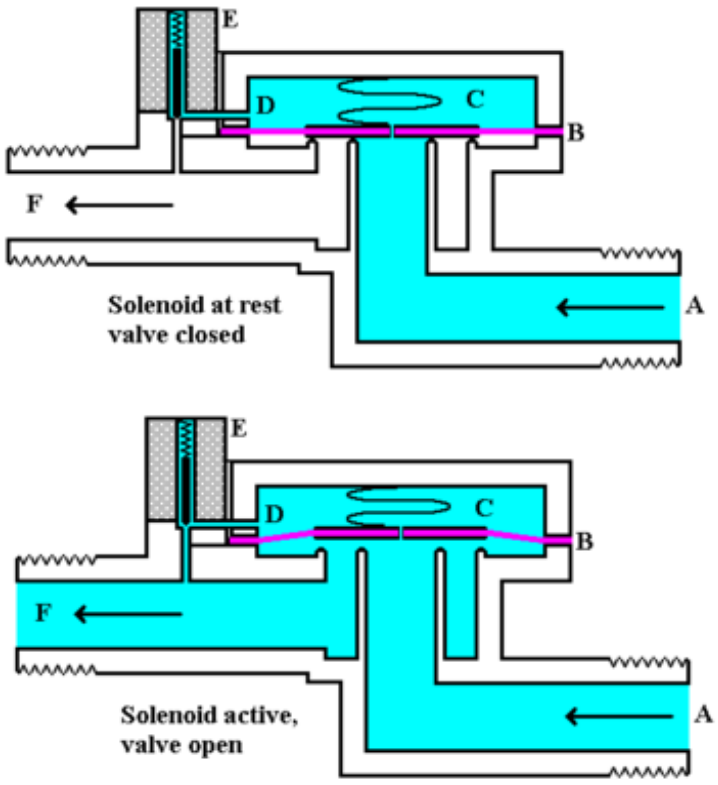

Figure 2-6 Working principle of a solenoid valve. (A- Input side, B- Diaphragm, C- Pressure chamber, D- Pressure relief conduit, E- Solenoid, F- Output side.) [65]

At the top of Figure 2-6 is the valve in its closed state. The gas or liquid enters at A under pressure. B is an elastic diaphragm and there is a weak spring above it pushing it down. The pressure is equal on both sides of the diaphragm and the compressed spring supplies a downward force. Conduit D is blocked by the armature of the solenoid and E is pushed down by a spring. If the solenoid is activated by a constant flow of electrical current, the pin is drawn upwards by magnetic force; the fluid will flow from input side A through the conduit D to output side F. However, if the electrical current through the solenoid coil stops, the spring pushes the diaphragm down again, the pressure between chambers equals, and the main valve closes [65].

2.1.2.3 Vapor pressure in a liquid CO_2 tank

Vapor pressure is the pressure of the vapor in the headspace above its liquid under the thermodynamic equilibrium at a given temperature in a closed system. The pressure inside a cylinder containing liquid CO_2 is determined by the characteristic vapor pressure of the chemical, not the mass of CO_2 in the cylinder.

There are four basic factors that influence vapor pressure: the polarity of the molecules, the surface area of the liquid that is exposed in a cylinder (cylinder diameter), the concentration of the vapor molecules above the liquid, and temperature [66]. Since polar substances have stronger intermolecular forces and the liquid molecules are more easily kept in a liquid state, they have lower vapor pressures at a given temperature. Non-polar molecules like liquid CO_2, on the other hand, have weaker intermolecular forces to keep them in a liquid state [66]. Therefore, vapor pressure of liquid CO_2 is characteristically higher than those of polar molecules.

In the case of a closed liquid CO_2 cylinder under the equilibrium, everything else is fixed, so temperature is the only factor that controls the CO_2 vapor pressure, which means temperature

controls the pressure inside the tank. As long as the liquid CO_2 cylinder is at a constant temperature (such as room temperature) and under normal operation circumstances, the vapor pressure is constant as well.

Increase in the temperature of the liquid CO_2 tank can increase the average kinetic energy and the liquid CO_2 will be able to overcome the intermolecular forces and will become vapor. The relationship between the temperature and the vapor pressure is defined by the Clausius-Clapyron Equation [67]:

$$P = A\ exp(\frac{-\Delta H_{vap}}{RT}) \qquad \text{Equation 2-1}$$

Where R is the universal gas law constant (= 8.314 J mol^{-1} K^{-1}), A is the gas constant, and ΔH_{vap} is the enthalpy of vaporization. If P_1 and P_2 are the pressures and T_1 and T_2 are their temperatures, the equation has the form:

$$In\left(\frac{P_2}{P_1}\right) = \left(\frac{\Delta H_{vap}}{R}\right)\left(\frac{1}{T_2} - \frac{1}{T_1}\right) \qquad \text{Equation 2-2}$$

If the vapor pressure and the enthalpy of vaporization are known to be at a certain temperature, the Clausius-Clapeyron equation can estimate the vapor pressure at another temperature.

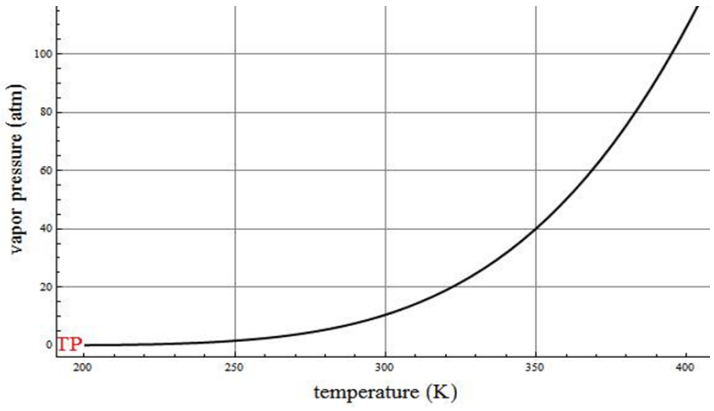

Figure 2-7 The Clausius-Clapeyron relationship between temperature and vapor pressure [67].

2.2 Improvement and evaluation of traditional cold fiber system

2.2.1 Improvement of solenoid valve body temperature control

In the traditional cold fiber system with a solenoid valve, the body temperature of the valve increases after working for a long time since the solenoid coil produces extra heat while applying the electric current to keep the solenoid valve open. The high solenoid coil temperature reduces the sensitivity of the spring coil to open and close the valve. Therefore, the delivery of liquid CO_2 passing through the valve is influenced by this heat effect, resulting in less accuracy in the coating temperature control. In order to reduce valve body and solenoid coil temperature, dry ice is added around the solenoid valve, which cools down the solenoid valve system temperature. The drawback of this strategy is that the solenoid valve body temperature cannot easily be controlled near room temperature, and the coating temperature always drops much lower than its preset value. A new strategy to cool down the solenoid temperature was to install a fan for the solenoid valve, which kept the body temperature neither too high nor too low. Figure 2-8 shows the comparison of valve body temperature at an “extreme” working condition with and without the fan. The electrical current was applied to the solenoid coil and the valve was kept open all the time during the test.

At beginning of the test, the body temperatures for the two strategies were close to each other and the temperatures gradually increased with a longer working time. The valve body temperature without the fan increased faster than with the fan. After 10 min continuous working with the electric current was applied, the increase rate of solenoid body temperature with the fan was 30% slower than that without the fan. Therefore, installing a fan can effectively slow down the increase of solenoid body temperature.

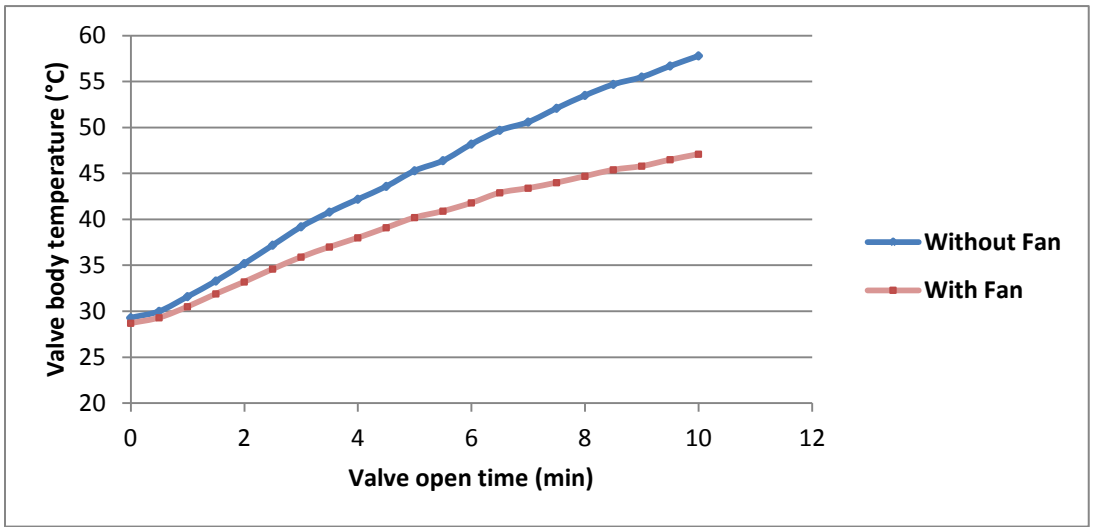

Figure 2-8 Comparison of valve body temperature with and without the fan (the electrical current was applied to the solenoid coil and the valve was kept open during the test).

Figure 2-8 illustrates an extreme working condition in which the electric current was applied to the solenoid and the value produces extra heat the whole time. Under normal working conditions, the valve switched between *open* and *closed* according to the coating temperature. Since extra heat was only produced when the value was open, the temperature of the valve body was much lower when it was actually working. Table 2-1 monitors the valve body temperature in a real working process. After working for 45 min, the valve body temperature can stay around 45 ℃, which promises good sensitivity for the coil spring to control the liquid CO_2 delivery.

Table 2-1 Valve body temperature under normal working conditions (T_s = 180 ℃ T_f = 30 ℃).

Working time	Valve body temperature (℃)
2 min	27.7
5 min	33.4
15 min	42.2
30 min	44.4
45 min	45.8
60 min	48.2

2.2.2 Coating temperature fluctuation under different conditions

In a cold fiber SPME system, the fiber coating should be kept at a low temperature while it is exposed to a hot headspace. In a real extraction process, there is a fluctuation zone for the coating temperature around its preset value. In order to obtain more stable extraction results, the coating temperature fluctuation should be controlled as little as possible. There are several factors that influence the fluctuation. These include the solenoid valve body temperature, which was discussed in the last section; The position of the thermocouple wires inside the hollow fiber, which is very important for the coating temperature control of the system; As well as the temperature gradient at the different positions from the coating to the headspace.

2.2.2.1 Coating temperature fluctuation with thermocouple probe at different position

In section 2.1, the design of the cold fiber has been introduced. One end of the thermocouple wires connects to a temperature controller in order to monitor temperature and the other end is put inside at the tip of the syringe fiber. This end of the thermocouple wires is welded together with the seal cement to make sure the movement of the fiber does not change the position of the thermocouple probe. However, under some circumstances, the thermocouple probe is not located at the syringe tip due to careless operation in syringe tip sealing and the transportation process.

Figure 2-9 compares the coating temperature fluctuation with thermocouple probe at two positions: one was at the tip of the syringe tubing and the other one was located about 1 cm away from the tip. Sample temperature (T_s) and coating temperature (T_f) were set at 120 ℃ and at 30 ℃, respectively. After exposing the fiber coating to the hot headspace, it took around 20 seconds to cool down to the preset coating temperature at both positions. The frequencies to switch the solenoid valve between *open* and *closed* were different at different probe locations. When the

thermocouple probe was located at the tip of syringe, the temperature fluctuation range was 30 ± 4 ℃, which was in a reasonable fluctuation range. The temperature fluctuation range was much larger when the probe was put 1 cm away from the syringe tip. Therefore, the thermocouple probe should be located at the tip of the syringe for a constant coating temperature fluctuation range.

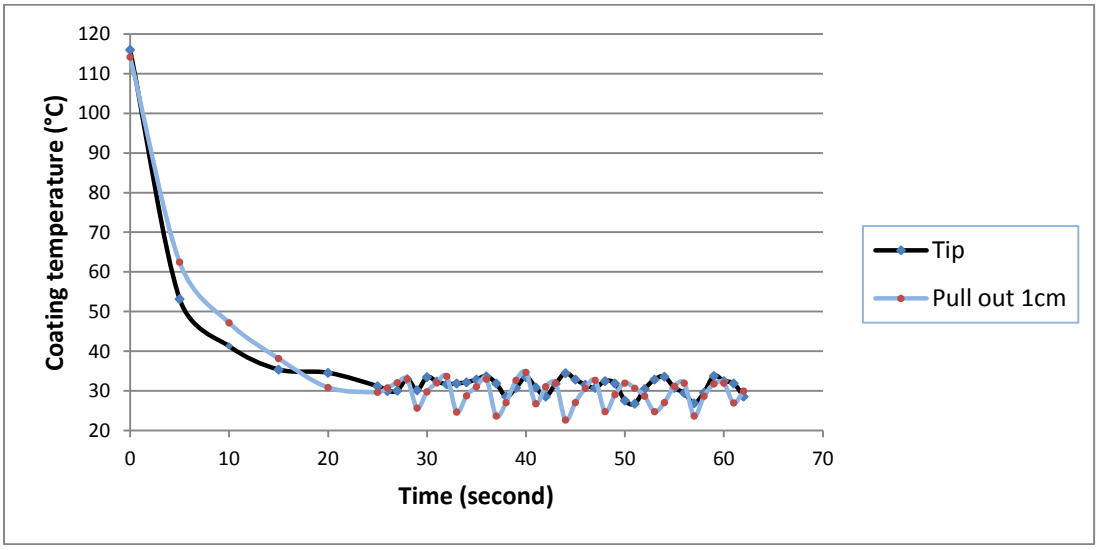

Figure 2-9 Monitoring of coating temperature with the thermocouple probe at different positions (T_s = 120 ℃, T_f = 30 ℃).

2.2.2.2 Temperature gradient at the different positions from coating to headspace.

In a headspace cold fiber SPME system, the sample, as well as the headspace, is in a high temperature environment, while the coating temperature is very low. After the fiber coating is exposed to the headspace for extraction, there is a temperature gradient from the core of the coating to the headspace. Investigating the temperature gradient is essential for studying the partition of the analytes between the extraction phase and the headspace. In this section, several test points from A to E have been investigated as showed in Figure 2-10.

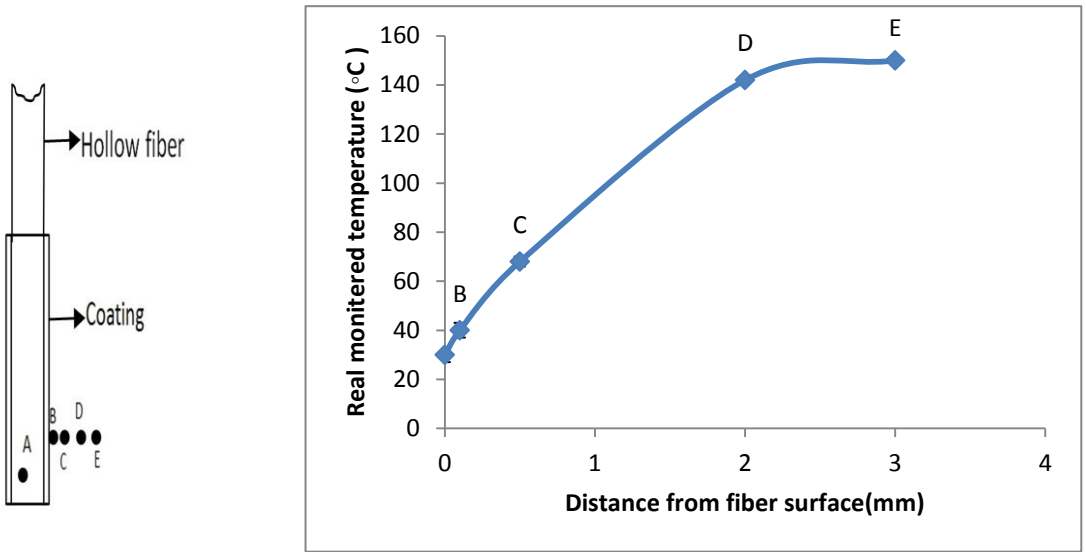

Figure 2-10 The distribution of the test points (left) and temperature gradient (right) from the fiber coating to the headspace. (A: Inside tubing, B: Coating surface, C: 0.5 mm away from coating, D: 2 mm away from coating, E: 3 mm away from coating, T_s = 180 ℃, T_f = 30 ℃)

The sample and coating temperatures were set at 180 ℃ and 30 ℃, respectively. Point A in Figure 2-10 was the probe of the thermocouples located inside the syringe tip, with a temperature around 30 ℃. The temperature at points B and C were tested by twisting the probe of thermocouples outside the coating surface tightly and loosely respectively. The temperature at point B can be considered as the coating surface temperature, which was around 40 ℃. Since the PDMS hollow coating is a unity, no test point was applicable in the extraction phase. However, the temperature distribution in the PDMS coating can be estimated by the test results from A to B, which was between 30 ℃ and 40 ℃. Temperature can achieve to 140 ℃ only 2 mm away from the coating surface to the headspace.

2.2.3 System evaluation

After the cold fiber system has been improved by minimizing the fluctuation range of coating temperature problems, system performance is evaluated by investigating the extraction of polycyclic aromatic hydrocarbons (PAHs). The evaluation includes coating temperature fluctuation, water content effect, system precision, and the temperature and time profiles for PAHs.

2.2.3.1 Chemicals and instrumental

PAHs (naphthalene, acenaphthylene, acenaphthene, fluorene, phenanthrene, anthracene, fluoranthene, pyrene, benzo(b)fluoranthene, and benzo(a)pyrene) were purchased from Supelco (Oakville, ON, Canada). Methanol (HPLC grade) was purchased from BDH (Toronto, ON, Canada). Helium (99.9%), nitrogen (99.9%), and compressed air were supplied by Praxair (Kitchener, ON, Canada) for GC. The SPME fiber used in all experiments was 1 cm PDMS hollow tubing with a thickness of 178 μm from Dow Corning (Midland, MI, USA).

Gas chromatography was performed on Varian 3800 equipped with flame ionization detection (FID) and a CTC Combi PAL autosampler (Zwingen, Switzerland). SLB-1 capillary column (30 m, 0.25 mm i.d., 0.25 μm film thickness) was purchased from Supelco. Helium was the carrier gas with a flow rate of 1 ml/min. Temperature for injector and detector were 250 ℃ and 300 ℃. For the analysis of PAHs, column temperature was maintained at 40 ℃ for 1 minutes, and then increased at a rate of 4 ℃/min to 204 ℃, 10 ℃/min to 250 ℃.

The stock standard solution of PAHs (100 mg/l) was prepared in methanol. 1 μl of the standard solution was spiked into 10 ml empty vials for the experiments of coating temperature

fluctuation, water content effect, and system precision. 1 μl of the standard solution was spiked into 10 ml vial loaded 1 g sand for the extraction temperature and time profiles tests for PAHs.

2.2.3.2 Evaluation of coating temperature fluctuation with different sample temperatures

Coating temperature fluctuation has been minimized by cooling the solenoid valve body temperature and precisely location of the thermocouple probe. The evaluation of the coating temperature fluctuation was performed with different sample temperatures from 80 ℃ to 200 ℃ and the coating temperature was between -10 ℃ and 40 ℃.

Table 2-2 illustrates the coating temperature fluctuation ranges at different sample temperatures. Coating temperature at 30 ℃ was taken as an example for discussion. With a lower sample temperature, the coating can easily drop to less than 30 ℃, and the temperature fluctuation range was slightly larger than those at higher sample temperatures. For higher sample temperatures, after the coating temperature reached higher than 30 ℃, it took more time to cool down, resulting in a larger fluctuation range. The fluctuation range of the coating temperature was ± 3 ℃ around the preset value for most tests in Table 2-2. Therefore, the coating temperature can be considered relatively constant in this system.

Table 2-2 Coating temperature fluctuation ranges with different sample temperatures.

T_s(℃)	T_f= -10(℃)	T_f = 0(℃)	T_f = 10(℃)	T_f = 20(℃)	T_f = 30(℃)	T_f = 40(℃)
80	-12.7~-7.0	-1.4~-2.6	8.7~11.8	15.4~23.2	**25.1~32.8**	-
100	-12.9~ -6.1	-3.8~3.2	8.8~13.1	17.8~23.5	**27.0~33.2**	-
120	-13.5~-6.0	-2.8~4.1	8.4~13.6	17.9~23.5	**27.8~32.7**	-
150	-	-2.1~4.2	7.9-14.6	18.7~23.6	**27.9~33.4**	37.5~43.7
180	-	-0.9~7.0	9.8~16.1	17.1~24.1	**28.3~34.5**	37.7~44.4
200	-	-2.9~8.4	9.4~16.9	18.6~24.2	**28.4~34.7**	37.5~44.8

2.2.3.3 The influence of water content on extraction

If water exists in the sample vial, when the temperature of the sample is higher than 100 ℃, the vapor pressure of water increases; as a result, more water molecules are present in the headspace. Since water has a high heat capacity, the presence of high water content can dramatically increase the difficulty in cooling down the coating temperature. This section studies the effect of water content in the cold fiber system.

To investigate the influence of water content levels, different amounts of water (0, 10, 20, 50 µl) were added into 10 ml empty vials. The coating temperature was monitored for the extraction of the spiked PAHs from empty vials with sample temperature was at 180 ℃. For no addition and 10 µl addition of water in the sample vial, the coating temperature could drop to lower than 30 ℃. But when more water was present in the system, the coating temperature was more difficult to cool because of the high heat capacity of water. The coating temperature can only drop to 60 ℃ and 100 ℃ after adding 20 and 50 µl water respectively.

With a high water content presence in the headspace, there is a risk that water molecules may cover the coating layer and influence the extraction efficiency of target analytes. PAHs standard solution was spiked in empty vials and different water content were loaded. 1 µl of the solution was spiked into 10 ml empty vials loaded with 0, 10, 20 µl water. In order to eliminate the extraction difference caused by different coating temperatures, the coating temperature was fixed to 60 ℃ for all levels of water added. After extraction at 180 ℃ for 10 min, the fiber was transferred to a GC injector for desorption at 250 ℃.

Figure 2-11 is the comparison the recoveries of PAHs with loaded different amounts of water. The recoveries for different compounds will not be discussed in this section since the extraction condition was not optimized. The comparison of recoveries with different water content for same

compound needs to be analyzed. Ten PAHs in Figure 2-11 are arranged by their molecular weight, from light to heavy. For the first five compounds with high volatility, the recoveries without water were slightly higher than that with water in the sample. For those compounds, the distribution coefficients are smaller than the other five compounds, so the existence of water influences the partition of the compounds with the coating. For the other five semi-volatile compounds, no significant differences in the recoveries were observed. Overall, water content did not show much effect on the extraction efficiency for any of the ten compounds investigated.

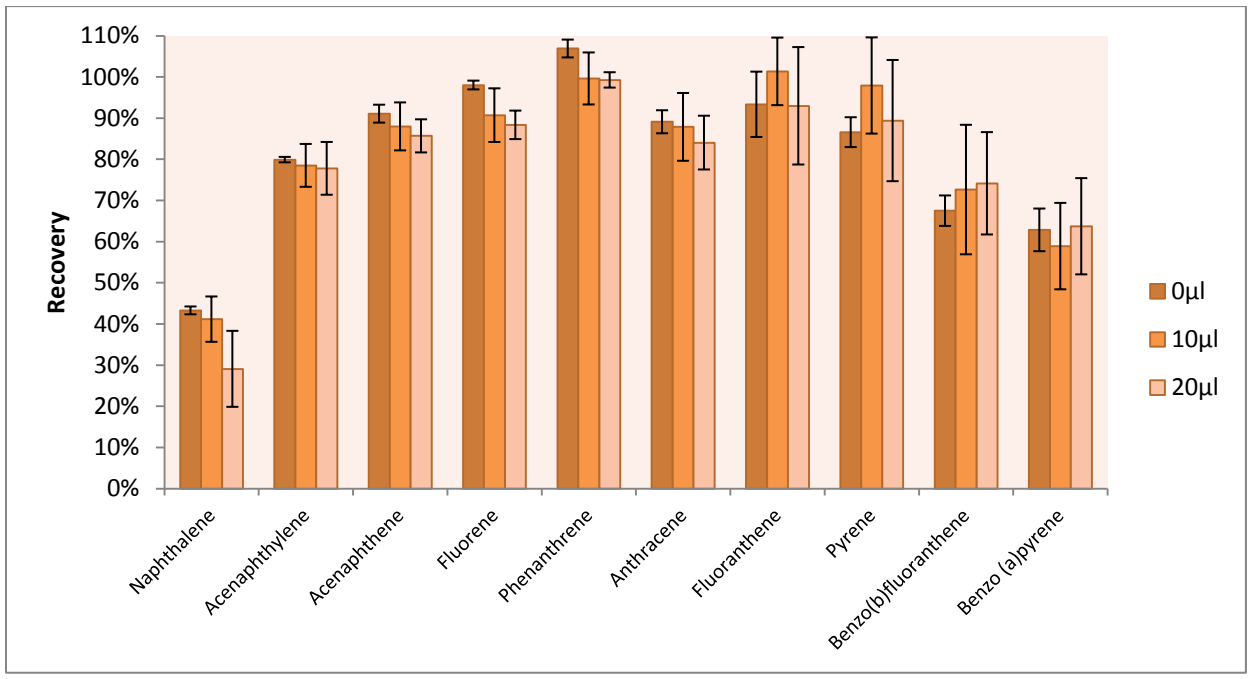

Figure 2-11 Extraction of PAHs with different amounts of water loaded in empty vials (T_s = 180 ℃, T_f = 60 ℃, t =10 min).

It was observed that the error bar range after adding water into the sample was much larger than that without water in the sample. Water existing in the sample may have a strong interference with the coating temperature fluctuation. The water content should be made smaller for the lower and more stable coating temperature.

2.2.3.4 Evaluation of system precision

The coating temperature fluctuation is considered constant, which has been discussed in the previous section. This section studies the system precision for the extraction of PAHs with a coating temperature fluctuation range within ± 3 ℃. The test samples were spiked by adding 1 µl of the spiking solution (100 mg/ml) into 10 ml empty vials. The samples were spiked 30 min before analyzing. The sample temperature and coating temperature were 150 ℃ and 30 ℃. The extraction time was 15 min, and desorption was at 250 ℃ for 1 min in GC injector. Six samples with exactly the same operation procedure were compared.

The peak area integration and relative standard division (RSD) are listed in Table 2-3. For all seven compounds analyzed, except anthracene with a RSD of 3.55%, the values of RSD for other analytes were lower than 2%. This can be explained that in a cold fiber system during the extraction, sample temperature, extraction time, desorption temperature and time can be precisely controlled by the autosampler system; the coating temperature fluctuation is in a small range as well. Therefore, it is reasonable to have good precision for extraction with the cold fiber SPME system, which can be considered a reliable extraction strategy with good stability.

Table 2-3 Peak area and RSD for PAHs extracted from spiked samples (n = 6).

	Naphthalene	Acenaphthylene	Acenaphthene	Fluorene	Anthracene	Fluoranthene	Pyrene
Run_1	749507	928128	948128	962731	877961	898058	827418
Run_2	770982	912204	961226	969948	859756	925867	855309
Run_3	752630	904220	950455	942869	831034	925839	855376
Run_4	771480	901293	954589	943360	810168	910685	856795
Run_5	749575	887801	931703	931650	823922	900646	844332
Run_6	756005	915131	975765	967937	883583	935192	869413
Average	758363	908130	953644	953083	847737	916048	851441
RSD (%)	**1.54**	**1.32**	**0.60**	**1.44**	**3.55**	**1.47**	**1.46**

2.2.3.5 Evaluation of extraction temperature and time profiles for PAHs

In the cold fiber SPME system, the extraction parameters can be precisely controlled, which provides good stability in the extraction. The system evaluation with extraction temperature profiles and extraction time profiles are studied this section with PAHs.

2.2.3.5.1 Evaluation of extraction temperature profiles for PAHs

For the evaluation of the system with extraction temperature profiles, the sample temperature was set from 80 ℃ to 200 ℃, while with coating temperature was fixed to 30 ℃ for all extractions. The test samples were spiked by adding 1 µl of the spiking solution (100 mg/ml) into 10 ml vials loaded 1 g sand. The samples were spiked 15 min before analyzing. The extraction time was 30 min, and desorption was at 250 ℃ for 5 min in GC injector.

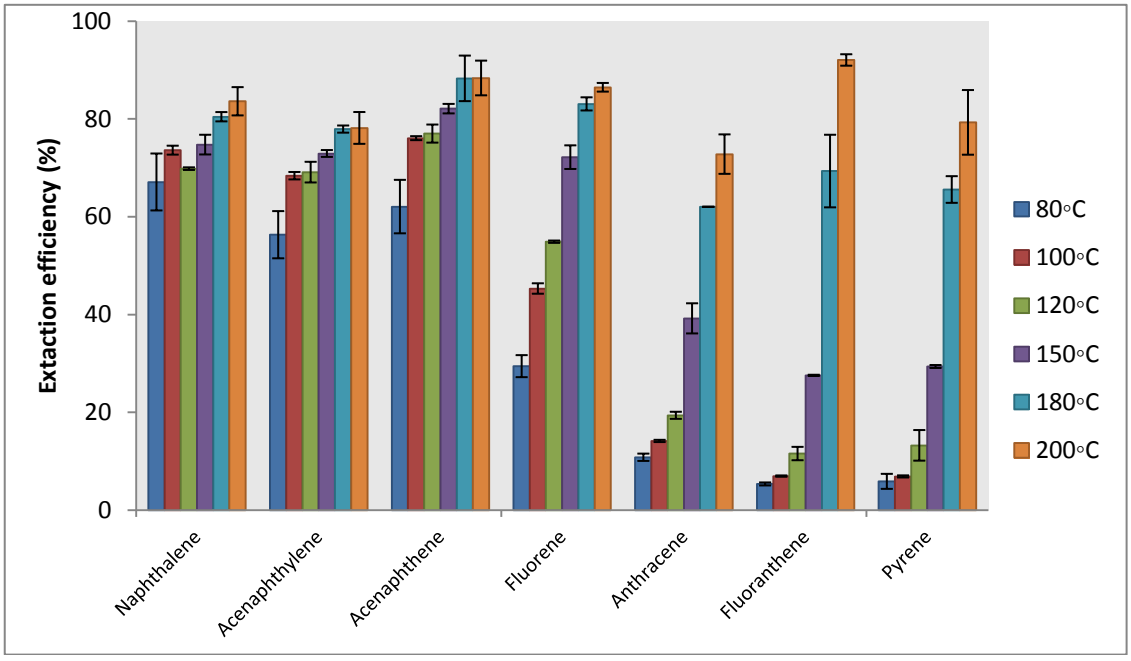

Figure 2-12 The extraction temperature profiles for PAHs from freshly spiked sand samples (T_f = 30 ℃, t = 30min).

The extraction efficiency was calculated by dividing the amount of analytes extracted by the coating with the total amount of analytes originally present in the sample and multiplying this result by 100 to convert it into a percentage. Figure 2-12 shows that almost all PAHs' extraction efficiency kept increasing with the elevated temperatures, but to a different extent for each one.

For the more volatile compounds such as naphthalene, acenaphthylene and acenaphthene, the increase of the extraction amount from 80 ℃ to 100 ℃ was very obvious, and similar to the total increase of amount between 100 ℃ and 200 ℃. The extraction efficiency did not show a rise with the sample at 180 ℃ and higher.

For those semi-volatile compounds, with the increase of extraction temperature, extraction efficiency of all PAHs kept increasing dramatically. Especially in the case of fluoranthene, the recovery could reach higher than 90% at 200 ℃, which was only 5% at 80 ℃. This is an example of the advantage of cold fiber SPME for the extraction of semi-volatile compounds. The increasing rates of the extracted amounts for the anthracene, fluoranthene and pyrene were more significant at temperatures between 150 and 200 ℃ than that from 100 to 150 ℃. Extraction at higher temperatures would help the semi-volatile compounds release from the matrix.

2.2.3.5.2 Evaluation of extraction time profiles for PAHs

For the system evaluation with extraction time profiles, the extraction time varied from 2 min to 120 min while the sample temperature and the coating temperature was fixed at 180 ℃ and 30 ℃. The test samples were spiked by adding 1 μl of the spiking solution (100 mg/ml) into 10 ml vials loaded 1 g sand. The samples were spiked 15 min before analyzing. Desorption conditions were the same as that in previous section. The extraction efficiency was calculated by dividing the amount of analytes extracted by the coating with the total amount of analyte originally present in

the sample and multiplying this result by 100 to convert it into a percentage. The extraction result was split into two parts according to the volatility of PAHs in Figure 2-13.

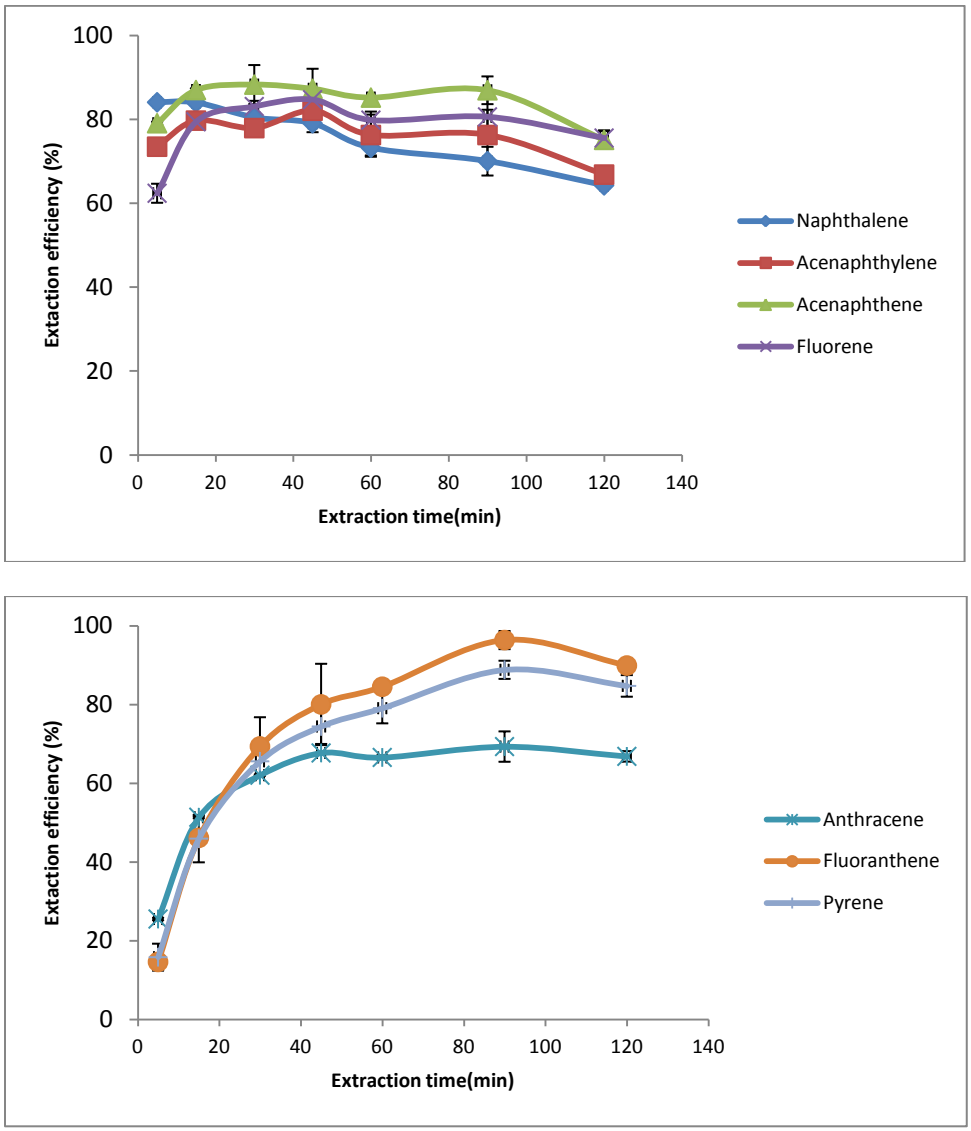

Figure 2-13 The extraction time profiles for PAHs from freshly spiked sand samples (T_s = 180 ℃, T_f = 30 ℃).

For naphthalene, acenaphthylene, the extraction amount was not sensitive during the extraction process with different extraction time, which remained around 80% consistently. For the acenaphthene and fluorene, equilibriums were achieved after extraction for 15 min. With the increase of extraction time, the extraction amounts of semi-volatile compounds kept increasing.

The equilibrium time was 45 min for Anthracene and around 90 min for fluoranthene and pyrene. The extraction amounts did not increase with longer extraction time after the equilibrium.

2.3 Cold fiber system without the solenoid valve

2.3.1 Introduction

The solenoid is an important component in the traditional cold fiber system to control the delivery of liquid CO_2 from the CO_2 tank to the fiber coating. However, using the solenoid valve may enhance the risk of coating temperature fluctuation, as well as adding to the complexity and cost of the system. A simplified cold fiber system without the solenoid was modified as shown in Figure 2-14 that connecting CO_2 delivery tubing directly to the tank valve by a stainless steel connector. Graphite ferrules with different inner diameter were applied to make sure there was no leakage at the joint for the different sizes of tubing. Thermocouples were connected to a temperature controller to monitor the fiber temperature. A heating plate with the proper position for the sample vial was applied to provide the heating source of the sample during the extraction.

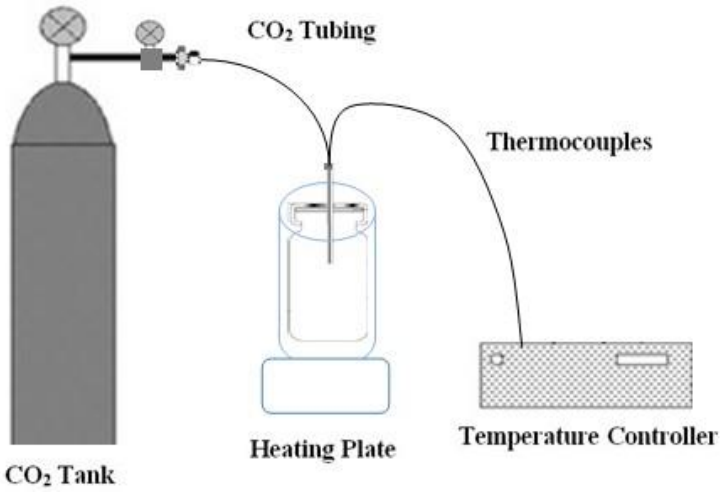

Figure 2-14 Scheme of modified cold fiber system without the solenoid valve.

In this simplified system, the switches of liquid CO_2 supply *on* and *off* the must be operated manually. After turning on the valve of the liquid CO_2 tank, fiber temperature starts to cool down and then is kept constant after the equilibrium is reached. In a liquid CO_2 tank, temperature is the only parameter that influences the vapor pressure above the liquid CO_2. Since the temperature of the tank is always the same as room temperature, the vapor pressure of CO_2 is constant under normal operation circumstance. As a result, the flow rate of liquid CO_2 in the same size delivery tubing is constant as well. In this system, the sample temperature is fixed, and the flow rate of the liquid CO_2 is constant, resulting in constant fiber temperature under equilibrium.

2.3.2 Comparison of the delivery efficiency of liquid CO_2 with different size tubings

Since the vapor pressure of liquid CO_2 is constant in a closed tank, CO_2 delivery tubing with larger inner diameter has stronger delivery efficiency. The cooling effect of different sizes of CO_2 delivery tubings is compared in this section. Table 2-4 shows the outer diameter and inner diameter of different tubings and Figure 2-15 show the fiber temperature trends for four delivery tubings with different sample temperatures.

Table 2-4 Outer diameter and inner diameter of different tubings.

Tubing	Outer diameter	Inner diameter
30RW	0.0012"+0.0005/-0	0.006" +0.001/-.0005
33RW	0.008"+0.0005/-0	0.004" +0.001/-.0005
34RW	0.007"+0.0005/-0	0.003"+0.001/-.0005
35RW	0.005"+0.0005/-0	0.002"+0.001/-.0005

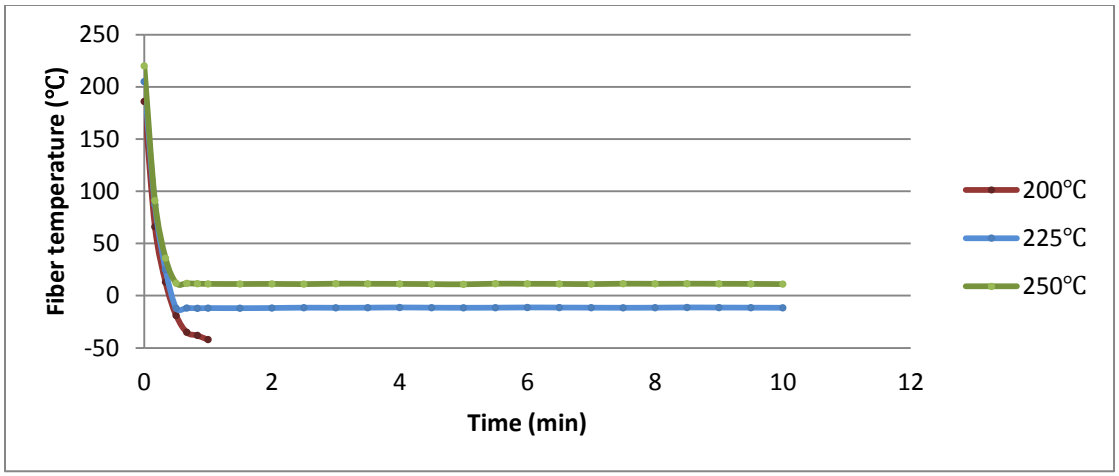

Figure 2-15(a) Fiber temperature trend for 30RW tubing with sample temperature at 200, 225 and 250 ℃.

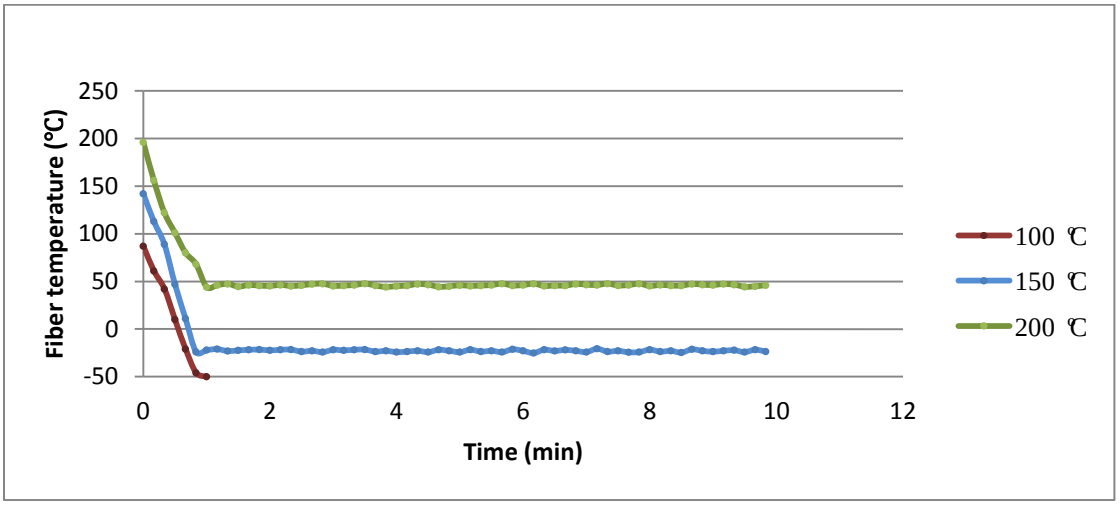

Figure 2-15(b) Fiber temperature trend for 33RW tubing with sample temperature at 100, 150 and 200 ℃.

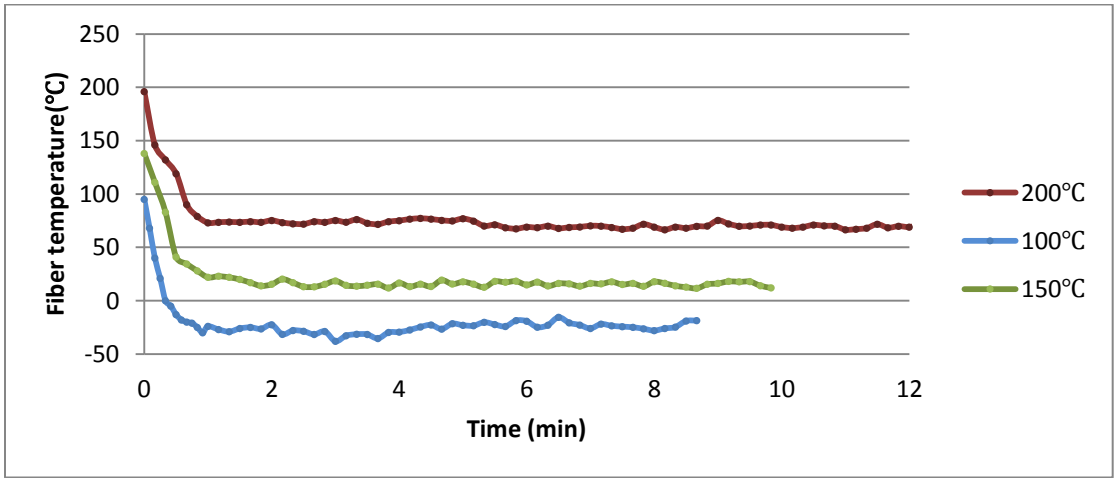

Figure 2-15(c) Fiber temperature trend for 34RW tubing with sample temperature at 100, 150 and 200 ℃.

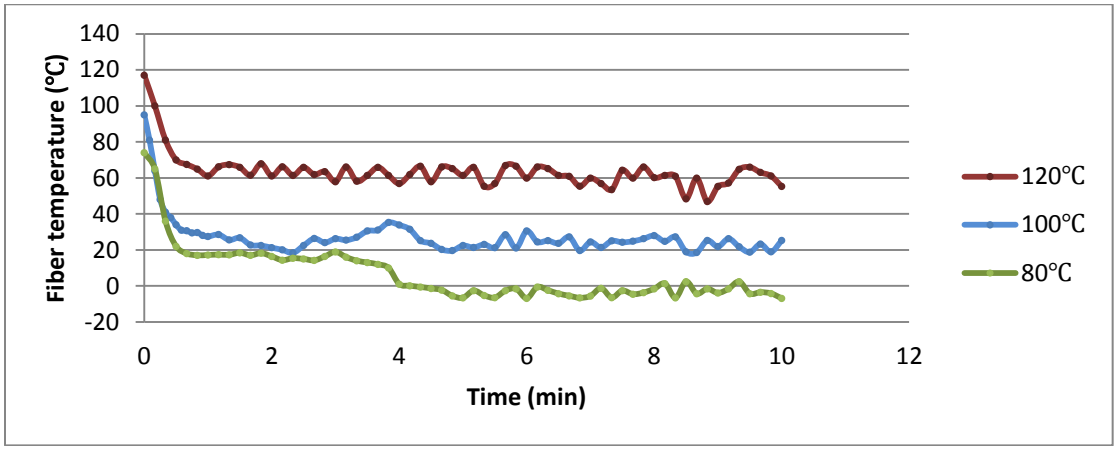

Figure 2-15(d) Fiber temperature trend for 35RW tubing with sample temperature at 80,100 and 120 ℃.

After analyzing the fiber temperature trends for four different sizes of tubings in Figure 2-15, it is easy to find that tubings with a large inner diameter have strong delivery efficiency, so the fiber temperature can drop to very low. For some of those large tubings, if the equilibrium temperatures are lower than -50 ℃, frosting will appear at the tubing end. The fluctuations of fiber temperature in small tubings are much more significant than that in large tubings: ±0.5 ℃ for 30RW tubing, ±2 ℃ for 33RW tubing, ±4 ℃ for 34RW tubing, and ±6 ℃ for 35RW tubing.

Figure 2-16 summaries the fiber temperature fluctuation ranges after equilibrium for different sizes of tubings under various sample temperatures. In the selection of liquid CO_2 delivery tubings, larger tubing is preferred because of their strong delivery efficiency and good stability, but the sample temperature must be very high to avoid frosting. A smaller size of tubing like 34RW, on the other hand, has more applications since the fiber temperatures are widely distributed when the sample temperatures are less than 200 ℃.

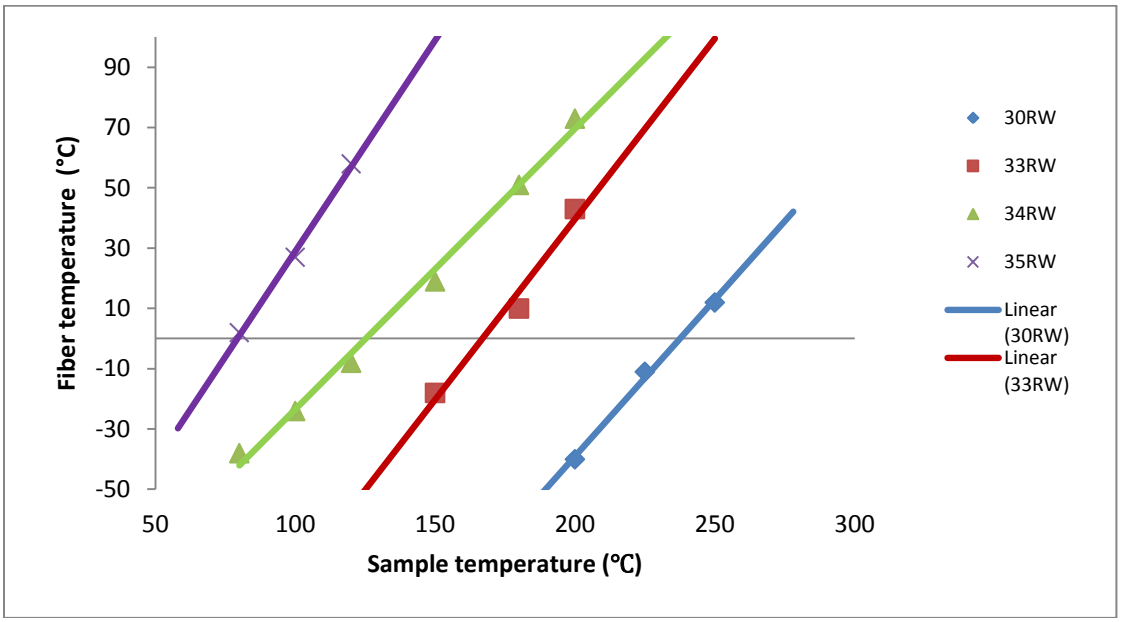

Table 2-16 Distribution of fiber temperatures after equilibrium under various sample temperatures for different tubings.

2.3.3 Evaluation of the robustness of CO_2 delivery tubings in terms of balanced fiber temperature

For the same delivery tubing, the fiber temperature should be constant under equilibrium. In order to study the distribution of balanced temperatures for different tubings with the same size, six 33RW tubings were compared with a sample temperature of 200 ℃. In Figure 2-17, 1-6 in the x axis represent six different tubings, and test 1, test 2, and test 3 are independent of each other. This means that for those three tests, firstly the tubings were cut from the liquid CO_2 cylinder and the cold fiber device, and then were connected with the liquid CO_2 cylinder and cold fiber device before the start of the test. If the tubing is connecting to the liquid CO_2 cylinder and cold fiber device the whole time, the balanced fiber temperatures are very close to each other with the same tubing and the fluctuation is in the range of ± 2 ℃, which is the same result in the previous section. For the tests with different tubings and independent tests, there is a distribution

range in ±5 ℃ around 50 ℃ for the balanced fiber temperature according to the results in Figure 2-17. This is understandable because in this system some factors may affect liquid CO_2 delivery. These factors include the length of delivery tubing, the length of CO_2 tubing inserted into the cylinder connector, and the distance of the tubing end and the syringe tip. These factors are discussed in following sections.

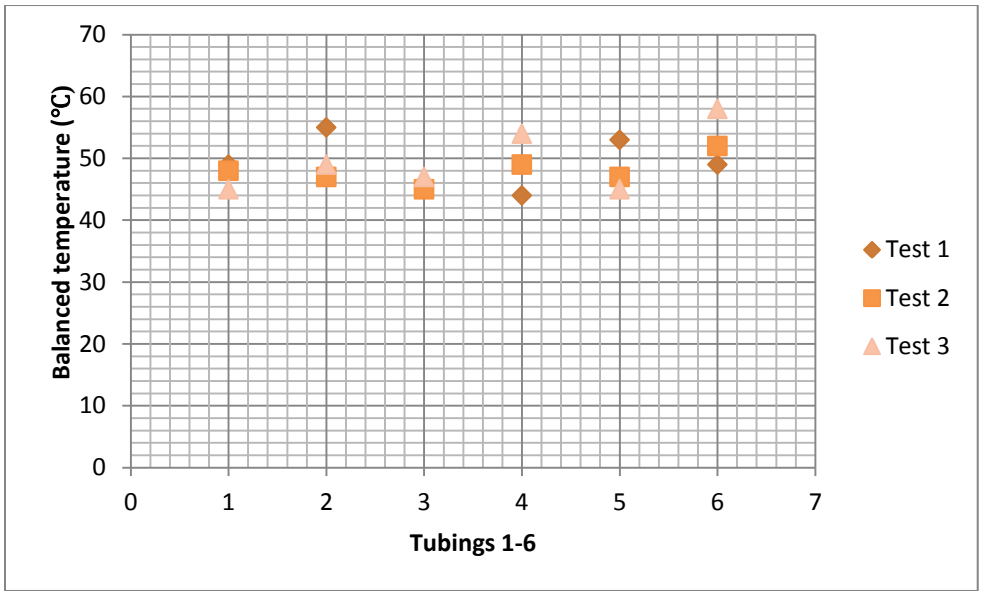

Figure 2-17 Comparison of the balanced temperature for six same size CO_2 delivery tubings with three independent tests (33RW tubing with sample temperature at 200 ℃).

2.3.3.1 Investigation of the influence of the length of CO_2 delivery tubing to balanced fiber temperature

In the last section, there was a large distribution range of independent tests for the same size of tubing. The length of liquid CO_2 delivery tubing may have effects on the cooling process. Two 33RW tubings were studied with sample temperature was at 200 ℃. The original length of both tubings was 165 cm, and 10 cm of the tubings were cut off each time before testing. Seven data points from 165-105 cm were applicable since 105 cm was the shortest tubing length that could

be used in this system. The balanced fiber temperatures for Tubing A and Tubing B are shown in Figure 2-18.

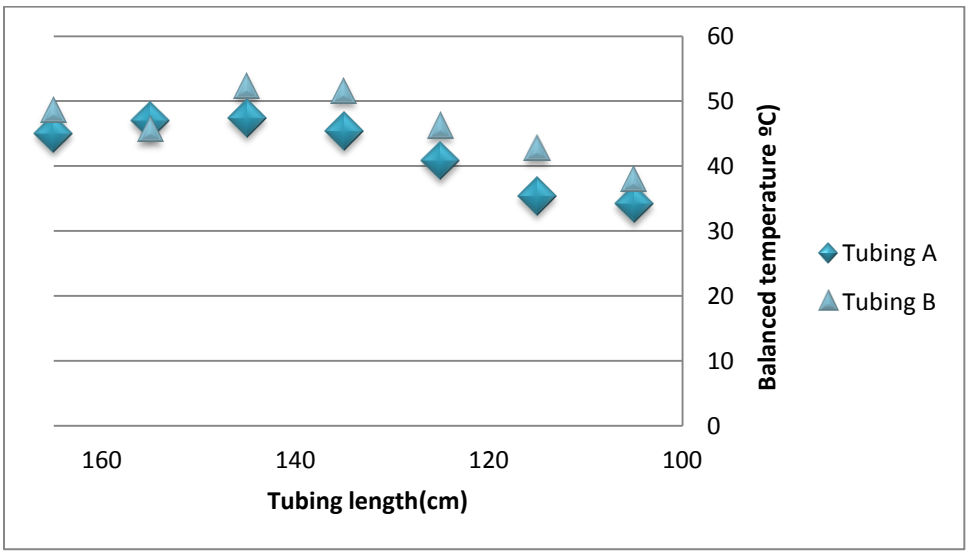

Figure 2-18 Comparison of the balanced temperatures for different CO_2 delivery tubing lengths (33RW tubings with sample temperature at 200 ℃).

For both tubings, the balanced temperatures were relatively constant for the tubing lengths were from 165 to 135 cm, with the fluctuation range within 5 ℃. The balanced fiber temperature started to decrease when the tubings were shorter than 125 cm. Since the tubings were with a length of 160 ± 5 cm from the supplier, under a normal operation without cutting the tubing, the fiber temperature will not be influenced by the slight difference of the tubing lengths.

2.3.3.2 Investigation of the influence of the length of CO_2 delivery tubing inserted into cylinder connector

In this simplified system, one end of liquid CO_2 delivery tubing is directly connected to the valve of the cylinder by a stainless steel connector. The effects of different lengths of delivery tubing inserted into the connecter on the cooling process are investigated in this study. Two 34RW tubings were studied with a sample temperature of 200 ℃. The lengths of the delivery tubings

inserted into the connecter were 5 cm, 4 cm and 3 cm. In Table 2-5, test 1 and test 2 were independent of each other; meaning that for those two tests, tubings were firstly cut from the liquid CO_2 cylinder and cold fiber device, and then were connected with the liquid CO_2 cylinder and cold fiber device before the start of the test.

Table 2-5 Comparison of the balanced temperature for different lengths of CO_2 delivery tubing inserted into the connector (34RW tubings when sample temperature was at 200 ℃).

	Balanced fiber temperature (℃)			
Tubing size	Insert length	5cm	4cm	3cm
34RW_C	Test1	85.0	85.2	86.7
	Test2	87.4	88.7	88.1
34RW_D	Test1	90.2	91.3	90.7
	Test2	91.4	90.0	92.1

The balanced fiber temperatures with the tubing insert lengths from 5 to 3cm fluctuated within 3 ℃ for tubing C and within 2 ℃ for tubing D. According to Table 2-5, the fiber temperature was not influenced by the insert length of tubing into the connector. It was observed that the balanced fiber temperature was 5 ℃ higher for tubing D in all tests than that for Tubing C. This can be explained in that some tubings may have been squeezed by an unknown external force and the inner diameter was slightly smaller than its original size, which could influence the delivery efficiency for liquid CO_2. Overall, the balanced temperatures of the same size of tubings were close to one another.

2.3.3.3 Investigation of the influence of the distance between CO_2 delivery tubing end and the syringe tip

One end of liquid CO_2 delivery tubing is directly connected with the cylinder valve, and the other end inserted into the syringe tip. The effect of different lengths of the delivery tubing

inserted into the connecter on the balanced temperature has been discussed in last section. This section studies the influence of the distance of CO_2 delivery tubing end from the syringe tip. Two 33RW tubings: Tubing E and Tubing F were tested at a sample temperature of 200 ℃. The distances of the delivery tubings from the syringe tip inserted into the syringe were 0 cm, 0.5 cm, 1 cm, and 1.5 cm.

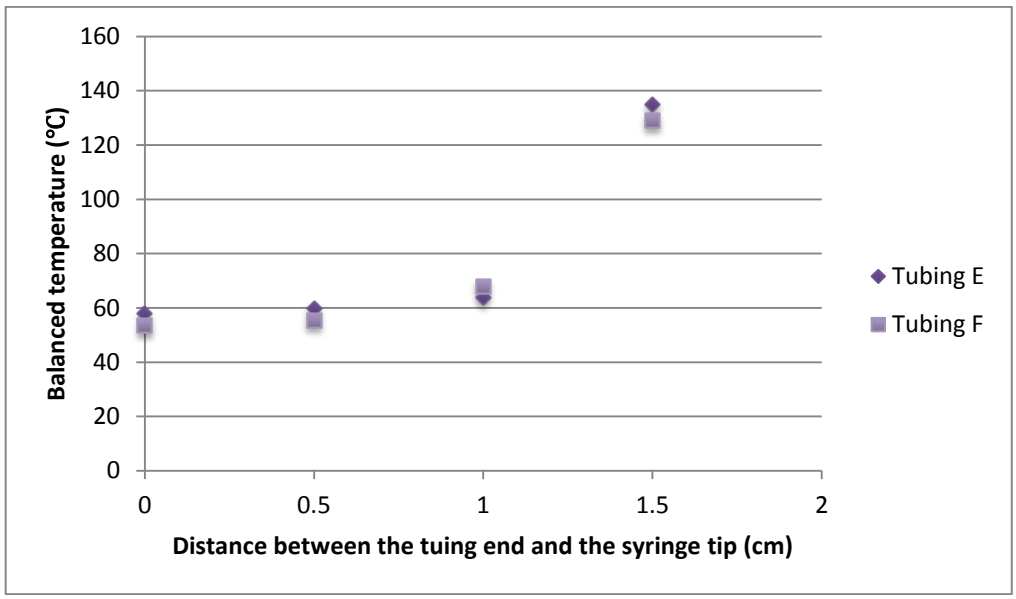

Figure 2-19 Comparison of the balanced temperature for distance between CO_2 delivery tubing end and the syringe tip (33RW tubings with sample temperature at 200 ℃).

In Figure 2-19, when the distance between delivery tubing end and syringe tip was less than 0.5 cm, no significant change of the balanced fiber temperature was observed. When the distance between those two was around 1 cm, the balanced temperature increased around 10 ℃. The balanced fiber temperature increased significantly if there was 1 cm to 1.5 cm distance between the end of the delivery tubing and the syringe tip. In order to keep the balanced temperature low and constant, the delivery tubing should be put very close to the syringe tip.

2.4 Conclusion

This chapter introduced the design and automation of the cold fiber device with details. A fan was installed for the solenoid valve that successfully reduced the valve body and solenoid coil temperature, as well as controlling the coating temperature fluctuation within a reasonable range. The temperature distribution from the core of the coating to the headspace was investigated and the temperature increased dramatically, in that can achieve 140 ℃ only 2 mm away from the coating. In the study of the water content effect in the sample, no significant differences in the recoveries were observed after adding different amounts of water.

After the cold fiber system was improved by minimizing the coating temperature fluctuation, the performance of the system was evaluated by investigating the extraction of PAHs. The evaluation includes the coating temperature fluctuation, system precision and the temperature and time profiles for PAHs. Overall, the coating temperature can be controlled with in ± 3 ℃ around its preset value and RSDs were smaller than 2% for six of seven analytes. Therefore, cold fiber SPME can be considered a reliable extraction strategy with good stability.

A simplified cold fiber system without the solenoid valve was modified to connect CO_2 delivery tubing directly with the valve of tank. In this simplified system, CO_2 delivery tubing with larger inner diameter has stronger delivery efficiency and smaller temperature fluctuation range. The robustness of this system was evaluated with different sizes of CO_2 delivery tubings that a distribution range in ± 5 ℃ of balanced fiber temperature was observed. Other factors may have effects on liquid CO_2 delivery, such as the length of delivery tubing, the length of CO_2 tubing inserted into cylinder connector, and the distance between the tubing end and the syringe tip. The simplified system is stable, has a low cost, and can easily be controlled, which provides a supplementary extraction strategy besides the traditional cold fiber system.

Chapter 3

Verification of the performance of cold fiber SPME

3.1 Theory

The thermodynamic extraction process of cold fiber headspace SPME is described by Zhang and Pawliszyn [68]. It is assumed that only one analyte is extracted at a constant pressure and most molecules of that analyte are transferred into the headspace. In this system, only two phases are taken into account: the headspace and the extraction phase. Before the extraction, it is assumed that the two phases are isolated from each other. At the beginning in the headspace at temperature T_s and pressure P_s, there is n_0 mole analyte and n_h mole air in a container with the volume of V_s. In the SPME coating, there is n_c mole analyte at temperature T_f [68].

As soon as the extraction begins, the analyte starts to partition between the headspace and the extraction phase. The temperature and the pressure of the extraction phase and the headspace are maintained at their initial values during the extraction. Finally, the extraction phase and the

headspace reach a dynamic equilibrium (with n_s mol of the analyte in the headspace and n_f mol of the analyte in the extraction phase; $n_0 = n_s + n_f$). After the equilibrium is reached, the absorption rate of the analyte by the coating and the desorption rate of the analyte from the coating equals. Route A in Figure 3-1illustrates this process.

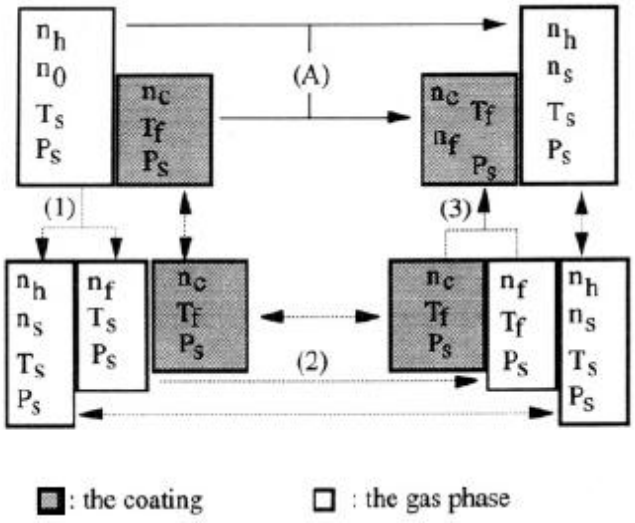

Figure 3-1 Analyte transferring process during cold fiber SPME sampling. Steps 1, 2, and 3 are the designed thermodynamic alternative routes; n_0, n_h, and n_c are molar numbers of the analyte, air, and the coating materials, respectively; n_f ($n_s + n_f = n_0$) and n_s are molar numbers of the analyte in the coating and the gas phase, respectively; T_f and T_s are the temperature of fiber coating and gas phase, respectively; P_s is the gas phase pressure; and the two-headed arrow indicates no changes occur [68].

Increases in thermodynamic entropy can drive the transfer of the analyte from the headspace to the extraction phase. When the equilibrium is established, transferring an extremely small amount of the analyte between the headspace and the extraction phase will not change the entropy in the system.

The change of entropy (ΔS) in a system is determined by the entropy from a initial state to a final state. It is independent of how the system changes between its initial state and its final state. ΔS of a system can be calculated by designing an artificial route which the system undergoes and has the same initial and final state. Figure 3-1 shows the initial and final states of the cold fiber

SPME sampling and an alternative route with three simple steps is designed to calculate the change of entropy (steps 1, 2 and 3 in Figure 3-1). ΔS of the cold fiber sampling can be calculated by adding the entropy changes of three steps in the designed route as expressed in Equation 3-1:

$$\Delta S = \Delta S_1 + \Delta S_2 + \Delta S_3 \qquad \text{Equation 3-1}$$

Step one is a process under constant temperature and pressure. ΔS_1 can be calculated using the Gibbs free energy change (ΔG) in this process. The detailed calculation steps of entropy changes are discussed in the reference [68]. The entropy change of the analyte for step one can be described as:

$$\Delta S_1 = -n_s R ln \frac{n_s}{n_h} + n_0 R ln \frac{n_0}{n_h} \qquad \text{Equation 3-2}$$

Where n_s is the amount of the analyte still in the headspace when the equilibrium is reached, n_0 is the amount of the analyte initially present in the headspace, R is the gas constant, and n_h is the amount of the mixing air in the headspace, which remains constant during the extraction. It is assumed that the air in the headspace will behave ideally and $n_h >> n_0$.

In the second alternative route, the fraction of analyte molecules which will be extracted by coating, are cooled from the sample temperature (T_s) to the fiber temperature (T_f). The entropy change in step two is the sum of the entropy change of the analyte and that of the surrounding environment. The change of the entropy in step two can be written as:

$$\Delta S_2 = n_f C_p (\frac{T_s - T_f}{T_f} + ln \frac{T_f}{T_s}) = n_f C_p (\frac{\Delta T}{T_f} + ln \frac{T_f}{T_s}) \qquad \text{Equation 3-3}$$

Where n_f is the amount of the analyte to be extracted from the headspace to the extraction phase; C_p is the heat capacity of the analyte; and ΔT is temperature difference between the headspace and the fiber coating. In this equation, it is assumed that the heat capacity of the analyte remains constant during the temperature change process [68].

In the third step, the analyte molecules that are separated (in step one) and cooled to the fiber temperature (in step two) are transferred from the headspace to the fiber coating at constant temperature and pressure. The entropy change for step three is calculated by:

$$\Delta S_3 = -n_f R ln(\frac{T_f n_f V_s}{T_s V_f K_0 n_h}) \qquad \text{Equation 3-4}$$

Where n_f is the amount of the analyte extracted by the coating at temperature T_f and pressure P_s. Other parameters are described in the previous step. It is assumed that the air in the headspace is ideal and $n_h >> n_0$.

After the equilibrium has been reached, the entropy will not change by small amount transfer of the analyte between the headspace and the extraction phase:

$$\frac{\partial \Delta S}{\partial n_f} = 0 \qquad \text{Equation 3-5}$$

Since the amount of the analyte initially existed in the headspace equals the sum amount of the analyte that is extracted in the coating and the analytes residues in the headspace ($n = n_f + n_s$), ΔS of the cold fiber sampling can be calculated by adding the entropy changes of three steps, resulting in the following equation:

$$C_p(\frac{\Delta T}{T_f} + ln\frac{T_f}{T_s}) - \mathrm{R}ln(\frac{T_f n_f V_s}{T_s V_f K_0 n_s})=0 \qquad \text{Equation 3-6}$$

The partition coefficient of the analyte between the fiber coating and the headspace is defined as $K_T = C_f/C_s = n_f V_s/n_s V_f$, Equation 3-6 can be rewritten as:

$$K_T = K_0 \frac{T_s}{T_f} Exp[\frac{C_p}{R}(\frac{\Delta T}{T_f} + ln\frac{T_f}{T_s})] \qquad \text{Equation 3-7}$$

where K_0 is the partition coefficient of the analytes between the headspace and the fiber coating when both phases are at the same temperature T_s; T_s and T_f are the temperatures of the sample and the fiber coating respectively; ΔT is the temperature difference between two phases; C_p is the heat capacity of the analytes; R is the gas constant. There are three main parameters that affect the value of partition coefficient of a particular analyte: K_0, T_s and T_f. With the larger K_0, the lower the fiber temperature, maintaining the sample at a high temperature and a large temperature gap between the fiber coating and the headspace can significantly increase the partition coefficient.

Since the value of K_0 and R are constant for the analyte; T_s and T_f are known in a specific system; C_p values for different temperatures can be obtained from thermodynamic databases or handbooks, the partition coefficients (K_T) for the analytes between the headspace and the fiber coating at different temperatures can be calculated. After the partition coefficient of the analyte in the cold fiber SPME is calculated, the recovery of the analyte in a specific system can be estimated in advance.

3.2 Verification of the theoretical calculation of the cold fiber SPME

3.2.1 Experimental

The verification of the theoretical calculation was investigated by the extraction of spiked BTEX from empty vials. No matrix was added to the vial to avoid any interference.

3.2.1.1 Chemicals and instrumental

BTEX (Benzene, Toluene, Ethylbenzene, and o-Xylene) were purchased from Supelco (Oakville, ON, Canada). Methanol (HPLC grade) was purchased from BDH (Toronto, ON, Canada). Helium (99.9%), nitrogen (99.9%), and compressed air were supplied by Praxair (Kitchener, ON, Canada) for GC. SPME fiber used in all experiments was 1 cm PDMS hollow tubing with a thickness of 178 μm from Dow Corning (Midland, MI, USA).

Gas chromatography was performed on Varian 3800 equipped with flame ionization detection (FID) and a CTC Combi PAL autosampler (Zwingen, Switzerland). SLB-1 capillary column (30 m, 0.25 mm i.d., 0.25 μm film thickness) was purchased from Supelco. Helium was the carrier gas with a flow rate of 1 ml/min. Temperature for the injector and the detector were 250 ℃ and 300 ℃. For the analysis of BTEX, column temperature was maintained at 40 ℃ for 2 minutes, and then increased at a rate of 20 ℃/min to 180 ℃.

3.2.1.2 Sample preparation and extraction condition

The stock standard solution of BTEX (100 mg/l) was prepared in methanol. 1 μl of the standard solution was spiked into a 10 ml empty vial and analyzed 15 min after spiking. The extraction time was 5 min, and desorption was at 250 ℃ for 1 min in the GC injector. The sample temperature was at 100 ℃ and the coating temperatures were -45 ℃ and -30 ℃ in this section.

3.2.2 Calculation of the partition coefficients for BTEX

The partition coefficient (K_T) for the analyte between the headspace and the fiber coating at different temperatures can be calculated according to Equation 3-7. At 298 K, K_0 is 493 for

benzene, 1322 for toluene, 3266 for ethylbenzene and 4417 for o-xylene [68]. C_p values were collected from CRC handbook. When the sample matrix temperature is fixed to 100 ℃ (313 K) and fiber temperatures are from -45 ℃ (228 K) to 15 ℃ (288 K), K_T values for BTEX that calculate from Equation 3-7 are illustrated in Table 3-1.

Table 3-1(a) Calculations of K_T values for benzene under specific coating temperatures.

$T_s(K)$	$T_f(K)$	$\Delta T(K)$	$C_p(J/K*mol)$	K_0	K_T/k_0	K_T
373	228	145	105	498	10.05	5.0E+03
373	248	125	105	496	5.05	2.5E+03
373	268	105	105	495	3.02	1.5E+03
373	278	95	105	494	2.45	1.2E+03
373	288	85	105	494	2.05	1.0E+03

Table 3-1(b) Calculations of K_T values for toluene under specific coating temperatures.

$T_s(K)$	$T_f(K)$	$\Delta T(K)$	$C_p(J/K*mol)$	K_0	K_T/k_0	K_T
373	228	145	131	1330	15.76	2.1E+04
373	248	125	131	1327	6.82	9.0E+03
373	268	105	131	1325	3.65	4.8E+03
373	278	95	131	1324	2.85	3.8E+03
373	288	85	131	1323	2.30	3.0E+03

Table 3-1(c) Calculations of K_T values for ethylbenzene under specific coating temperatures.

$T_s(K)$	$T_f(K)$	$\Delta T(K)$	$C_p(J/K*mol)$	K_0	K_T/k_0	K_T
373	228	145	159	3281	25.58	8.4E+04
373	248	125	159	3276	9.42	3.1E+04
373	268	105	159	3271	4.49	1.5E+04
373	278	95	159	3269	3.35	1.1E+04
373	288	85	159	3268	2.60	8.5E+03

Table 3-1(d) Calculations of K_T values for o-xylene under specific coating temperatures.

$T_s(K)$	$T_f(K)$	$\Delta T(K)$	$C_p(J/K*mol)$	K_0	K_T/k_0	K_T
373	228	145	161	4427	26.45	1.2E+05
373	248	125	161	4424	8.82	3.9E+04
373	268	105	161	4421	4.20	1.9E+04
373	278	95	161	4419	3.10	1.4E+04
373	288	85	161	4418	2.42	1.1E+04

In Table 3-1, if the sample temperature is maintained at 100 ℃ as coating temperature decreases, the coating/headspace partition coefficient (K_T) of the analyte increases dramatically. For

example, ethylbenzene has a partition coefficient of 8511 when the coating is at 15 ℃. This value increases to 83914 when the coating temperature is -45 ℃ with the sample temperature is kept at 100 ℃.

3.2.3 Calculation of the extraction amounts for BTEX and comparison with the experimental results

The extraction is considered to be complete when the analyte concentration has reached equilibrium between the sample matrix and the extraction phase. At this time, exposing the fiber for a longer time does not result in the accumulation of more analytes. It is assumed that all the analytes are transported into the headspace and there are only the headspace and the fiber coating in this system. The value of extraction amount after the equilibrium conditions can be calculated by Equation 1-2:

$$n = \frac{K_{fs} V_f V_s C_0}{K_{fs} V_f + V_s} \qquad \text{Equation 1-2}$$

Where n is the amount of the analyte extracted by the coating; K_{fs} is the distribution coefficient between the fiber coating and the sample matrix, which has been calculated in the last section for BTEX; V_s is the volume of the fiber coating that is 2.4 µl for this hollow PDMS tubing; V_f is the headspace volume in this system as well as the sample vial volume (10 ml). C_0 is the initial concentration of the analyte in the sample.

With all parameters known, the extraction amount can be calculated theoretically in advance and the values can be compared with the experimental result under the same extraction condition. Table 3-2 shows the comparison of extraction from the calculation and that of the experiment with sample temperature at 100 ℃ (373 K) and the fiber temperatures at -45 ℃ (228 K) and -30 ℃ (243 K) for BTEX.

Quantitative extraction can be achieved if the amount of the analyte extracted by the fiber coating is larger than 90% of the total amount of the analyte initially in the sample matrix. For a sample with 10 ml headspace, the value of K_T should be larger than 37500 for quantitative extraction. The theoretical result indicates that with sample temperature at 100 ℃, for ethylbenzene and o-xylene, quantitative extraction can be met when coating temperature is at about -30 ℃; while for benzene and toluene, with the coating temperature even as low as to -45 ℃, quantitative extraction cannot be achieved due to the extremely low partition coefficient with PDMS coating.

Table 3-2 Comparison of the theoretical calculation with the experiment results for BTEX.

Extraction amount (ng)	Temperature (℃)		Benzene	Toluene	Ethylbenzene	o-Xylene
	Matrix	Coating				
Theoretical calculation	100	-30	41.3	72.4	90.3	92.8
	100	-45	54.6	83.4	95.3	96.6
Experimental results	100	-30	58.3	81.7	94.1	97.7
	100	-45	76.1	88.6	100.7	102.8

In Table 3-2, the extraction amount for the experimental results was very close to that of the theoretical calculations, especially for ethylbenzene and the o-xylene, with errors in 10% range. For benzene, the extraction amount for experiment was higher than that of calculation. This could be explained as the temperature of fiber coating during the extraction not being uniform, which always reached a lower temperature than was preset before turning off the solenoid valve in a cycle. Overall, the theoretical calculations for the cold fiber system involving the coating/headspace partition coefficient (K_T), as well as the extraction amount of the analyte, can

be verified with cold fiber SPME. In the following sections, those theoretical calculations are used as a guide for comparison with the experimental results.

3.3 Evaluation the performance of cold fiber SPME

The last section introduced the calculation of the extraction amount for BTEX, and the result was in accordance with that of the experiment without a matrix under the same extraction parameters. In a real extraction process, there are many factors influence the extraction efficiency, such as the lack of sufficient desorption of the analyte from the matrix and the leakage from the headspace during the extraction at a high temperature. By comparing the extraction amounts in real extraction processes with the values of theoretical calculation, it could be easier to find out the source of loss.

3.3.1 Experimental

The performance of the cold fiber SPME system was evaluated by extracting BTEX from spiked samples.

3.3.1.1 Chemicals and instrumental

BTEX (Benzene, Toluene, Ethylbenzene, and o-Xylene) were purchased from Supelco (Oakville, ON, Canada). Methanol (HPLC grade) was purchased from BDH (Toronto, ON, Canada). Helium (99.9%), nitrogen (99.9%), and compressed air were supplied by Praxair (Kitchener, ON, Canada) for GC. SPME fiber used in all experiments was 1 cm PDMS hollow tubing with a thickness of 178 μm from Dow Corning (Midland, MI, USA).

Gas chromatography was performed on Varian 3800 equipped with flame ionization detection (FID) and a CTC Combi PAL autosampler (Zwingen, Switzerland). SLB-1 capillary column (30 m, 0.25 mm i.d., 0.25 μm film thickness) was purchased from Supelco. Helium was the carrier gas with a flow rate of 1 ml/min. For the analysis of BTEX, column temperature was maintained at 40 ℃ for 2 minutes, and then increased at a rate of 20 ℃/min to 180 ℃. Temperature for the injector and the detector were 250 ℃ and 300 ℃.

3.3.1.2 Sample preparation and extraction condition

The stock standard solution of BTEX (100 mg/l) was prepared in methanol. 1 μl of the standard solution was spiked into 10 ml empty vials or 10 ml vials with 1 g sand loaded. The freshly spiked samples were analyzed 15 min after spiking, and the aged spiked samples were analyzed 30 days after spiking. The extraction time was 5 min if there was no notification in the specific section. The coating temperature and sample temperature varied according different tests. Desorption time was 1 min at 250 ℃ in GC injector.

3.3.2 Investigation of the performance of cold fiber SPME at various coating temperatures

According to the literature [69], the extraction property of PDMS coating, especially at a very low temperature, would be similar to a rigid rubber-like material and may affect the extraction and the diffusion of analytes through the coating. In order to investigate the performance of the PDMS coating at low temperature, samples of freshly spiked BTEX in empty vials were extracted under different coating temperatures when the sample temperature was set at 100 ℃.

The extraction amounts of BTEX with sample temperature at 100 ℃ (373 K) and the fiber temperature at 0 ℃ (273 K), -20 ℃ (253 K), -40 ℃ (233 K) were calculated. The extraction

amounts of the calculation and the experiment are compared in Figure 3-2. This result was the same as that in the previous section, in which the extraction amount for experiment was very close to the calculated result. This result verified that the property of the PDMS did not change at low coating temperatures and the performance of the PDMS was not influenced as well. Additionally, when the sample temperature was at 100 ℃ or lower, the leakage from the cap septa can be negotiable.

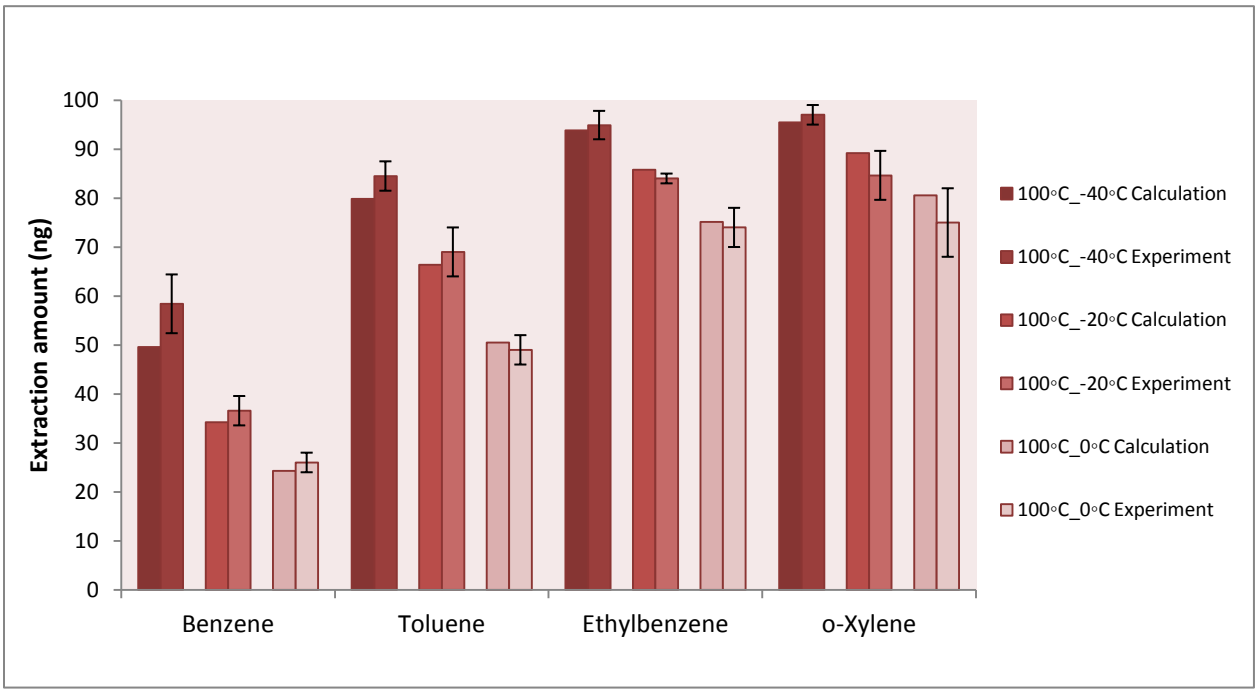

Figure 3-2 Comparison of the theoretically calculation and experimental results for BTEX with different coating temperatures (T_s = 100 ℃, T_f = -40 ℃, -20 ℃, 0 ℃, t = 5 min).

3.3.3 Investigation of the loss during the extraction at elevated sample temperatures with cold fiber SPME

In a cold fiber SPME with high sample temperature, it is always difficult to avoid the leakage of the analyte from the sample container to the outside due to the leakage through the cap septa of the sample vial [61, 70]. In order to investigate the extent of the leakage and its relationship with

sample temperature, freshly spiked BTEX samples in empty vials were extracted under elevated sample temperatures from 60 ℃ (333 K) to 140 ℃ (413 K). The coating temperature was constant for all tests. The extraction time was 5 min and the coating temperature was -20 ℃ (253 K). The extraction amount by the calculation is also presented for comparison with the experimental results, which are illustrated in Table 3-3.

Table 3-3 Comparison the extraction amounts of theoretical calculation and experimental results for BTEX with elevated sample temperatures (T_f = -20 ℃, T_s = 60 ℃, 80 ℃, 100 ℃, 120 ℃ and 140 ℃, t = 5 min).

	Temperature (℃)					
Extraction amount (ng)	Matrix	Coating	Benzene	Toluene	Ethylbenzene	o-Xylene
Theoretical calculation	60	-20	19.9	42.9	67.7	74.3
	80	-20	25.8	52.9	77.2	82.3
	100	-20	34.2	66.4	85.8	89.2
	120	-20	45.5	78.1	90.0	94.2
	140	-20	59.0	86.2	94.9	97.2
Experimental results	60	-20	31.8	55.5	71.1	75.5
	80	-20	33.2	61.8	76.5	79.1
	100	-20	36.6	69.9	84.2	84.6
	120	-20	35.2	66.5	84.9	85.9
	140	-20	30.6	65.9	86.1	87.3

When the matrix temperature increased from 60 to 100 ℃, the extraction amounts for the experiment were similar to the calculated value beforehand. There was no loss from the extraction or transport process for BTEX. Nevertheless, when the matrix temperature was higher than 100 ℃, the extraction amounts of the experiment became lower than that of calculation and the trend was more obvious with the higher sample temperatures. For benzene and toluene, the extraction amount even decreased with elevated sample temperatures. For ethylbenzene and o-

xylene, although the extraction amount kept increasing when the sample temperature was enhanced, but the extent of the increase was much smaller than that predicted in the calculation.

No loss of the analyte was found in the extraction and the transport with the sample temperature was lower than 100 ℃ for BTEX. When the temperature was higher than 100 ℃, the extraction amount of the experiment was lower than that of the calculation, this may due to the leakage from the cap septa of the sample vial during the extraction.

3.3.4 Investigation of the performance of different vial cap septa at high sample temperatures

The outer needle of cold fiber SPME is applied to protect the fiber from damage and to pierce through the thick septa of the sample vial and GC injector. The outer diameter of the outer needle is around 1.2 mm, which is much larger than that of an injection syringe and a regular SPME fiber needle. When the extraction begins, this large size needle pierces through the sample vial septa and the fiber is exposed to the headspace. During the extraction at high temperatures, the pressure inside of the sample vial is greater than the air pressure outside. The analyte in the headspace may be lost due to leakage. Different vial cap septa may have different effects on the elimination of the leakage. A series of different septa were compared in this study.

In this test, six different septa (one regular screw cap and five crimp caps) were compared: a - PTFE/Silicone crimp cap; b - PTFE/Silicone screw cap; c - Washer & PTFE/Silicone crimp cap; d - Teflon/Silicone crimp cap; e - Butyl/PTFE crimp cap; and f - PTFE/Silicone/PTFE crimp cap (Supelco, Canada). 1 μl BTEX standard solution (100 mg/l) was spiked in empty vials for the extraction with different septa. Since no leakage was observed with sample temperature was lower than 100 ℃ for BTEX in the last section, the proposed sample temperature had to be

higher than 100 ℃ to investigate the performance of septa. The sample temperature was set at 120 ℃. The coating temperature was -20 ℃ and the extraction time was 5 min.

No loss of the analyte was found in the extraction and the transport with the sample temperature was lower than 100 ℃ for BTEX. When the temperature was higher than 100 ℃, the extraction amount of the experiment was lower than that of the calculation, this may due to the leakage from the cap septa of the sample vial during extraction for all tests. The extraction amount of the calculation was also compared with that of experimental results for six different septa. The comparison of performance for different septa is illustrated in Figure 3-3.

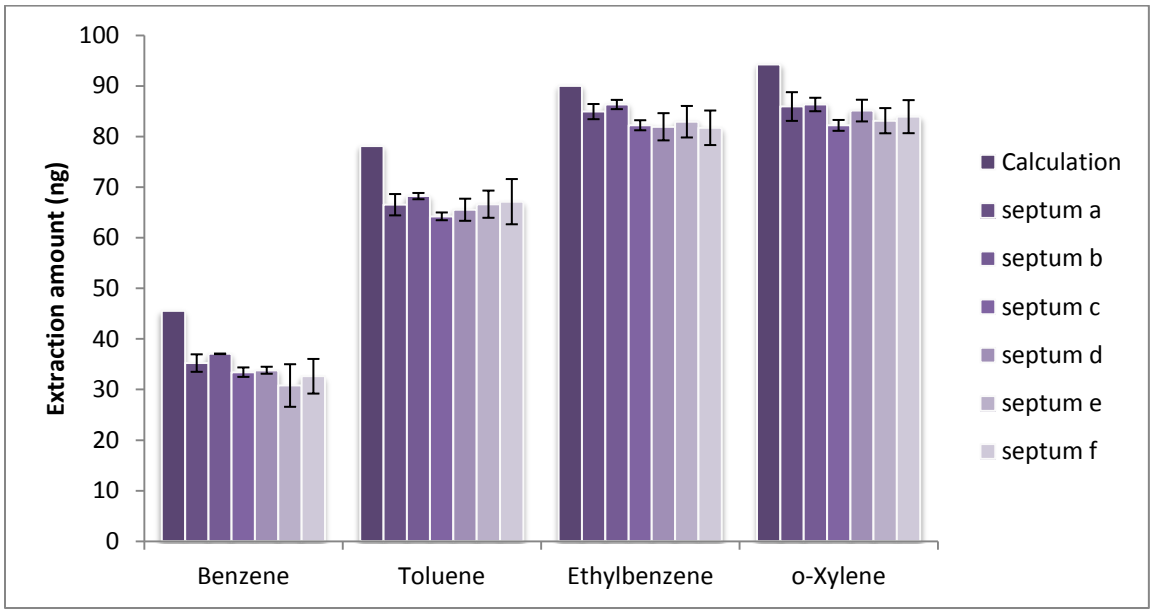

Figure 3-3 Comparison of the extraction amounts for different cap septa with that of calculation. (a: PTFE/Silicone crimp cap; b: PTFE/Silicone screw cap; c: Washer & PTFE/Silicone crimp cap; d: Teflon/Silicone crimp cap; e: Butyl/PTFE crimp cap; and f: PTFE/Silicone/PTFE crimp cap. T_f = -20 ℃, T_s = 120 ℃, t = 5 min)

According to the extraction amount shown in Figure 3-3, there was no significant difference in the extraction amount between cap septa. The extraction amount with a regular screw cap was slightly higher than that of other caps and the extraction amount with Butyl/PTFE crimp cap was

a marginally lower than that of other caps. The ratios between the average extraction amounts of the different septa to that of the theoretical calculations for benzene and toluene were 75% and 85%, and there were around 20% loss of benzene and toluene during the extraction. The ratios were 92% for ethylbenzene and o-xylene, which meant fewer molecules of the analytes were lost in the extraction. However, the ratios between the average extraction amounts of the different septa to that of the theoretical calculation was 107%, 105%, 98%, and 95% for four compounds when the sample temperature was 100 ℃. Increasing the temperature of the sample and the headspace could cause the loss of the compounds during extraction.

According to the comparison of extraction amounts with different septa, none of them showed obviously better results in reducing the leakage. The loss through the cap may be caused by the rapid increase of the analyte's vapor in the headspace. One way to reduce the loss is to slow down the headspace expansion rate. This could be achieved by increasing the sample temperate gradually during the extraction process. Since the volume of container is constant, the transfer of the analyte from the gas phase to the coating will reduce the pressure expansion.

3.3.5 Investigation the extraction efficiency using the theoretical calculation as a guide

This study investigated and compared the extraction efficiency for aged spiked BTEX with the calculated results. The aged spiking samples were prepared by adding 1 µl of the standard solution into 10 ml vials with 1 g sand loaded and stocked for 48 hours before the analysis. The extraction amount of BTEX from aged spiked samples was compared with freshly spiked samples in empty vials and the calculated results. The sample temperature was set at 100 ℃ and the coating temperatures were at -40 ℃ and -20 ℃. Extraction time was 5 min and desorption

time was 1 min at 250 ℃. The comparison of extraction amounts with the different extraction conditions is illustrated in Figure 3-4.

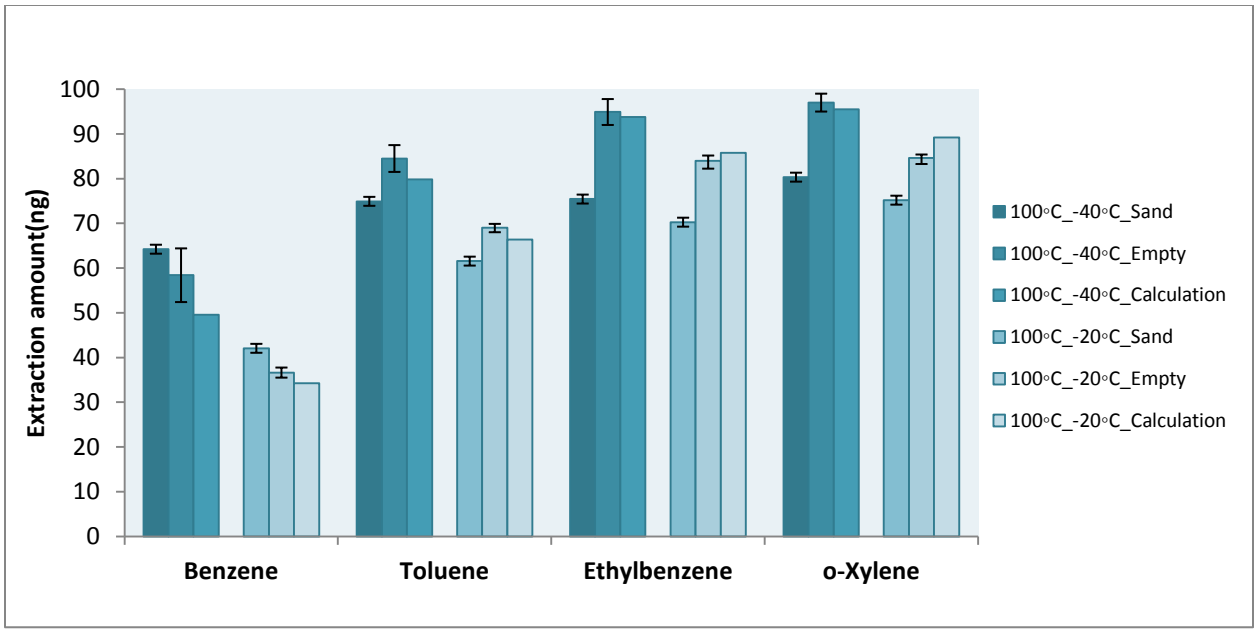

Figure 3-4 Comparison of the extraction amounts of BTEX with aged spiked sand sample, freshly spiked empty sample and calculation (T_s =100 ℃, T_f = -40 ℃, -20 ℃, t = 5 min).

Three groups of data are shown for different comparisons. Freshly spiked BTEX in empty vials were used to explore the ideal extraction without the influence of the sample matrix. Samples of aged spiked BTEX in sand were used for considering the interaction between the analytes and the sand matrix, and the desorption efficiency of the analytes from that matrix. Finally, theoretical calculation was utilized as a guide to check the extraction efficiency for the real samples. The performance of the extraction amounts of the four compounds was very similar at two different coating temperatures.

It was surprising that for benzene, the extraction amount in sand sample was higher than that of the freshly spiked empty sample and the calculation. This is because, for the empty spiked sample, some benzene molecules possibly diffused outside the vial when they were extracted in

the high sample temperature. For the spiked sand sample of benzene, a portion of the analyte that bonded with the sand matrix was released into the headspace gradually. It was then extracted by the cold fiber, reducing the chance for loss. However, the extraction amounts under both extraction modes were still higher than the calculated results. This can be explained by the fact that the fiber temperature was not uniform, it fluctuated around the preset value. Benzene was very sensitive to the low coating temperature. When the fiber temperature was lower than the preset temperature, extra benzene molecules were absorbed by the cold fiber and it was therefore possible that the extraction amount was higher in the experiment than the calculated value.

However, the ratios between the extraction amounts of the sand spiked samples to that of the theoretical calculation were 93% for toluene and only around 84% for ethylbenzene and o-xylene. This is because, under that extraction condition, some molecules of those three compounds were still bonded with the sand matrix. More energy was required to accelerate the molecules to overcome the interaction and finally release into the headspace. Prolonging the extraction time and enhancing the sample temperature are the two most common approaches.

The extraction time profiles for aged spiked BTEX observed the trend of the extraction with different extraction times. The sample temperature was set at 100 ℃ and the coating temperature was at -20 ℃. 1 µl standard solution was spiked into 10 ml vials with 1 g sand loaded and the spiking time was 72 hours before the analysis. Extraction time varied from 1 min to 20 min and desorption time was 1 min at 250 ℃. The extraction amounts of the different extraction times are illustrated in Figure 3-5.

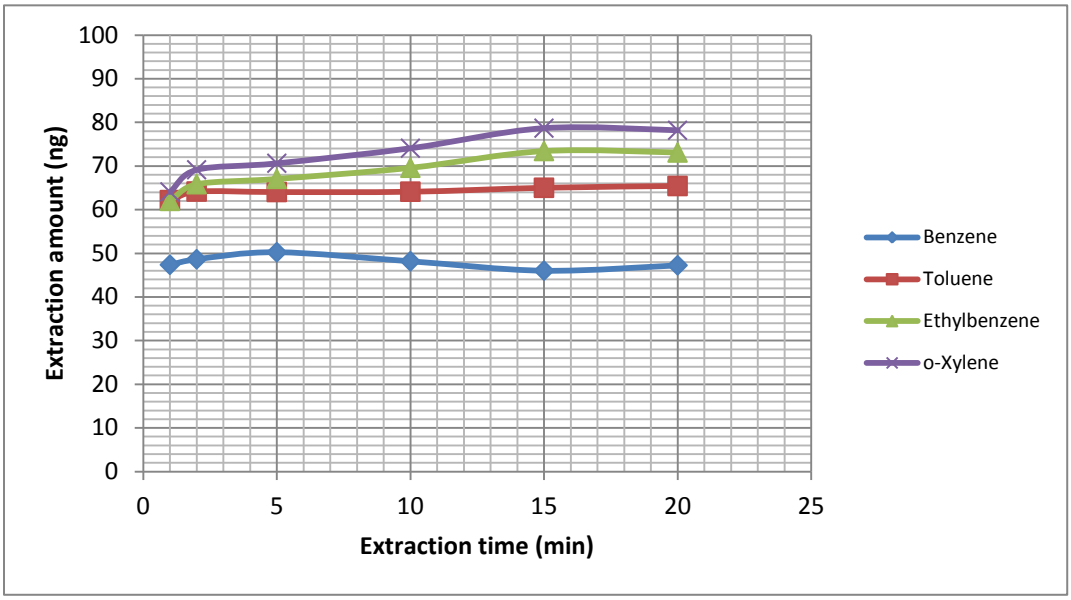

Figure 3-5 The extraction time profiles for aged spiked BETX (T_s = 100 ℃, T_f = -30 ℃).

If we assume that most analytes are released into the headspace from the sample matrix during the extraction, only two phases are taken into consideration in the headspace SPME sampling: the headspace, and the fiber coating. Under this mode, equilibrium can be established between the sample matrix and the extraction phase if the extraction time is long enough. When equilibrium is reached, exposing the fiber for a longer time does not result in the accumulation of more analytes.

For benzene and toluene, the extraction amount was not sensitive during the extraction process with different extraction times. This is due to the fast release rate of those two compounds from the sand matrix and rapid partition equilibrium between the headspace and the coating during the extraction. For ethylbenzene and o-xylene, the extraction amount increased rapidly during the first two minutes; after that, the extraction amount was keeping increasing with a slow rate. The interactions of those two analytes with the sand matrix were stronger than that of benzene and

toluene. The optimum extraction time for BTEX was around 15 min. Prolonging the extraction time did not result a significant increase in the extraction amount for BTEX from the aged spiked sample in this section.

3.3.6 Investigation of the extraction efficiency for aged spiked PAHs

The last section discussed the extraction of the analytes from the aged spiked sand samples that extra energy was required to help the compounds to overcome the molecular interaction with the matrix and finally be released into the headspace. However, prolonging the extraction time was not effective for aged spiked BTEX samples; enhancing the sample temperature could be more significant for semi-volatile compounds. In this study, two PAH compounds: anthracene and pyrene were applied to investigate the extraction efficiency at elevated sample temperatures with the cold fiber SPME system.

3.3.6.1 Experimental

PAHs (anthracene and pyrene) were purchased from Supelco (Oakville, ON, Canada). Methanol (HPLC grade) was purchased from BDH (Toronto, ON, Canada). Helium (99.9%), nitrogen (99.9%), and compressed air were supplied by Praxair (Kitchener, ON, Canada) for GC. SPME fiber used in all experiments was 1 cm PDMS hollow tubing with a thickness of 178 μm from Dow Corning (Midland, MI, USA).

Gas chromatography was performed on Varian 3800 equipped with FID and a CTC Combi PAL autosampler (Zwingen, Switzerland). SLB-1 capillary column (30 m, 0.25 mm i.d., 0.25 μm film thickness) was purchased from Supelco. Helium was the carrier gas with a flow rate of 1 ml/min. The column temperature was initially set at 50 ℃ for 1 min, then increased to 270 ℃ at a rate of

20 ℃ /min and held at 13 min. The temperatures set for the injector and the detector were 250 ℃ and 300 ℃.

The stock standard solution of anthracene and pyrene (100 mg/l) was prepared in methanol. 1 µl of the standard solution was spiked into 10 ml empty vials or 10 ml vials with 1 g sand loaded. The freshly spiked samples were analyzed 15 min after spiking, and the aged spiked samples were analyzed 30 days after spiking. The extraction time was 30 min. The sample temperatures for two PAHs were from 100 ℃ to 200 ℃. Desorption time was 5 min at 250 ℃ in GC injector.

3.3.6.2 Result and discussion

Two processes are involved in the headspace SPME: the analytes are released from their matrix to the headspace and then are extracted by the fiber coating. In the extraction process, quantitative extraction is impossible to reach if a significant portion of analytes are strongly retained by the sample matrix. The majority of the analytes should be released into the headspace for better quantitative extraction. It is critical to choose optimized extraction conditions that are able to facilitate the release of the majority analytes from the matrix. Thermal desorption can usually release most volatile organic compounds and semi-volatile compounds from simple matrices like sand.

The theoretical extraction amount for PAHs was calculated by the same approach as the calculation for BTEX in the previous sections. The distribution coefficients of PAHs are much higher than that of BTEX with the sample and coating both at the same temperature T_s. Therefore, it is reasonable to conclude that the theoretical extraction amounts for PAHs shows in Figure 3-6 are very high. The calculated extraction amounts for anthracene and pyrene are close to each other under the same condition. When most analytes are released into the headspace from the matrix, quantitative extraction can be achieved if the target analytes coating exhibit very large

partition coefficients between the headspace and the fiber coating. The extraction results for those two compounds with the empty spiked samples were similar to that of the calculation, which verified that without the interference of the matrix, the performance was ideal for the PAHs with the cold fiber SPME system.

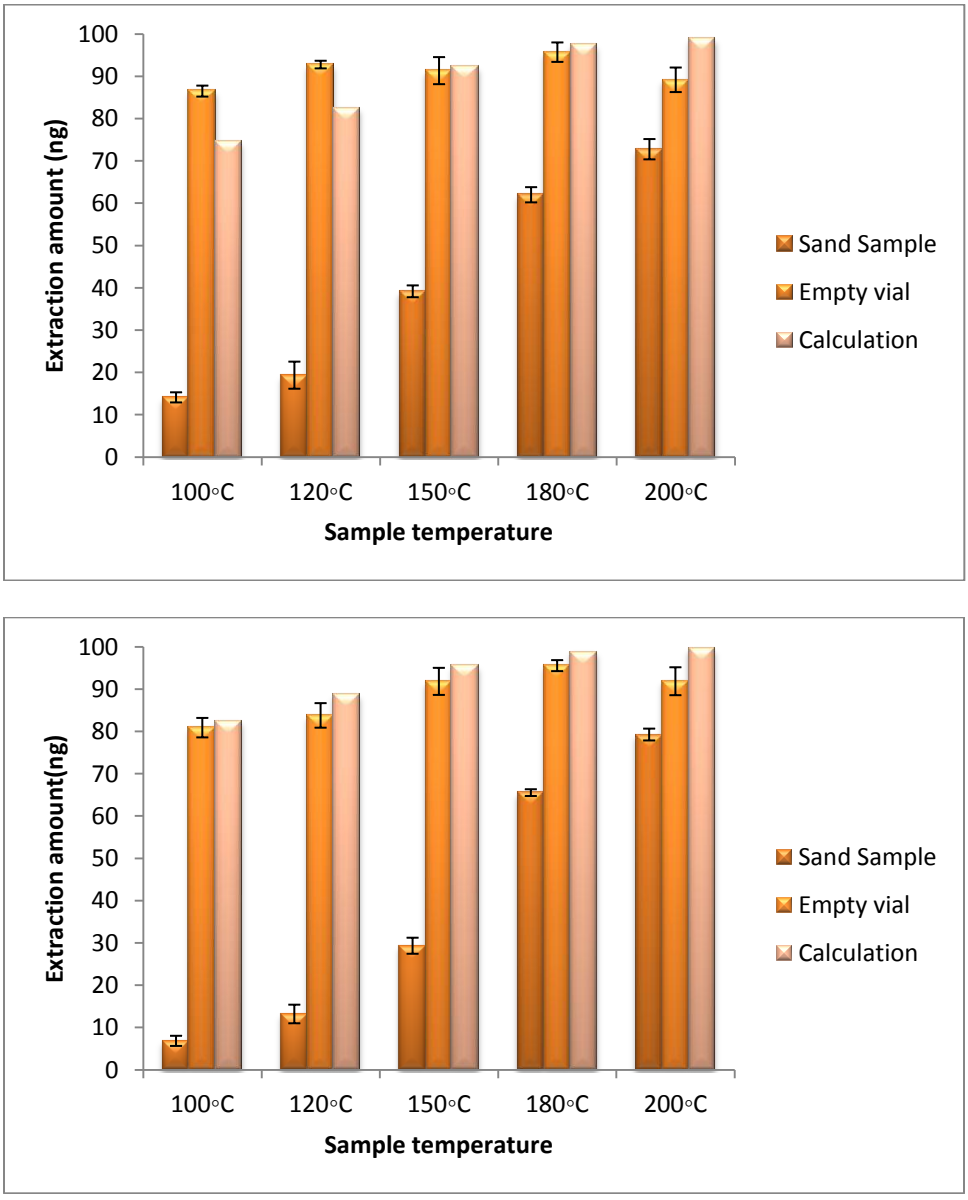

Figure 3-6 Comparison the extraction amounts of anthracene (above) and pyrene (bottom) with aged spiked sand samples, freshly spiked empty samples and calculation (T_s = 100-200 ℃, T_f = 30 ℃, t = 30min).

For the aged spiked samples when the extraction temperature was at 100 ℃, recoveries for anthracene and pyrene were only 14% and 7%. This is because most molecules of the analytes were still not desorbed from the sand matrix at this temperature, and a higher sample temperature was required to help the molecules to be released from the matrix into the headspace for the further extraction. After enhancing the sample temperature to 200 ℃ with the coating temperature remaining constant, the extraction amount for both compounds increased dramatically. This illustrates that enhancing the sample temperature effectively increased the analytes desorption from the interacted matrix, and finally increased the extraction amount.

3.4 Conclusion

This chapter calculated the partition coefficient (K_T) for the analyte between the headspace and the fiber coating at different temperatures, and estimated the recovery of the analyte in a specific system in advance.

The verification of the theoretical calculation was investigated by extracting of freshly spiked BTEX samples without matrix. The extraction amounts of experimental results were very close to that of the theoretical calculation. Therefore, the calculated results in a cold fiber system involving the coating/headspace partition coefficient, as well as the extraction amount of the analyte, can be verified with the cold fiber SPME.

By using theoretical calculations for guidance, it is easier to find the source of loss during the real extraction. After studying the extraction of BTEX with various coating temperatures, it was concluded that the property of the PDMS did not change at low coating temperature to -40 ℃ and the performance of the PDMS was not influenced as well. However, with elevated sample temperatures higher than 100 ℃ for BTEX, the extraction amounts of the experiment became

lower than the calculated value. This trend was more obvious with higher sample temperatures, which may be due to leakage from the cap septa of the sample vial during extraction. The performance for six different cap septa was compared and no significant difference of extraction amounts between cap septa can be found.

Theoretical calculations were applied to investigate the desorption efficiency of the analyte from the matrix for aged spiked samples. For aged spiked BTEX, prolonging the extraction time may increase the extraction efficiency for ethylbenzene and o-xylene, but in a slow rate. For aged spiked PAHs, the extraction efficiency with elevated sample temperatures up to 200 ℃ was increased dramatically, which leads to a conclusion that enhancing the sample temperature can effectively increase the desorption of the analytes from the interacted matrix, and finally increase the extraction amount.

After the comparison with the calculated extraction amount and the extraction amount for the empty spiked samples, the performance of the cold fiber SPME system is verified as ideal for exhaustive extraction.

Chapter 4

Method optimization for PAHs from solid samples

4.1 Introduction

4.1.1 PAHs in the environment

Polycyclic aromatic hydrocarbons (PAHs) are a group of about 10,000 compounds, representing an important class of hazardous organic chemicals consisting of two or more benzene rings in linear, angular or cluster arrangements [71]. They are important pollutants, present in the environment, and released from incomplete burning of carbon containing materials, such as oil, wood, garbage, or coal [72-74]. PAHs from fires can bind to ashes and move long distances through the air [75]. Since some lighter PAHs (containing up to four benzene rings) are water-soluble they can also be found in rivers and groundwater [76]. Most PAHs in the environment derive from incomplete burning accumulated in soil, sediment, and sludge.

PAHs can persist in the environment and accumulate under the right conditions, so that the

potential for adverse health effects is high. Exposure to PAHs is considered an environmental concern. Over 120 PAH compounds have been detected and classified as pollution by the U. S. Environmental Protection Agency (EPA), among them 16 PAHs are classified as priority pollutants [77]. PAHs are not commonly associated with adverse health effects in humans. However, the U.S. Department of Health and Human Services has determined that some PAHs, particularly 4- and 6-ringed PAHs, can potentially cause cancer [78].

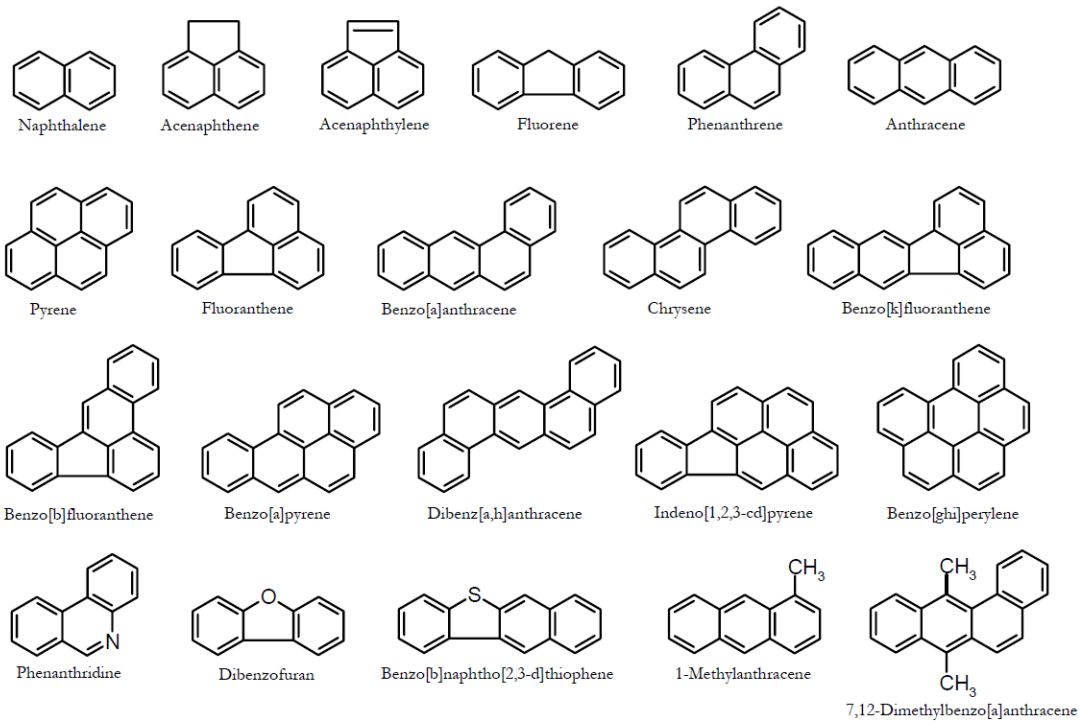

Figure 4-1 Structures of the 16 US-EPA PAHs and selected alkyl-PAHs [77].

Generally, PAHs show high affinity for organic matter. However, individual PAHs differ substantially in their properties. As shown in Table 4-1, from two to six benzene rings in the PAH-molecule, properties such as vapor pressure and aqueous solubility range in twelve and five orders of magnitude. Low molecular weight PAHs are much more water soluble and volatile than high molecular weight PAHs, which have higher hydrophobicity [79]. The difference also

reflects the octanol-water partitioning coefficient (K_{OW}) shown in Table 4-1. These properties of PAHs largely determine their environmental behavior. The semi-volatile nature of the low molecular PAHs means that they partly exist in the atmosphere as vapors and they could be partly dissolved in aqueous environments. On the other hand, the high molecular weight PAHs, are primarily associated with particles in the environment [73, 80].

Table 4-1 Properties of the 16 US-EPA PAHs [79].

PAHs	Number of rings	Molecular weight	Aqueous solubility (mg/l)	Vapor pressure (Pa)	Log K_{ow}
Naphthalene	2	128	31	$1.0x10^{2}$	3.37
Acenaphthylene	3	152	16	$9.0x10^{-1}$	4.00
Acenaphthene	3	154	3.8	$3.0x10^{-1}$	3.92
Fluorene	3	166	1.9	$9.0x10^{-2}$	4.18
Phenanthrene	3	178	1.1	$2.0x10^{-2}$	4.57
Anthracene	3	178	0.045	$1.0x10^{-3}$	4.54
Pyrene	4	202	0.13	$6.0x10^{-4}$	5.18
Fluoranthene	4	202	0.26	$1.2x10^{-3}$	5.22
Benzo[a]anthracene	4	228	0.011	$2.8x10^{-5}$	5.91
Chrysene	4	228	0.006	$5.7x10^{-7}$	5.91
Benzo[b]fluoranthene	5	252	0.0015	-	5.80
Benzo[k]fluoranthene	5	252	0.0008	$5.2x10^{-8}$	6.00
Benzo[a]pyrene	5	252	0.0038	$7.0x10^{-7}$	5.91
Dibenzo[a,h]anthracene	6	278	0.0006	$3.7x10^{-10}$	6.75
Indeno[1,2,3-cd]pyrene	6	276	0.00019	-	6.50
Benzo[ghi]perylene	6	276	0.00026	$1.4x10^{-8}$	6.50

In soil, most PAHs are strongly bonded to organic matter, some light molecular weight PAHs are partly lost through degradation processes, most PAHs can remain in the soil for many centuries [73]. The effect of sorption with the soil generally increases with increasing the number of benzene rings in the molecule [81, 82]. The processes of sorption and aging limit the

degradability and reduce the toxicity of the soil contaminants by lowering the available fraction [83, 84].

Concentrations of PAHs are generally higher near the emission sources of environmental pollutants. Elevated concentrations of PAHS have been found in urban soils and very high concentrations have been reported at contaminated sites. These sites usually involved production or use of fossil fuels [85].

More attention has been given to the subject of pollution in the environment due to continuously increasing industrial activities. Because of the high environmental stability and high hydrophobicity of PAHs, human beings are exposed to PAHs via the air and drinking water but mostly through the intake of food, which results from the accumulation of the trophic chain with in which the human body is the final destination.

As shown in the previous information about soil contamination in the environment and the levels of toxicity, the distributions of PAHs in the environment and potential human health risks have become the focus of much attention. Therefore there are increasing demands for the use of analytical methods to study PAHs in the environment. Because PAHs are often present in lower concentrations, they may be difficult to identify in the complex mixtures in these environmental samples. It is therefore essential to use powerful analytical tools to extract, separate, and identify the analytes in the environment. Furthermore, powerful extraction techniques are required to release these strongly sorbed contaminants from the soil material for analysis of PAHs in soil.

4.1.2 Sorption and desorption mechanisms of organic compounds with soil

Soil is a complex matrix consisting of organic and mineral fractions. The organic fraction consists of unaltered debris, combustion residues, degraded organic materials, and non-aqueous

phase liquids. The mineral fraction consists of silicates that are coated with various metal oxides and with organic matter [86]. Furthermore, soil contains pore water with dissolved organic matter, dissolved ions, and suspended minerals [87].

The on-site presence of large amounts of chemicals is a potential source of soil contamination [88]. Sorption rates of organic contaminants from soil can predict the transportation of these compounds between different environmental media at contaminated sites [89]. Furthermore, the sorption process also affects the biological availability, bioaccumulation, biodegradation, and potential toxic effects on organisms [90, 91]. Also, sorption models predicting the organic contaminants behavior towards soils is essential in evaluating the risk of these compounds to the environment.

Organic chemicals can be associated with soils via adsorption or absorption. Adsorption refers to molecules attaching to a two-dimensional surface, while absorption refers to molecules penetrating a three-dimensional matrix. The different sorption processes for the apparent sorption coefficient of a soil depend on the properties of sorbate and sorbent. The sorption mechanisms are shown in Figure 4-2.

Absorption between the soil and the aqueous phase usually takes place in the organic fraction of the soil. This process is driven by the energy difference in the aqueous phase and in the organic phase to form a cavity [92]. The larger compounds have stronger interactions with the soil matrix so those compounds have a higher the sorption coefficient to the organic phase. This interaction is often the most important sorption of non-polar hydrophobic organic compounds. In this absorption process, chemicals are absorbed in the organic fraction of the soil, the sorption coefficient (K_{OC}) can be described as:

$$K_{oc} = \frac{K_D}{f_{oc}}$$ Equation 4-1

Where f_{OC} is the organic carbon fraction and K_D is the sorption coefficient. Absorption processes is considered to be independent of the concentration.

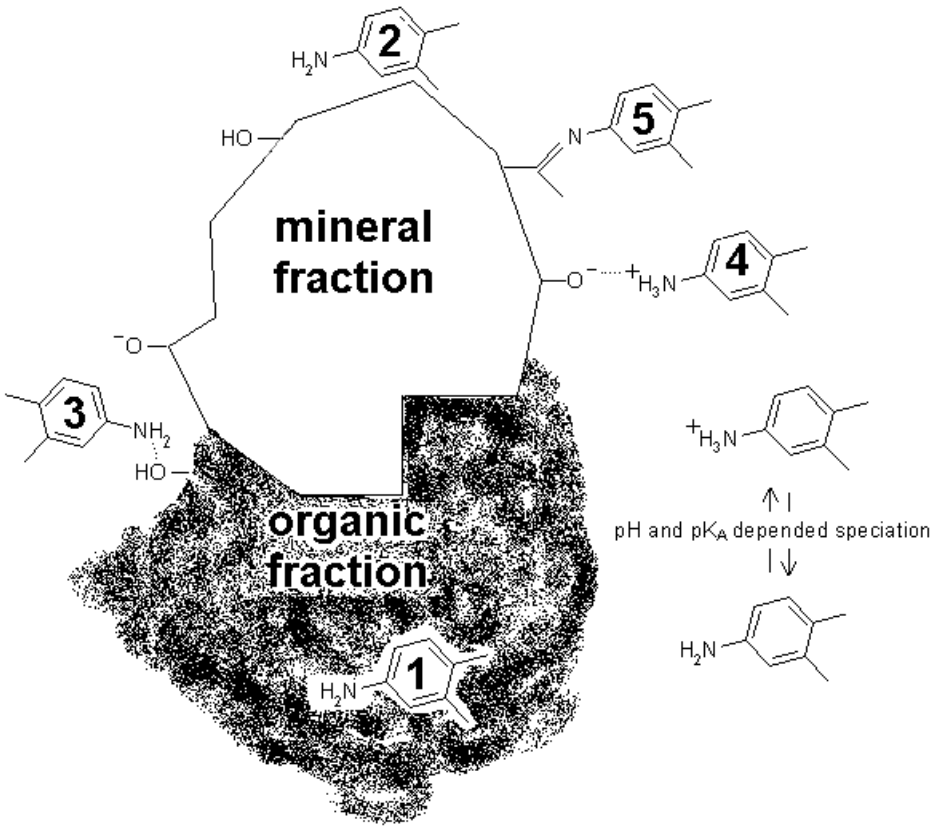

Figure 4-2 The sorption mechanisms of a chemical with soil. (1) Neutral sorbate escapes water and absorbs in to the organic material of the soil; (2) Neutral sorbate adsorbs by van der Waals interactions to organic and mineral soil surfaces; (3) Neutral sorbate adsorbs by hydrogen bonds to mineral and organic soil surfaces; (4) Charged sorbate adsorbs by non-specific electrostatic attraction or ionic bonding to mineral soil surfaces with oppositely charged surface groups; (5) Reactive moiety of sorbate covalently bonds with reactive moiety of mineral or organic sorbent [87].

Adsorption always takes place on the surface of the soil constituent. Polar organic chemicals with hydrogen accepting/donating groups can form hydrogen bonds with mineral, water and organic the surface of the soil. Besides that, ionized organic compounds can adsorb oppositely

charged surfaces by non-specific electrostatic attraction. Furthermore, compounds can sorb by chemical reactions that leads to covalent bonds [86, 87].

The sorption coefficients of the adsorption often depend on the compound concentration, since the number of sorption sites is limited for the compounds [86, 87]. As a result, non-linear sorption isotherms are often observed. Freundlich isotherm is a common mathematical approach to fit the changing sorption coefficients with concentration:

$$C_s = K_D C_{aq}^n \qquad \text{Equation 4-2}$$

Where the K_D is the sorption coefficient at a defined aqueous concentration; C_{aq} is the aqueous concentration; and n is the parameter describing the sorption linearity. The sorption coefficient increases with increasing aqueous concentration if n is larger than one, and the sorption coefficient decreases with increasing sorption coefficient if n is smaller than one. If adsorption of molecules occurs at homogeneous surfaces with a limited number of sorption sites (Γ_{max}) and equal adsorption energies, the mechanistic model can be described by the Langmuir equation:

$$C_s = \frac{\Gamma_{max} K_D C_{aq}}{1 + K_D C_{aq}} \qquad \text{Equation 4-3}$$

The organic domain includes sorbent organic matter (SOM). The organic matter that is present in soils includes: recognizable biochemicals (proteins, nucleic acids, lipids, and cellulose) and macromolecular residues formed through diagenesis [93]. SOM normally contains oxygen-containing functional groups, which are polar. However, the hydrophobic and hydrophilic domains are decided by the number of such polar groups, which may vary significantly [98]. Hydrophobic organic contaminants (HOCs) are persistent contaminants, which include wide classes of chemicals, including aromatic compounds such as PAHs [94]. The affinity of SOM

for non-polar hydrophobic organic compounds depends on aromatic carbon content and the polarity of soils [94].

Non-aqueous phase liquids (NAPLs) are organic liquids like dry fuel oil, gasoline, and organic solvents that are associated with human activities [95]. NAPLs are often considered homogeneous with no interfacial resistance in mass transportation [94].

There are a variety of sorption sites available for the organic compounds in soils due to their complex nature. Partitioning models based on instant equilibrium were not adequate to describe all the mass transport situations. Kinetic terms rather than equilibrium terms were applied to explain desorption of organic compounds from natural sorbents. Desorption of organic compounds from/through soils models are built by considering various possible rate-limiting steps.

One possible rate-limiting parameter is the activation energy of molecular diffusion and sorptive bonds [96]. Desorption kinetic energy is the sum of the thermodynamic energy of adsorption and the activation energy of absorption. Desorption kinetics of HOCs in soils have been proved to occur in two stages: an initial fast release phase (from minutes to hours) followed by a slower stage (from weeks to years) [97].

Adsorption to flat and rigid surfaces is generally inactivated or slightly activated with a very short lifetime [96]. Therefore, desorption of small molecules from rigid surfaces are not expected to be the reason for slow desorption of organic compounds.

Slow kinetics of desorption is generally described by molecular diffusion; that is, random movements of molecules caused by concentration gradient [96]. For the sorbed molecules to leave the porous particle, they need to pass through solid phases (matrix diffusion), pores within

the particle (pore diffusion), the liquid "film" on the solid surface (film diffusion), and the bulk liquid [96]. Currently, the most common model that explains desorption of organic compounds is based on diffusion in SOM [89]. Polymer theory is applied to explain diffusion through SOM assuming that SOM structure is similar to polymers. While the organic compounds diffusion through the glassy (hard) SOM is known to be fast, and the diffusion of organic compounds through the rubbery (soft) SOM is considered slow (the rate limiting step for desorption) [89]. Desorption data of molecular diffusion models are based on Fick's second law [89].

4.2 Experimental

4.2.1 Reagents and supplies

HPLC grade methanol was purchased from BDH (Toronto, ON, Canada). Naphthalene, acenaphthylene, acenaphthene, fluorene, phenanthrene, anthracene, fluoranthene, pyrene, benzo(b)fluoranthene, and benzo (a)pyrene were purchased from Supelco (Oakville, ON, Canada). Ultrapure water was collected from a Barnstead/Thermolyne NANO pure water system (Dubuque, IA, USA). Diethylamine was purchased from BDH (Toronto, ON, Canada). 99% aniline, HPLC grade acentonitrile and hexane were all provided by Sigma-Aldrich. The stock standard solutions of naphthalene, acenaphthene, acenaphthylene, fluorene, anthracene, fluoranthene, and pyrene (100 mg/l) were prepared in methanol. PAHs working standard solutions were prepared by appropriate dilutions of the mixing the standard stock solutions with methanol. All stocks and working standard solutions for PAHs were stored at 4 ℃.

The sand matrix was purchased from the EM science (NJ, USA). All the gases were supplied by Praxair (Kitchener, Canada). CRM 172-100 certified reference soil of was purchased from Sigma-Aldrich. 10 ml sample vials with magnetic crimp caps and PTFE coated silicone septa

were used for the automated analysis (Supelco). PDMS liquid polymer hollow tubing with a thickness of 178 μm was purchased from Dow Corning (Midland, MI, USA).

4.2.2 Instrumental

A CTC Combi PAL autosampler (Zwingen, Switzerland) with Cycle Composer software and a Varian 3800 gas chromatography (GC) coupled with FID were utilized for the sample analysis. The CTC Combi PAL autosampler was equipped with a temperature controlled six-vial agitator tray and a SPME syringe holder. Separations were performed using a 30 m×0.25 mm×0.25 μm SLB-5 fused silica column from Sigma-Aldrich. The carrier gas was helium and the flow rate was set at 1 ml/min. The GC injector was in a splitless mode with injector temperature was maintained at 250 ℃ for 5 min, and then increased at 1 ℃ /min to 270 ℃ and held constant until the end of the total run time.

For the analysis of seven PAHs (naphthalene, acenaphthylene, acenaphthene, fluorene, anthracene, fluoranthene, and pyrene) laboratory spiked samples in the sand, the column temperature was initially set at 50 ℃ for 1 min, then increased to 270 ℃ at a rate of 20 ℃ /min and held at 13 min. For the analysis of ten PAHs (naphthalene, acenaphthylene, acenaphthene, fluorene, phenanthrene, anthracene, fluoranthene, pyrene, benzo(b)fluoranthene, and benzo(a)pyrene) in certified reference soil , the column temperature was initially set at 50 ℃ for 1 min. It was increased to 200 ℃ at a rate of 10 ℃ /min and held at 13 min, and finally ramped at 20 ℃ /min to 270 ℃ and held constant until the end of the 50 min total run time. The detector temperature was set at 300 ℃ with gas flows for makeup gas (nitrogen), hydrogen, and high purity air set at 25, 30, and 300 ml/min, respectively. The automated cold fiber SPME system coupled with GC-FID coating was used for all experiments.

4.2.3 Experimental procedure

The experimental design involved an optimization the extraction of PAHs from laboratory spiked sand samples and the extraction of PAHs from certified reference soil samples. The optimization procedure was carried out by determining the optimized extraction time, sample temperature, and coating temperature.

Sand samples used in the optimization process were prepared by spiking 1 µl standard solution into 10 ml vials loaded with 1 g sand, capped immediately to prevent any possible losses. For the freshly spiked samples, the sample vials were put on a vertex for 1 min and analyzed 25 min after spiking; for the aged spiked samples, the samples were placed on a mechanical shaker (Fisher Vortex Genie) for 60 min, and stored at 4 ℃ for at least 14 days before the analysis. Each vial was used for one extraction.

The reference certified soil samples used in the extraction process were prepared by weighting 0.1 g soil into 10 ml empty vials, adding specific volume of modifier if required. The sample vials must be capped immediately to prevent any possible losses and then placed on a vertex for at least 1 min before the analysis.

After extraction, the fiber was transferred to a GC injector for thermal desorption. Desorption time was 5 min for the laboratory sand samples and 8 min for the certified reference soil samples. The longer desorption time chosen for the soil samples was meant to prevent any form of carryover.

4.3 Results and discussion

4.3.1 Effect of the pre-agitation

In the procedure of traditional extraction, pre-agitation at high temperatures was applied in order to accelerate the equilibrium between the sand matrix and the headspace. In this process prior to the extraction, the sample vial was agitated at a speed of 200 rpm for 15 min in the agitator of autosampler, which was normally set at a high temperature up to 200 ℃. After the extraction began, agitation was stopped and the fiber coating was exposed to the headspace for extraction. Agitation was not applicable during extraction because the external needle of the cold fiber was not flexible.

However, this high temperature pre-agitation (or preheating) resulted in a much higher temperature in the sample vial than room temperature. This temperature difference would lead to a pressure gap between the headspace of the sample vial and the ambient air before the extraction, which may result in a leakage during the needle piercing at the very beginning and the loss during the extraction. A proposed extraction procedure without pre-agitation process replaced the high temperature pre-agitation by a room temperature vortex prior to the extraction, and then immediately started extracting after the sample vial was put in the agitator.

Experiments with and without the pre-agitation were preformed to compare sand spiked PAHs samples with different spiking times, extraction temperatures, and extraction times. Figure 4-4 shows a typical result for the extraction. The extraction efficiency was calculated by dividing the amount of analytes extracted by the coating with the total amount of analytes originally present in the sample and multiplying this result by 100 to convert into percentage. Better extraction efficiency was shown for all compounds without the pre-agitation procedure than that of a previous 15 min agitation process, except in the case of naphthalene. Then the author repeated

the experiments comparing different extraction times and found that the extraction amount for naphthalene was very close under both extraction strategies. This can be explained that the extraction equilibrium for naphthalene was very fast to achieve, so this analyte was more easily to be absorbed by the low temperature coating rather than lost to the outside.

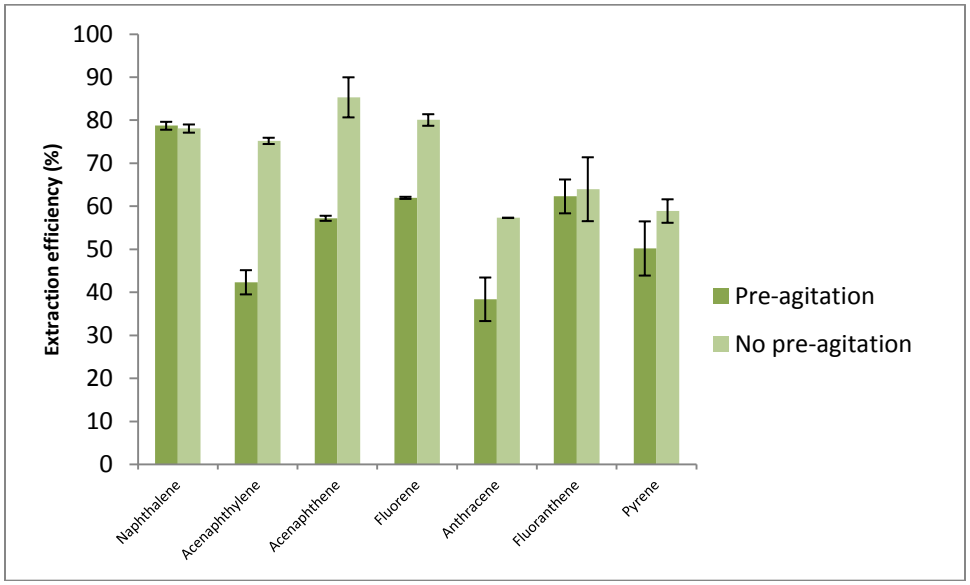

Figure 4-4 Extraction of PAHs from spiked sand samples with and without pre-agitation (T_s = 180 ℃, T_f = 30 ℃, t = 30 min).

4.3.2 Effect of the extraction temperature and extraction time without pre-agitation

Extraction time and temperature profiles for PAHs from spiked sand samples were studied by monitoring the extraction amounts of PAHs as a function of the extraction time and sample temperature using the cold fiber SPME system. The extraction results for fluorene and pyrene in Figure 4-5 represent the extraction efficiency for typical volatile compounds and semi-volatile compounds respectively. The increase in the extraction amounts observed corresponded with the increase of the sample temperature. For volatile compounds, the increases in the extraction

amounts were less significant at the higher sample temperatures compared to that at the lower temperatures. For high boiling point compounds, however, the increasing rates of the extraction amounts were around ten times higher at 200 ℃ than the extraction amounts when the sample was at 80 ℃. For extraction time profiles of PAHs in sand samples from 5 to 120 min, the extraction amounts increased with a longer extraction time.

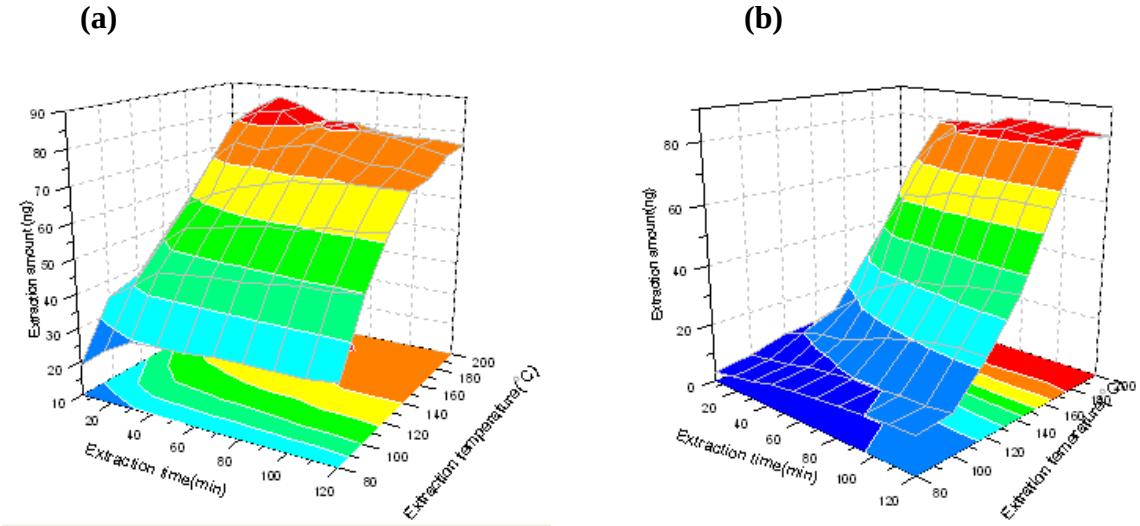

Figure 4-5 Extraction amounts at different extraction times and temperatures for (a) fluorene and (b) pyrene without pre-agitation (T_s = 80-200 ℃, T_f = 30 ℃, t = 5-120 min).

The optimized extraction sample temperature for PAHs in this case was 200 ℃ based on the highest extraction amounts for all analytes. The optimized extraction time was selected to be 30 min since too long of the extraction time should be avoided for method optimization. However, compared to the theoretical value, the extraction amounts at optimized temperature and time were still low in Figure 4-6. In exhaustive extraction, 90% of the total molecules of analytes should be extracted. Only fluoranthene in all seven compounds achieved the exhaustive extraction level. Therefore, new extraction strategies are required to achieve better extraction efficiencies for all target compounds.

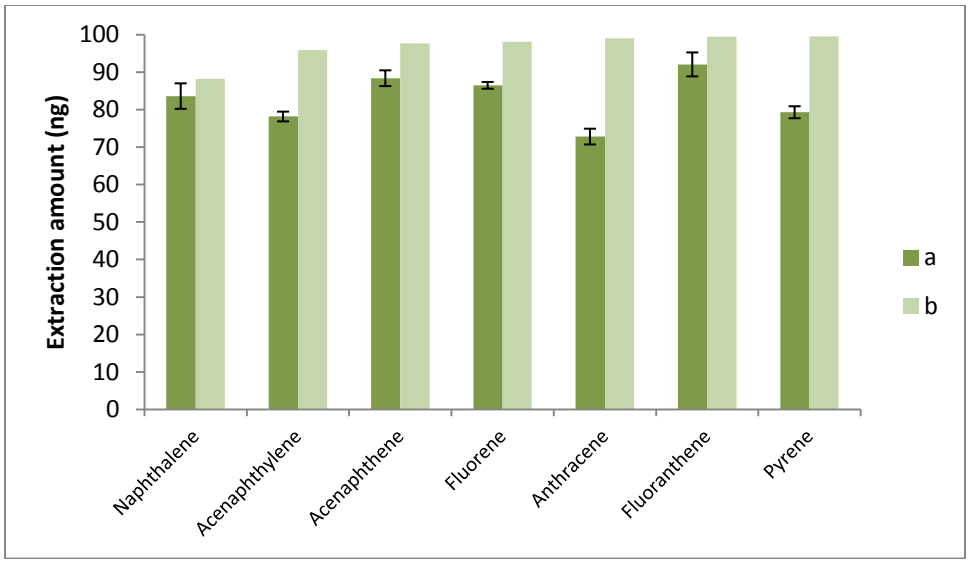

Figure 4-6 Extraction amounts for PAHs under optimized extraction condition compared with the theoretical calculation. (a) PAHs from spiked sand samples (T_s = 200 ℃, T_f = 30 ℃, t = 30 min) and (b) the theoretical calculation at the same condition (Calculation see chapter 3).

4.3.3 Multivariate optimization of the extraction strategy

For the analysis of mixture PAHs with different volatilities, the main objective in this section is to improve the extraction efficiencies for all compounds in a minimal extraction time. For volatile compounds, decreasing the coating temperature can increase the partition coefficient of the compounds with PDMS coating, which is in agreement with Equation 1-2. For heavier compounds such as pyrene, on the other hand, a relatively higher coating temperature could yield higher extraction amounts within a shorter extraction time. To achieve better extraction efficiency for all target compounds with different volatilities, keeping the coating temperature constant at a relatively higher temperature for some time, and then cooling the coating to a lower temperature during the extraction is an effective strategy [69].

This extraction strategy of changing coating temperatures can be referred to as “programmed coating temperature”, in contrast with the traditional constant coating temperature method. See Figure 4-7 for the comparison with the extraction efficiency for these two methods.

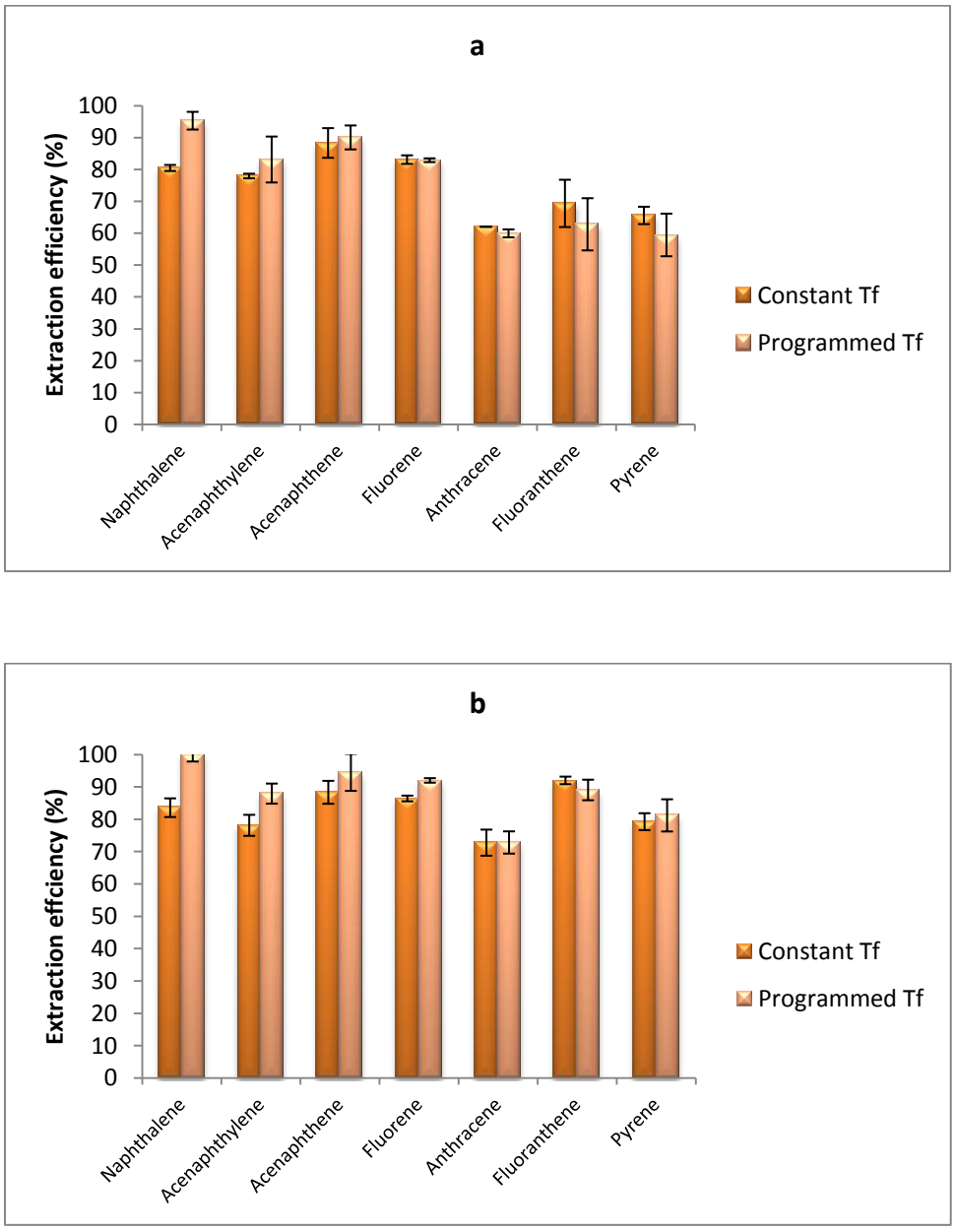

Figure 4-7 Comparison of the extraction efficiency for PAHs with constant coating temperature and programmed coating temperature at a: T_s = 180 ℃ and b: T_s = 200 ℃. (T_f = 30 ℃ for 30 min for constant fiber temperature, T_f = 30 ℃ for 25 min and then 10 ℃ for last 5 min for programmed fiber temperature, total extraction time 30 min for all extractions.)

For volatile compounds, i.e. naphthalene and acenaphthylene, the extraction efficiency with the programmed coating temperature method was higher than that of the traditional constant coating temperature method. The optimum coating temperature for these compounds was lower than 30

℃. The extraction results for semi-volatile compounds were similar with or slightly lower with the new programmed coating temperature method than that with the traditional constant coating temperature method. However, this programmed coating temperature method can shorten the equilibrium time for those compounds.

The programmed coating temperature method led to higher extraction efficiency for most studied analytes compared to the traditional methods. Further studies were focused on the optimization of the extraction with the programmed coating temperature method to obtain the ultimate extraction efficiency. Several parameters should be taken into consideration here: sample temperature (T_s), total extraction time (t), first stage coating temperature (T_{f1}) and time (t_1), second stage coating temperature (T_{f2}), and time (t_2).

4.3.3.1 Optimization of T_s and T_{f1}

Sample temperature is an important parameter for desorption of the analytes from the matrix into the headspace and then diffusion through the fiber coating. Higher temperatures can accelerate the compounds, especially the heavier analytes, to release from binding with the solid matrix. Extraction temperature profiles for PAHs in sand samples were studied in the last section, which showed that 200 ℃ was the optimum extraction temperature for extraction of PAHs from the sand matrix.

In order to maximize the value of partition coefficient at a constant sample temperature, it is very important to get a greater temperature gap between the sample and the fiber coating. For volatile compounds, the extraction efficiency can be improved by cooling down the coating temperature, and the equilibrium can be reached very fast. However, in case of semi-volatile compounds at a lower coating temperature, a longer extraction time is required to reach the equilibrium.

Therefore, in order to achieve equilibrium in a short extraction time for those compounds, the coating temperature cannot be too low. 30 ℃ was selected as the first staged coating temperature due to the behavior of these compounds under the different coating temperatures.

4.3.3.2 Optimization of t

Extraction time profiles for PAHs from spiked sand samples with programmed coating temperature were studied by monitoring the extraction efficiency of PAHs as a function of the extraction time using the cold fiber SPME system. As results show in Figure 4-8, the extraction efficiency was around 100% for naphthalene with different total extraction times, which indicates that the lower temperature in last 5-10 min in the extraction was the most important step for these compounds to be extracted by the coating. For acenaphthylene, acenaphthene and fluorene, the effects of the different extraction times were not significant. This is due to the fast partition equilibrium between the headspace and the extraction phase for those compounds. For the semi-volatile compounds such as anthracene, fluoranthene, and pyrene, a longer extraction time improved extraction efficiency, which is because long extraction time was required to reach the partition equilibrium for those compounds.

Those results indicate that the optimum extraction conditions for the volatile compounds meant cooling down the coating temperature during extraction while optimum extraction conditions for semi-volatile compounds involved a longer extraction time. Therefore, a combination of those two conditions could have a good result for all the compounds. Considering the extraction efficiency for all compounds, too long extraction time should be avoided in method optimization. Since a total extraction time of 45 min had good extraction efficiency for most compounds, 45 min was selected as the total extraction time in method optimization.

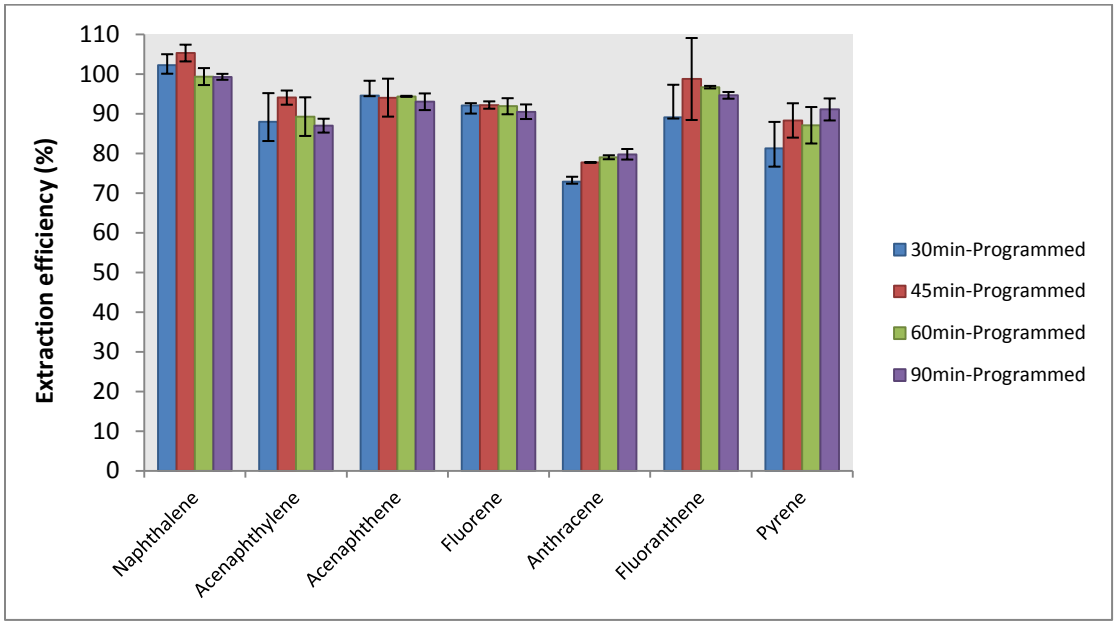

Figure 4-8 Comparison of the extraction efficiency for PAHs with programmed coating temperature at different extraction times from 30 min to 90 min (T_s = 200 ℃).

[30min-programmed]: keep coating temperature at 30 ℃ for 25 min and then at 10 ℃ for 5 min.
[45min-programmed]: keep coating temperature at 30 ℃ for 40 min and then at 10 ℃ for 10 min.
[60min-programmed]: keep coating temperature at 30 ℃ for 50 min and then at 10 ℃ for 10 min.
[90min-programmed]: keep coating temperature at 30 ℃ for 80 min and then at 10 ℃ for 10 min.

4.3.3.3 Optimization of t_2 and T_{f2}

In the previous sections, the optimized sample temperature and first staged coating temperature were 200 ℃ and 30 ℃ respectively, and the total extraction time was 45 min. In this section, the optimization of the second staged extraction time and temperature need to be determined to maximize the extraction efficiency. In the selection of the second staged coating temperature, other parameters were fixed and the second staged coating temperatures were set from 5 to 30 ℃.

The extraction efficiency did not show significant difference with different T_{f2} in Figure 4-9, but the result with 5 ℃ as the second coating temperature was not as good as that of other

temperatures except in the case of naphthalene, which indicated that low coating temperature was favored for volatile compounds. For most compounds, extraction efficiency with 10 ℃ as the second staged coating temperature was slightly better than that of other coating temperatures. Those results indicated that the optimum coating temperature was related to the volatility of the compounds. The lower coating temperature was preferred for higher volatile compounds, and the higher optimum coating temperature during the extraction was beneficial for the semi-volatile compounds. 30 ℃ and 10 ℃ were selected as the first and the second staged coating temperature while keeping the total extraction time at 45 min.

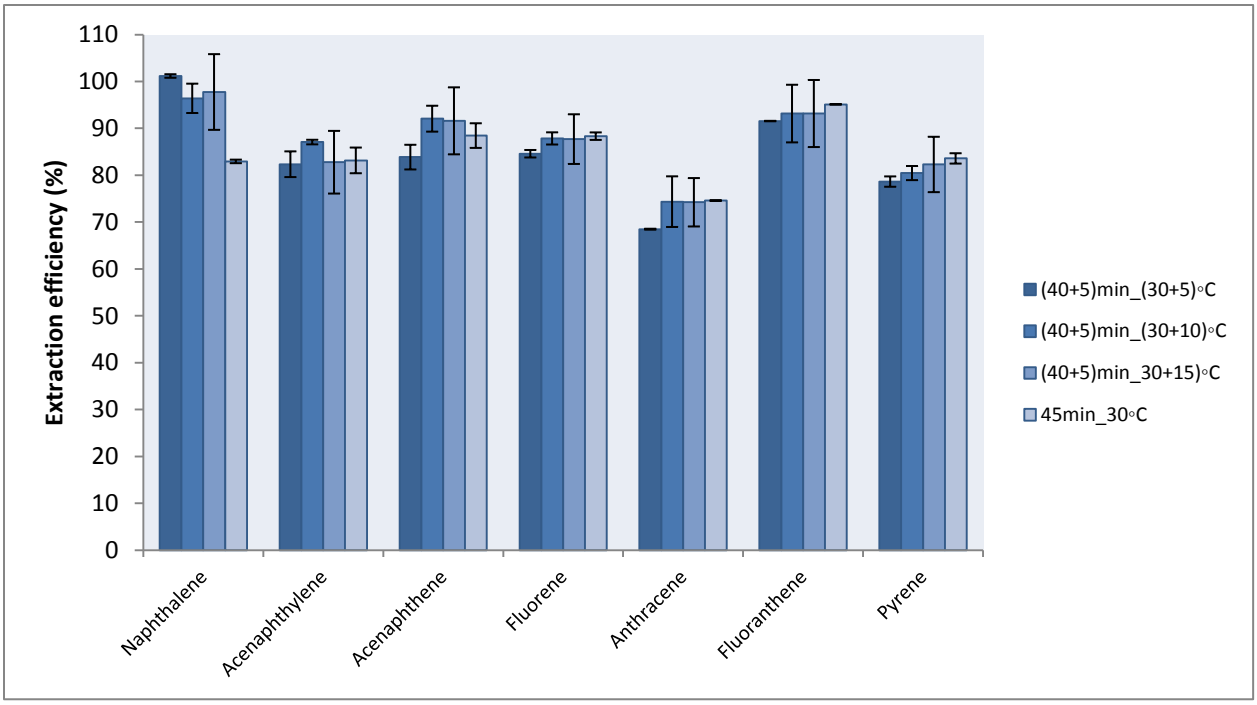

Figure 4-9 Comparison of the extraction efficiency for PAHs with different second staged coating temperatures (T_s = 200 ℃, T_{f1} = 30 ℃, t = 45 min).

[(45+5) min_ (30+5) ℃]: keep coating temperature at 30 ℃ for 40min and then at 5 ℃ for 5 min.
[(45+5) min_ (30+10) ℃]: keep coating temperature at 30 ℃ for 40min and then at 10 ℃ for 5 min.
[(45+5) min_ (30+15) ℃]: keep coating temperature at 30 ℃ for 40min and then at 15 ℃ for 5 min.
[45 min_30 ℃]: keep coating temperature at 30 ℃ for 45 min.

In the selection of the second staged coating time, the procedure involved fixing the sample temperature at 200 ℃ and the total extraction time at 45 min; keeping the first staged coating temperature T_{f1} at 30 ℃ and the second staged temperature T_{f2} at 10 ℃. The only flexible parameter was the time of the second staged program, which was set from 0 to 15 min. With the total extraction time fixed, a short extraction time at lower coating temperature was preferred for semi-volatile compounds because those compounds required a longer time for partition under that condition. On the other hand, volatile compounds like naphthalene were beneficial from a lower coating temperature. Overall, the extraction for PAHs had the best result with second staged temperature at 10 ℃ for 10 min.

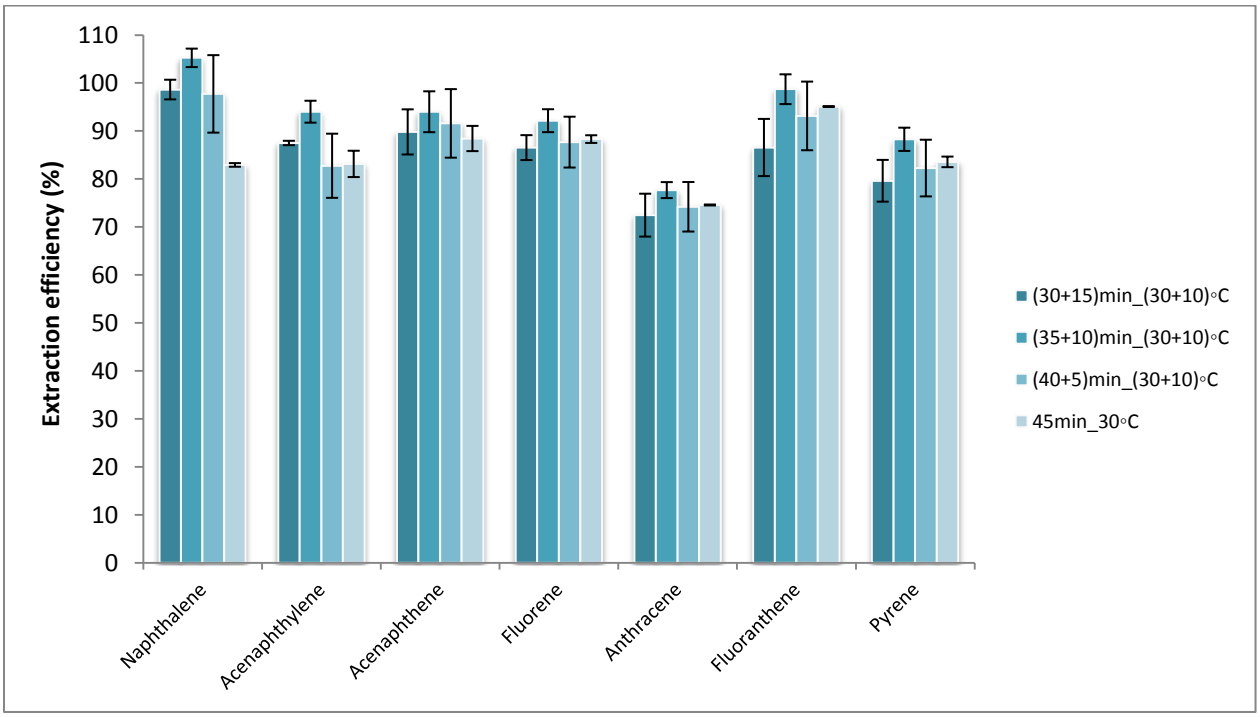

Figure 4-10 Comparison of the extraction efficiency for PAHs with different second staged coating times (T_s = 200 ℃, T_{f1} = 30 ℃, T_{f2} = 10 ℃, t = 45 min).

[(30+15) min_ (30+10) ℃]: keep coating temperature at 30 ℃ for 30 min and then at 10 ℃ for 10 min.
[(35+10) min_ (30+10) ℃]: keep coating temperature at 30 ℃ for 35 min and then at 10 ℃ for 10 min.
[(40+5) min_ (30+10) ℃]: keep coating temperature at 30 ℃ for 40 min and then at 10 ℃ for 5 min.
[45 min_30 ℃]: keep coating temperature at 30 ℃ for 45 min.

4.3.3.4 Optimized extraction condition for multivariate optimization

The optimized extraction condition for multivariate optimization was as following: the sample temperature was 200 ℃; the coating temperature was kept at 30 ℃ for 35 min, and then switched to 10 ℃ for 10 min with a total extraction time of 45 min. Under this optimized condition, the recoveries for naphthalene and fluoranthene were around 100% while more than 90% for other compounds except anthracene. Six of seven selected compounds were quantitative extracted with this optimized method.

Table 4-2 Optimized extraction condition for PAHs from laboratory spiked samples.

200◦C	•Sample temperature
45min	•Total extraction time
30 ◦C for 35min	•T_{f1} temperature and time
10◦C for 10min	•T_{f2} temperature and time

Figure 4-11 compares the extraction amounts for PAHs with the proposed programmed coating temperature strategy, the traditional constant coating method, and the calculation values. Extraction amounts increased by 10-20% for all analytes using the programmed coating temperature strategy compared to the traditional extraction methods. Therefore, this proposed programmed coating temperature strategy has improved the extraction efficiency for all target analytes compared to the traditional constant coating method.

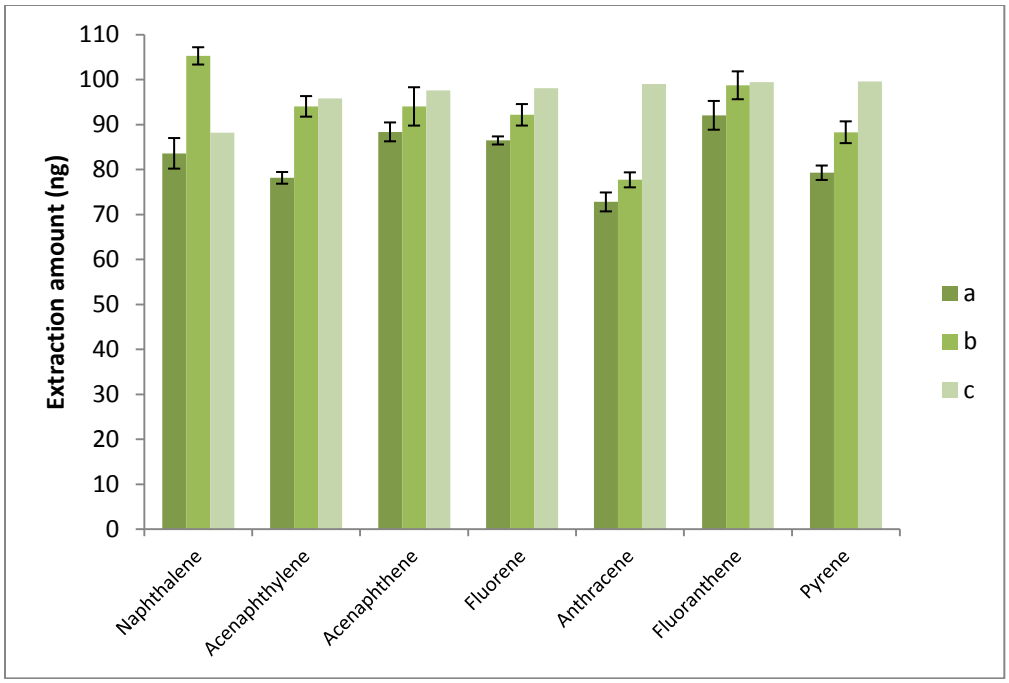

Figure 4-11 Comparison of the extraction amount for PAHs under different extraction strategies compared with theoretical calculation. (a) Optimized constant coating method (T_s = 200 ℃, T_f = 30 ℃, t = 30 min), (b) Optimized programmed coating method (T_s = 200 ℃, fiber temperature: keeping 30 ℃ for 30 min and cooling to 10 ℃ for 15 min), and (c) Theoretical calculation at the same condition.

For naphthalene, the extraction amount with the proposed method was higher than that of calculation. This could be explained as the temperature of the fiber coating during the extraction was not uniform, which means that it will always reached a lower temperature than preset before turning off the solenoid valve in a cycle. The ratios between the extraction amounts of acenaphthylene, acenaphthene, fluorene and fluoranthene to that of the theoretical calculation were 99%, 97%, 94%, and 99%, which illustrated that the high extraction efficiency can be obtained with the cold fiber SPME system. For pyrene, around 90% of total molecules were extracted under this optimized method. Due to the lower volatility of pyrene and strong bonds with the sand matrix, its recovery can be higher if more molecules can be released into the headspace from the sand matrix. However, only around 80% of the total molecules were extracted for anthracene, which was not surprising since the recovery for the optimized tradition method was even lower. This may be caused by the strong interaction of anthracene with the

sand matrix. Higher sample temperatures and/or the addition of a modifier could help the analyte to desorb from the matrix.

4.3.4 Determination of PAHs from soil samples

In real soil sample analysis, the extraction amount is strongly influenced by the interactions between the analytes and the soil matrix. Quantitative analysis in soil model is not feasible unless a nearly exhaustive extraction can be realized. Ordinary headspace SPME is less suited for accurate quantitative measurements of semi-volatile compounds in soil. Cold fiber SPME could be a good solution for the extraction of those compounds from soil matrix.

In this section, cold fiber SPME was applied to extract PAHs from soil. The soil sample in this study was the certified reference loamy soil containing PAHs with referenced concentration. The reference certified soil samples were prepared by weighting a specific amount soil into 10 ml empty vials, adding a small amount of modifier if required. The sample vial must be capped immediately to prevent any possible losses and then placed on vertex for minimize 1 min before the analysis.

Different amounts of reference soils from 50 mg to 1 g were analyzed using cold fiber SPME. The sample and coating temperatures were 200 ℃ and 30 ℃, and the extraction time was 30 min. The results revealed that by using more than 100 mg of the sample, a hump shape baseline was evident in the chromatogram (from 5 to 20 min). However, if the sample amount was too small, the detection amount was reduced. Therefore, 100 mg was used as the sample mass for the extraction.

Initially the extraction was conducted without adding any modifier. For most volatile analytes, the recoveries were only more than 50%, and for some semi-volatiles, the recoveries were even

less than 20%. This can be explained by the strong binding between the soil matrix and the analytes, especially for the heavier compounds. Two approaches can accelerate the release of those compounds from the matrix: increasing desorption energy by higher sample temperatures, and/or adding an organic modifier. Since the extraction temperature for sample was 200 ℃, which was the highest temperature that the system can reach. Therefore, in order to improve the extraction efficiency, organic modifiers were added into the soil sample for better desorption.

Small amounts of acetonitrile, hexane, acetic acid, aniline and diethylamine were added to soil samples. The extraction time was 30 min with the sample and coating temperatures were 200 ℃ and 30 ℃ respectively for all samples. Table 4-3 illustrates the comparison of extraction amounts with the addition of different modifiers. The addition of acetonitrile, hexane, and acetic acid did not show significant improvement in the extraction efficiency. But after adding amines, on the other hand, the extraction amounts were dramatically increased, especially for the heavier PAHs.

Table 4-3 Comparison of the extraction amounts of PAHs from soil with/without modifiers.

Extraction amount (ng/g)	Certified value	No modifier	Acetonitrile 5 µl	Hexane 5 µl	Acetic acid 2 µl	Aniline 1 µl	Diethylamine 1 µl
Naphthalene	140 ±38	64	88	68	—	—	**110**
Acenaphthylene	55 ±18	41	45	41	41	—	**69**
Acenaphthene	95 ±25	33	34	35	32	—	**124**
Fluorene	66 ±11	40	56	46	42	—	**53**
Phenanthrene	168 ±7	61	113	64	—	228	**126**
Anthracene	18 ±3	44	—	56	47	—	**92**
Fluoranthene	634 ±82	70	142	72	—	263	**128**
Pyrene	86 ±13	49	49	—	—	83	**89**
Benzo(b)fluoranthene	177 ±25	105	118	113	—	105	**128**
Benzo (a)pyrene	34 ±11	—	—	—	—	20	**—**

Note: "—" in the table indicates not detectable.

Since aniline and diethylamine can have strong interactions with PAHs in the soil, which significantly enhanced the extraction efficiency. The boiling point of aniline is close to that of the first four low-molecular PAHs, so the huge peak of aniline in chromatogram interfered with the peaks of those analytes. Interestingly, diethylamine was used successfully to enhance the recoveries of high molecular weight PAHs because it was capable to interact with the aromatic rings of the PAHs and release them from the carbon-rich matrix.

After selecting diethylamine as the modifier, the author investigated the different addition volumes and extraction times to explore the optimum extraction condition. With the extraction time fixed at 30 min, 1-10 μl diethylamine was added. The result revealed that a larger volume of diethylamine would increase the extraction amounts for heavier analytes. However, after adding too much diethylamine, there were huge interferences with retention time at 5-20 min, so the first 3-4 analytes were mixed with the interferences.

For the different extraction time up to 90 min with the volume of diethylamine was fixed at 2 μl, the extraction amounts showed increasing trend for most compounds with a longer extraction time. However, with too long extraction time, similar to the addition of a large volume of diethylamide described before, the huge interferences appeared in first 20 min in the chromatogram. Those interferences appeared with a large addition volume of diethylamine and/or a long extraction time. Figure 4-12 and 4-13 are the typical chromatograms for the extraction in certified reference soil without and with interferences.

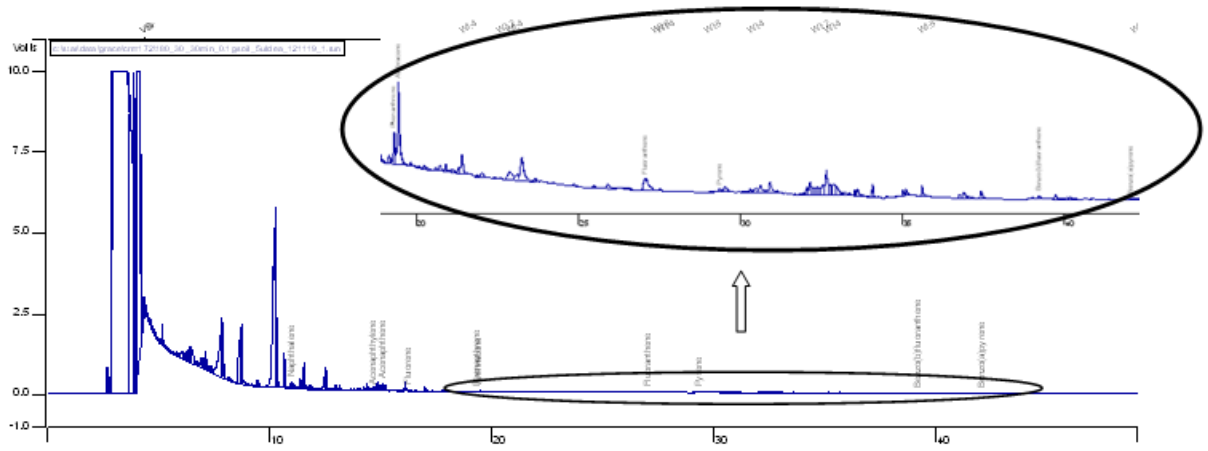

Figure 4-12 Typical chromatogram for PAHs in certified reference soil without interferences.

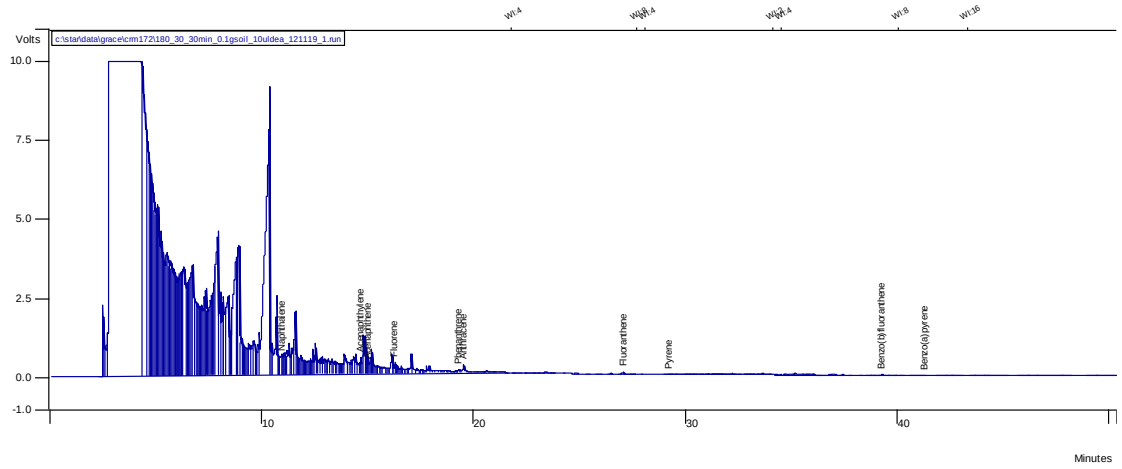

Figure 4-13 Typical chromatogram for PAHs in certified reference soil with interferences.

Therefore, to optimize the extraction of all compounds, 5 μl diethylamide was added (too large of the addition volume would cause the interference problems) and the total extraction time was set at 45 min (too long of the extraction time would cause the interference problems). The coating temperature was the programmed coating temperature referred to the previous sections, that was 50 ℃ for first 35 min (optimized for extraction larger molecular weight compounds without extracting interferences) and 30 ℃ for the last 10 min (optimized for extraction lighter

compounds for short time without extracting too much interferences). As the results in Figure 4-14, satisfactory extraction amounts were obtained by the proposed method.

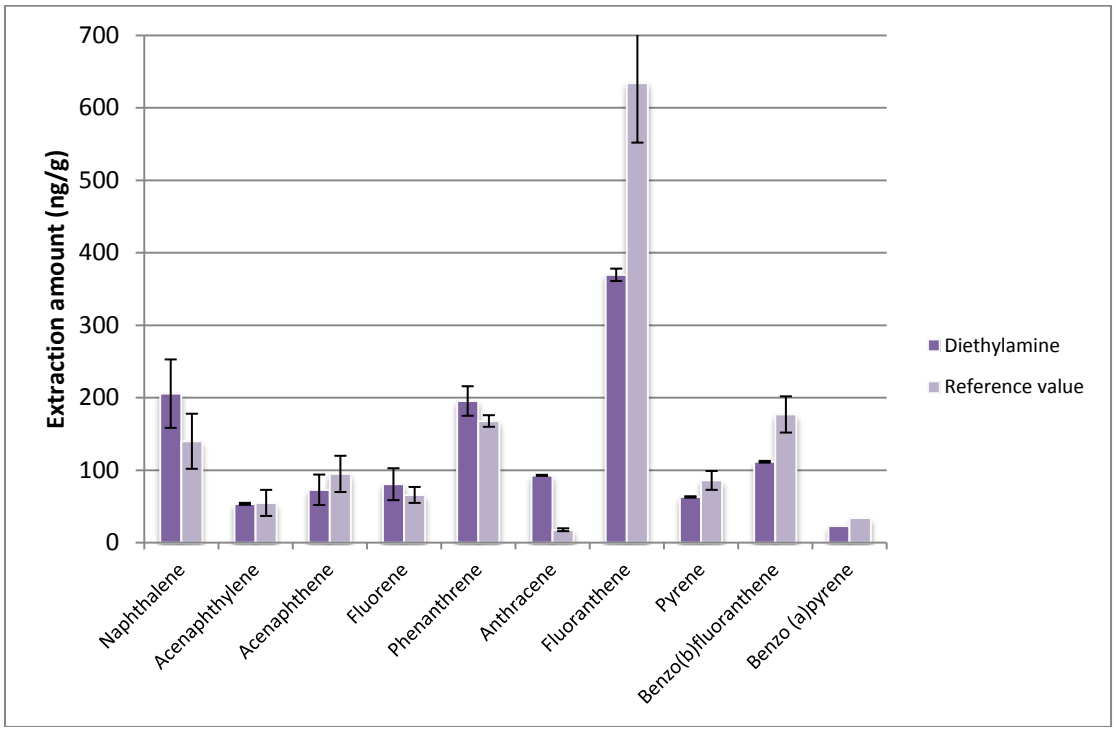

Figure 4-14 Comparison the extraction amounts for PAHs in certified reference soil with addition of diethylamide under optimized condition (T_s= 200 ℃, fiber temperature: keeping 50 ℃ for 35 min and cooling to 30 ℃ for 10 min), and the reference value.

Among the ten analytes investigated, extraction amounts for the first five PAHs (naphthalene, acenaphthylene, acenaphthene, fluorene, and phenanthrene) agreed with the reference values. The exhaustive extraction was realized for those analytes with the cold fiber SPME. For anthracene, however, the extraction amount with the proposed approach was much higher than that of the referenced value; this could be caused by the inference peak which may appear to have nearly the same retention time as the target compound. Mass spectrum is required for the further clarification of the possible inference peaks. The recoveries of fluoranthene, pyrene,

benzo(b)fluoranthene, and benzo(a)pyrene were around 60-75%. Considering the strong binding of those semi-volatile compounds with the soil matrix, these recoveries were acceptable. For all ten analytes investigated, satisfactory extraction amounts were met by the proposed method.

4.4 Conclusion

The comparison of extraction with and without pre-agitation revealed that the better extraction efficiency was achieved without pre-agitation for almost all compounds. After investigating the effects of extraction time and temperature, all compounds showed an increase in the extraction amounts, which corresponded with an increasing of the sample temperature and a prolonging of the extraction time.

In order to obtain better extraction amounts for PAHs, the programmed coating temperature method was developed, which led to higher extraction efficiencies for most studied analytes compared to the traditional methods. After the optimization of extraction with the programmed coating temperature method, the recoveries were around 100% for naphthalene and fluoranthene, and more than 90% for other compounds except anthracene. Six of seven selected compounds were quantitative extracted with this optimized method.

In real sample analysis, certified reference soils were analyzed using the proposed cold fiber SPME system. However, in the initial extraction without adding any modifier, recoveries for PAHs in the soil were very low. Several organic modifiers were added to improve the extraction efficiency. Among them, diethylamine was used successfully to realize the exhaustive extraction for volatile compounds and to enhance the recoveries to around 60-75% for semi-volatile compounds. Satisfactory extraction amounts were achieved for all compounds by the proposed method after the method optimization.

Chapter 5
Summary

5.1 Cold Fiber SPME

SPME is a simple, solvent-free, and reliable extraction technique that combines sampling, sample preparation, and pre-concentration into a single step before the chromatographic analysis. The headspace SPME technique has been widely used for the analysis of environmental pollutants in solid samples. Most applications have been assisted by sonication and microwaves due to the strong binding of the analytes with the solid matrix. The simplest and most effective way for desorption to take place is to heat the sample at a high temperature, which decreases the distribution coefficients of the analytes between the fiber coating and the sample matrix, and leads to poor extraction amounts.

The cold fiber SPME device was developed to overcome this drawback. In this system, the sample matrix is heated to a high temperature to accelerate desorption of the analytes from matrix; simultaneously, the fiber coating is kept cool to increase the distribution coefficients of

the analytes between the headspace and the extraction phase. In this heating-cooling system, a temperature gap is created between the hot sample/headspace and the cold fiber coating, which significantly increases the extraction efficiency.

The cold fiber SPME has been applied to many areas, but most target analytes was volatile compounds. More studies are required to extract both volatile and semi-volatile compounds from a complex solid matrix.

5.2 Contributions of this thesis

The cold fiber SPME system was improved by minimizing the coating temperature fluctuation range, and the performance of the system was evaluated by investigating the extraction of PAHs from spiked sand samples. The coating temperature can be controlled in ± 3 ℃ around the preset value and the RSDs were smaller than 2% for six in seven target analytes. A simplified cold fiber system without the solenoid valve was modified to connect CO_2 delivery tubing directly to the liquid CO_2 tank. The robustness of this system was evaluated with different sizes of CO_2 delivery tubings. The system is stable, low cost, and can easily be controlled, which provides a supplementary extraction strategy besides the traditional cold fiber system.

The partition coefficient for the analyte was calculated theoretically and the extraction amount of the analyte in a specific system was estimated in advance. The extraction amount of the experiment agreed with that of the calculation result. The cold fiber system was verified ideal if assumed that only the headspace and the extraction phase existed in the system. By using theoretical calculations for guidance, desorption efficiency for aged spiked samples was investigated. Enhancing the sample temperature was effective for increasing desorption of the analytes from the interacted matrix, and finally increased the extraction amount.

In order to achieve better extraction amounts for PAHs, the programmed coating temperature method was developed and optimized, which led to recoveries of more than 90% for six of seven selected compounds. In real sample analysis, certified reference soils were analyzed using cold fiber SPME. Diethylamine was added successfully to realize the exhaustive extraction for volatile compounds and to enhance the recoveries up to 75% for semi-volatile compounds. Satisfactory extraction amounts for all compounds were achieved with the proposed method after optimization.

5.3 Prospective

The fiber temperature evaluation results of the simplified system without the solenoid valve clearly demonstrate that this system has the potential to be applied to extract various samples. The distribution curve of fiber temperature and sample temperature can be seen as the basis for the selection of tubings. This simplified system can be applied in long time extraction, from several hours to several days.

The proposed method for traditional cold fiber SPME in environmental studies can be extended to investigate the desorption kinetics of organic chemicals from different solid matrices. For example, this system can be applied to extract n-alkanes, which are considered geological markers, from soils or rocks.

Currently, PDMS is the only coating for cold fiber system. If more coating types, especially the polar coatings, can be developed, the applications for this system will be broadened to various target analytes.

References

[1] J. Pawliszyn, J. Chromatogr. Sci., 31, 31-37, 1993.

[2] D. Louch, S. Motlagh, J. Pawliszyn, Anal. Chem., 64, 1187-1199, 1992.

[3] J. Pawliszyn, Sampling and Sample Preparation for Field and Laboratory, Elsevier, Amsterdam, 2002.

[4] J. Pare, J. Belanger, K. L. Stafford, S. J. Microcolumn. Sep., 7, 37-41, 1995.

[5] S. C. Lee, K.F. Ho, L.Y. Chan, et al., Atmos. Environ., 35, 5949-5960, 2001.

[6] T. Chetwittayachan, D. Shimazaki, K. Yamamoto, E. Atmosn., 36, 2027-2037, 2002.

[7] P. Yang, B. F. Gong, Y. Xiong, et al., Environ. Monit. China., 15, 1-20, 1999.

[8] B. E. Richter, et al., Anal. Chem., 68, 1033-1041, 1996.

[9] E. Bjorklund, T. Nilsson, S. Bowadt, Trends. Anal.Chem., 19, 434-445, 2000.

[10] M. M. Schantz, J. J. Nichols, S. A. Wise, Anal. Chem., 69, 4210-4219, 1997.

[11] M. Letellier, H. Budzinski, J. Bellocq, J. Conan, Org.Geochem., 30, 11, 1353-1365, 1999.

[12] M. Letellier, H. Budzinski, Analusis, 27, 3, 259-271, 1999.

[13] W. Wang, B. Meng, X. Lu, Y. Liu, S. Tao, Anal. Chim. Acta., 602, 2, 211-222, 2007.

[14] J. R. J Pare, J. M. R. Belanger, S. S. Stafford, Trends Anal. Chem., 13, 176-181, 1994.

[15] O. F. X. Donard, B. Lalere, F. Martin, R. Lobinski, Anal. Chem., 67, 4250-4258, 1995.

[16] C. Vale ère, Trends Anal. Chem., 19, 4, 229-231, 2000.

[17] Y. Y. Shu, R. C. Lao, C. H. Chiu, and R. Turle, Chemosphere, 41, 11, 1709-1716, 2000.

[18] S. E. Manahan, Environmental Chemistry, CRC Press, Boca Raton, Fla, USA, 8th edition, 2005.

[19] C. A. Meyer, American Society of Mechanical Engineers, New York, 1993.

[20] S. B. Hawthorne, Y. Yang, D. J. Miller, Anal. Chem., 66, 2912-2920, 1994.

[21] N. Itoh, M. Numata, Y. Aoyagi, T. Yarita, Anal. Chim. Acta., 612, 44, 2008.

[22] E. Moreno, J. Reza, A. Trejo, Polycycl. Aromat. Compd., 27, 239-251, 2007.

[23] D.W. Armstrong, Sep. Purif. Methods., 14, 213-225, 1982.

[24] V. Pino, J.H. Ayala, A.M. Afonso, V. Gonz ález, Talanta, 54, 15-22, 2001.

[25] V. Pino , V. Gonz ́alez, A. M. Afonso, J. Chromatogr. A., 1182, 145-152, 2008.

[26] E. V. Lau, S. Gan, H. K. Ng, Int. J. Ana. Chem., Article ID 398381, 2010.

[27] D. K. Banerjee, M. R. Gray, Environ. Sci. Technol., 31, 3, 646-650, 1997.

[28] N. Itoh, M. Numata, Y. Aovagi, T. Yarita, Anal. Chim. Acta., 612, 1, 44-52, 2008.

[29] P. Sun, L. K. Weavers, P. Taerakul, H.W. Walker, Chemosphere. 62, 2, 265-274, 2006.

[30] V. Lopez-Avila, R. Young, Anal. Chem., 66, 7, 1097-1106, 1994.

[31] L. Xu, H. K. Lee, J. Chromatogr. A., 1192, 2, 203-207, 2008.

[32] L. Ramos, J. J. Vreuls, U. A. T. Brinkman, J. Chromatogr. A., 891, 2, 275-286, 2000.

[33] M. Elektorowicz, T. Ayadat, J. Colloid. Interface. Sci., 309, 2, 445-452, 2007.

[34] E. Moreno, J. Reza, A. Trejo, Polycycl. Aromat. Compd., 27, 239, 2007.

[35] S. H. Haddadi, V. H. Niri, J. Pawliszyn, Anal. Chim. Acta., 652, 224-230, 2009.

[36] B. Vrana, D.Allan, R. Greenwood, G. A. Mills, et al., Trends Anal. Chem., 24, 845-858, 2005.

[37] T. Gorecki, J. Pawliszyn, Anal. Chem., 67, 3265-3274, 1995.

[38] K. Ridgway, S. P. D. Lalljie, R. M. Smith, J. Chromatogr. A., 1153, 36-53, 2007.

[39] R. Eisert, J. Pawliszyn, Anal. Chem., 60, 31-40, 1997.

[40] M.R. Negra˜o, M. de Fa´tima Alpendurada, J. Chromatogr. A., 823, 221-228, 1998.

[41] W. Wardencki, J. Curyło, J. Namieśnik, J. Biochem. Biophys. Methods, 70, 275-288, 2007.

[42] R. J. Krupadam, B. Bhagat, M.S. Khan. 397, 3097-106, 2010.

[43] J. A. Koziel, M. Odziemkowski, J. Pawliszyn, Anal. Chem., 73, 47-54, 2001.

[44] J. Pawliszyn, Solid Phase Microextraction -Theory and Practice, Wiley-VCH, New York, 1997.

[45] T. Górecki, X. Yu, J. Pawliszyn, Analyst, 124, 643-649, 1999.

[46] Z. Zhang, J. Pawliszyn, Anal. Chem. 67, 34-43, 1995.

[47] G. Ouyang, J. Pawliszyn, Anal. Bioanal. Chem. 386, 1059-1071, 2006.

[48] R. Dungan, Anal. Lett., 38, 2393-2405, 2005.

[49] O. Ezquerro, G. Ortiz, B. Pons, M.T. Tena, J. Chromatogr. A., 1035, 17-22, 2004.

[50] C. Devos, M. Vliegen, B. Willaert, F. David, et al., J.Chromatogr.A., 1079, 408-414, 2005.

[51] S. Fuster, J. Beltran, F. J. Lopez, F. Hernandez, J. Sep. Sci., 28, 98-103, 2005.

[52] K. J. Chia, T. Y. Lee, S. D. Huang, Anal. Chim. Acta., 527, 157-162, 2004.

[53] J. Carpinteiro, I. Rodriguez, R. Cela, Anal. Bioanal. Chem., 380, 853-857, 2004.

[54] P. Rearden, P. B. Harrington, Anal. Chim. Acta., 545, 13-20, 2005.

[55] A. Navalon, A. Prieto, L. Araujo, J. L. Vilchez, Anal. Bioanal. Chem., 379, 1100-1105, 2004.

[56] M. C. Wei, J. F. Jen, J. Chromatogr. A., 1012, 111-118, 2003.

[57] E. Carasek, J. Pawliszyn, J. Agric. Food. Chem., 54, 8688-8696, 2006.

[58] Y. Chen, F. Begnaud, A. Chaintreau, J. Pawliszyn, J. Sep. Sci., 30, 1037-1043, 2007.

[59] E. Carasek, E. Cudjoe, J. Pawliszyn, J. Chromatogr. A., 1138, 10-17, 2007.

[60] A. R. Ghiasvand, L. Setkova, J. Pawliszyn, Flavour. Frag. J., 22, 377-391, 2007.

[61] A. Ghiasvand, S. Hosseinzadeh, J. Pawlisyn, J. Chromatogr. A., 1124, 35-42, 2006.

[62] Y. Chen, J. Pawliszyn, Anal. Chem., 78, 5222-5226, 2006.

[63] PhD thesis, Y. Chen, New Calibration Approaches in SPME for On-site Analysis, 2004.

[64] Industrial Valve Resource, Miniature Solenoid Valves for Medical Devices. http://industrialvalveresource.com/category/valves/new-product-releases.html#item1186.

[65] Solenoid Valves in Wikipedia, http://en.wikipedia.org/wiki/Solenoid_valve.

[66] CO_2 Tanks, http://www.reefscapes.net/articles/breefcase/co2_tanks.html.

[67] J. C. M. Li, J. Chem. Phys., 25, 572-574, 1956.

[68] Z. Zhang, J. Pawliszyn, Anal. Chem., 67, 34-43, 1995.

[69] E. Martendala, E. Carasek, J. Chromatogr. A., 1218, 367-372, 2011.

[70] Y. Chen, J. Pawliszyn, Anal. Chem., 78, 5222-5226, 2006.

[71] D. Bal, J. Li, S.B. Chen, Environ. Sci. Technol., 35, 3936, 2001.

[72] R.G. Harvey, Polycyclic Aromatic Hydrocarbons, 1st edition, Wiley-VCH, New York, 1997.

[73] M.Howsam, K.C. Jones, The Handbook of Environmental Chemistry: PAHs and Related Compounds- Chemistry., Springer, Berlin Heidelberg New York, 137-174, 1998.

[74] A. L. C.Lima, J.W. Farrington, C. M. Reddy, Environ. Forensics., 6, 109-131, 2005.

[75] F. J. Santos, M. T. Galceran, Trends. Anal. Chem., 21, 672-685, 2002.

[76] D. Djozan, Y. Assadi, Microchem. J., 63, 276-284, 1999.

[77] U. S. Environmental Protection Agency. List of the Sixteen PAHs with Highest Carcinogenic Effect, London, 1984.

[78] D. Knopp, M. Seifert, V. Vaananen, R. Niessner, Environ. Sci.Technol., 34, 2035-2041, 2000.

[79] D. Mackay, W. Y. Shiu, K. C. Ma, Illustrated Handbook of Physical-chemical Properties and Environmental Fate for Organic Chemicals., Lewis Publishers, Michigan, USA. 1992.

[80] S. C. Wilson, K. C, Jones, Environ.Pollut., 81, 229-249, 1993.

[81] I. P. Bossert, R. Bartha, Bull. Environ.Contam.Toxicol., 37, 490-495, 1986.

[82] R. C. Sims, M. R. Overcash, Res.Rev., 88, 1-67, 1983.

[83] W. D. Weissenfels, H. J. Klewer, J. Langhoff, Appl. Microbiol. Biotechnol., 36, 689-696, 1992.

[84] M. Alexander, Environ. Sci. Technol., 29, 2713-2717, 1995.

[85] K. C. Jones, J. A. Stratford, K. S. Waterhouse, N. B. Vogt, Environ. Sci. Technol., 23, 540-550, 1989.

[86] M. B. McBride, Environmental Chemistry of Soils, Oxford University Press, Inc., New York, 1994.

[87] G. Sposito, The Chemistry of Soils, Oxford University Press, New York, 1989.

[88] J. H. C. Wong, C.H. Lim, G.L. Nolen, Design of Remediation Systems, CRC/Lewis Publishers, FL, USA, 1997.

[89] J. Birdwell, R. L. Cook, L. J. Thibodeaux, Environ. Toxicol. Chem., 26, 424-434, 2007.

[90] K.T. Semple, W. J. Morriss, G. I. Paton, Eur. J. Soil Sci., 54, 809-818, 2003.

[91] M. Alexander, Environ. Sci. Technol., 29, 2713-2717, 1995.

[92] K.U. Goss, R. P. Schwarzenbach, Sci. Educat., 80, 450-455, 2003.

[93] W. J. Weber, F. A. DiGiano, Process Dynamics in Environmental Systems, Wiley, New York, 1996.

[94] R. G. Luthy, et al., Environ. Sci. Technol., 31, 3341-3347, 1997.

[95] C. J. Werth, M. Reinhard, Environ. Sci. Technol., 31, 697-703, 1997.

[96] J. J. Pignatello, B. Xing, Environ. Sci. Technol., 30, 1-11, 1996.

[97] J. Farrell, M. Reinhard, Environ. Sci. Technol., 28, 63-72, 1994.

[98] R. P. Schawrzenbach, P. M. Gschwend, D. M. Imboden, Environmental Organic Chemistry, second edition, John Wiley, USA, 2003.